



UNIVERSITÀ DEGLI STUDI
DI MILANO



UNIVERSITÀ DEGLI STUDI
DI NAPOLI FEDERICO II

PhD degree in Systems Medicine (curriculum in Human Genetics)

European School of Molecular Medicine (SEMM),

University of Milan and University of Naples "Federico II"

Settore disciplinare: Med/03, XXXI ciclo

Analysis of TFEB nucleo-cytoplasmic shuttling dynamics in response to nutrient availability.

Valerio Benedetti

Tigem, Naples

Matricola n. R11474

Supervisor: Prof. Andrea Ballabio

Internal Supervisor: Prof. Carmine Settembre

External Supervisor: Prof. Romeo Ricci

Anno accademico 2018-2019

TABLE OF CONTENTS

TABLE OF CONTENTS	2
LIST OF ABBREVIATIONS	5
FIGURES INDEX	10
ABSTRACT	13
INTRODUCTION	14
1. THE LYSOSOME AS A SIGNALING HUB	14
1.1 The lysosome.....	14
1.2 Lysosomal degradation and secretion.....	15
1.3 Lysosomal signaling.....	15
2. MECHANISTIC TARGET OF RAPAMYCIN COMPLEX 1 (mTORC1).....	17
2.1 The mechanistic target of rapamycin (mTOR) complexes	17
2.2 Downstream targets of mTORC1	18
2.3 mTORC1 response to growth factors and stress	21
2.4 mTORC1 response to amino acids	21
3. MiT/TFE TRANSCRIPTION FACTORS	24
3.1 MiT/TFE family of transcription factors.....	24
3.2 Role of MiT/TFE transcription factors in cancer	27
4. TRANSCRIPTION FACTOR EB (TFEB).....	28
4.1 TFEB and TFE3 as master regulators of lysosomal function and autophagy	28
4.2 Physiological roles of TFEB <i>in vivo</i>	30
4.3 TFEB as a therapeutic target	32
4.4 Regulation of TFEB activity	33

5. NUCLEO-CYTOPLASMIC SHUTTILING PROTEINS	37
5.1 The mechanism of nucleo-cytoplasmic shuttling.....	37
AIMS OF THE STUDY.....	41
MATERIALS AND METHODS	42
Cell culture conditions.....	42
Materials	42
Plasmids	43
Transfection	45
Cell treatments.....	45
High-content analysis.....	46
Cell lysis and western blotting.....	46
Co-immunoprecipitation assay.....	47
RNA extraction and real-time PCR	47
Immunofluorescence and confocal microscopy	48
FRAP, FLIP and live cell imaging experiments	49
Statistical analysis.....	50
RESULTS	52
1. TFEB continuously shuttles between the cytosol and the nucleus through the activity of exportin CRM1	52
2. TFEB cytosolic relocalization is controlled by a nuclear export signal.....	55
3. TFEB nuclear export kinetics are modulated by nutrients	58
4. TFEB nuclear export is controlled by hierarchical phosphorylation	63
5. Phosphorylation on S142 and S138 is crucial for the interaction between TFEB and CRM1	65
6. Nuclear mTOR-dependent phosphorylation of TFEB during export	67
7. Analysis of lysosomal TFEB phosphorylation.....	68

DISCUSSION.....	81
BIBLIOGRAPHY	87
ACKNOWLEDGEMENTS.....	114

LIST OF ABBREVIATIONS

4E-BP1	eIF4E binding protein 1
AKT	Phosphoinositide-3-kinase–protein kinase B
AMPK	5' AMP-activated protein kinase
ARF1	ADP-ribosylation factor 1
Arg	Arginine
ATP	Nucleotide adenosine triphosphate
Bcl-2	B-cell lymphoma 2
bHLH	Basic helix-loop-helix domain
bHLH-Zip	Basic helix-loop-helix leucine-zipper
CAD	carbamoyl-phosphate synthetase2, aspartate transcarbamoylase, dihydroorotase
CASTOR1	Cytosolic arginine sensor for mTORC1 subunit 1
CLEAR	Coordinated lysosomal expression and regulation
CRM1	Chromosomal maintenance 1
DEPTOR	DEP domain containing mTOR-interacting protein
E-box	Enhancer box
eIF4A	Eukaryotic translation initiation factor 4A
eIF4B	Eukaryotic translation initiation factor 4B
eIF4E	Eukaryotic translation initiation factor 4E
eIF4F	Eukaryotic translation initiation factor 4F
ER	Endoplasmic reticulum
ERK	Extracellular signal-regulated kinase
FKBP12	12-kDa FK506-binding protein

FLCN	Folliculin
FLIP	Fluorescence loss in photobleaching
FNIP1/2	Folliculin-interacting protein 1/2
FRAP	Fluorescence recovery after photobleaching
FRB	FKBP12/rapamycin-binding domain
GAP	GTPase activating protein
GATOR	Gap activity toward rags
GDP	Guanosine diphosphate
GEF	Guanine nucleotide exchanging factor
GFP	Green fluorescent protein
GSK3β	Glycogen synthase kinase 3
GTP	Guanosine-5'-triphosphate
HIF-1α	Hypoxia-inducible factor 1-alpha
HIV	Human immunodeficiency virus
HPRT1	Hypoxanthine-guanine phosphoribosyltransferase 1
IGF-1	Insulin/insulin-like growth factor-1
KO	Knock-out
LAMP1	Lysosome-associated membrane protein
Lamtor1-5	Late endosomal/lysosomal adaptor, MAPK and mTOR activator 1-5
LMB	Leptomycin B
LSDs	Lysosomal storage disorders
Lys	Lysine
Lys-S6K	Lysosomal S6K
Lys-TFEB	Lysosomal TFEB

MALAT1	Metastasis associated lung adenocarcinoma transcript 1
MAP4K3	Mitogen-activated protein kinase kinase kinase kinase 3
MAPKAPK2	p38-activated kinase MK2
MCC	Mander's co-localization coefficient
MCOLN1	Mucolipin 1
MITF	Microphthalmia-associated transcription factor
MIT/TFE	Microphthalmia family of transcription factors
mLST8	Mammalian lethal with sec-13 protein 8
mSin1	Mammalian stress-activated map kinase-interacting protein 1
MTHFD2	Methylenetetrahydrofolate dehydrogenase (NADP+ dependent) 2
mTOR	Mammalian target of rapamycin
mTORC1	Mechanistic target of rapamycin complex 1
mTORC2	Mechanistic target of rapamycin complex 2
NES	Nuclear export signal
NFAT	Nuclear factor of activated T cells transcription factor
NF-kB	Nuclear factor kappa B
NLS	Nuclear localization signal
NPC	Nuclear pore complex
NR1D1	Nuclear receptor 1D1
PCR	Polymerase chain reaction
PDCD4	Programmed cells death protein 4
PKD1	Pyruvate dehydrogenase kinase 1

PGC1α	Peroxisome proliferator-activated receptor- γ coactivator 1 α
PIKK	PI3K-related kinase family
PKCβ	Protein kinase C β
PKD	Protein kinase D
PIK	Protein kinase inhibitor
PIP3	Phospholipid phosphatidylinositol 3-phosphate
PRAS40	Proline-rich Akt substrate 40 kDa
Protor1/2	Protein observed with rictor 1 and 2
Rag	Ras-related GTP-binding protein
Raptor	Regulatory-associated protein of mammalian target of rapamycin
Ran	Ras-related nuclear protein
RANKL	Receptor activator of nuclear factor κ B ligand
RCCs	Renal cell carcinomas
Rheb	Ras homolog enriched in brain
Rictor	Rapamycin-insensitive companion of mTOR
RPE	Retinal pigmented epithelium
RSK1	p90 ribosomal S6 kinase
RT-qPCR	Quantitative reverse transcription PCR
S6K1	p70S6 kinase 1
SESN2	Sestrin 2
SKAR	S6K1 Aly/REF-like substrate
SLC38A9	Sodium-coupled neutral amino acid transporter 9
SREBP1/2	Sterol regulatory element-binding protein 1/2
STUB1	STIP1 homology and U-box containing protein 1

TBC1D7	TBC1 domain family member 7
TFE3	Transcription factor E3
TFEB	Transcription factor EB
TFEC	Transcription factor EC
TOS	TOR-signaling motif
TSC	Tuberous sclerosis complex
ULK1	Unc-51 like autophagy activating kinase 1
v-ATPase	Vacuolar (H ⁺)-ATPases complex
VPS34	Vacuolar protein sorting 34
WNT	Wingless-related integration site
WT	Wild-type

FIGURES INDEX

Fig. 1. Function and regulation of lysosomes.....	16
Fig. 2. The nutrient sensing machinery that controls mTORC1 activity.....	23
Fig. 3. The microphthalmia family of transcription factors.....	26
Fig. 4. Overview of TFEB roles in cellular processes.....	30
Fig. 5. Model of TFEB regulation in response to nutrient availability.....	35
Fig. 6. Relevant TFEB phosphorylation sites and their regulatory effects.....	37
Fig. 7. Classic protein nuclear transport mediated by NLS and NES sequences..	39
Fig. 8. Time-lapse imaging of TFEB localization upon nutrient refeeding	52
Fig. 9. TFEB nuclear export impairment following leptomycin B treatment.....	53
Fig. 10. TFEB nucleo/cytoplasmic ratio in cells analysed by high-content imaging.....	53
Fig. 11. CRM1 RNA expression levels in silenced HeLa cells	54
Fig. 12. CRM1 depletion impairs TFEB nuclear export.....	54
Fig. 13. TFEB nuclear accumulation induced by leptomycin B treatment	55
Fig. 14. CRM1 consensus motif conserved among MiT/TFE members	56
Fig. 15. TFEB CRM1 consensus motif conserved among different species	56
Fig. 16. TFEB distribution in nuclear export signal (NES) mutants	57
Fig. 17. Fluorescence recovery after photobleaching (FRAP)	57
Fig. 18. Analysis of TFEB NES-mutants export kinetics by FRAP	58
Fig. 19. Analysis of TFEB export kinetics in the presence of nutrients by FRAP ..	59
Fig. 20. Analysis of TFEB export kinetics in the absence of nutrients by FRAP ...	60
Fig. 21. Fluorescence loss in photobleaching (FLIP)	61
Fig. 22. Analysis of nuclear export kinetics in response to nutrient availability by FLIP.....	61

Fig. 23. TFEB nuclear fluorescence decay measured by FLIP in response to nutrients	62
Fig. 24. Nuclear export kinetics of constitutive nuclear TFEB forms analysed by FRAP.....	64
Fig. 25. Hierarchical phosphorylation pattern of TFEB analysed with specific phospho-antibodies.....	65
Fig. 26. TFEB localization under leptomycin B and Torin1 treatment	66
Fig. 27. TFEB phosphorylation under leptomycin B and Torin1 treatment	66
Fig. 28. Nutrient-dependent phosphorylation of TFEB NES-mutant M144A	67
Fig. 29. Immunoblotting analysis of CRM1 interaction with wild-type TFEB or constitutive nuclear TFEB mutants.....	68
Fig. 30. Schematic representation of the constitutive Lys-TFEB construct	69
Fig. 31. Lys-TFEB localization in response to nutrient availability.....	69
Fig. 32. Lys-TFEB phosphorylation analysis in response to nutrient availability ...	71
Fig. 33. mTOR localization in HeLa cells expressing Lys-TFEB	71
Fig. 34. Analysis of mTOR co-localization with LAMP1 in cells expressing Lys-TFEB	72
Fig. 35. Schematic diagram of the constitutive Lys-S6K construct.....	72
Fig. 36. Lys-S6K localization in HeLa cells	73
Fig. 37. Lys-S6K phosphorylation analysis in response to nutrient availability	74
Fig. 38. mTOR localization in HeLa cells expressing lysosomal S6K	74
Fig. 39. Analysis of mTOR co-localization with LAMP1 in cells expressing Lys-S6K.....	75
Fig. 40. mTOR localization in RagA/B KO HEK293A cells expressing Lys-S6K ...	76
Fig. 41. mTOR and Lys-S6K co-localization analysis in RagA/B KO HEK293A cells	76
Fig. 42. Lys-S6K phosphorylation analysis in RagA/B KO HEK293A cells	77

Fig. 43. Lysosomal-S6K phosphorylation after Raptor silencing.....	77
Fig. 44. mTOR recruitment in cells expressing Lys-S6K after Raptor silencing	78
Fig. 45. mTOR localization in HeLa cells expressing Lys-S6K TOS-mutant.....	79
Fig. 46. Analysis of mTOR co-localization with Lys-S6K wild-type or TOS-mutant protein	79
Fig. 47. S6K phosphorylation analysis in cells expressing lysosomal-S6K TOS-mutant.....	80

ABSTRACT

The transcription factor EB (TFEB) is a key transcriptional regulator of lysosomal biogenesis and autophagy in response to variations in nutrient availability. TFEB subcellular localization and transcriptional activity are mainly controlled by its phosphorylation status. At the steady state, TFEB is normally phosphorylated and sequestered in the cytoplasm in an inactive form. Amino acids deprivation induces TFEB dephosphorylation and subsequent nuclear translocation, thus promoting the transcriptional activation of catabolic processes, including autophagy and lysosomal biogenesis. However, how nuclear TFEB is inactivated upon nutrient refeeding was until recently poorly understood. Our study on TFEB nucleo-cytoplasmic shuttling dynamics showed that TFEB continuously shuttles between the cytosol and the nucleus and highlighted the nuclear export as a new important checkpoint in the modulation of TFEB subcellular localization. TFEB nuclear export is mediated by the exportin CRM1, which recognizes a previously uncharacterized Nuclear Export Signal (NES) in the TFEB sequence. In addition, we found that this process requires a hierarchical multisite mTOR-dependent nuclear phosphorylation of TFEB on S142 and S138 residues, which allows its interaction with CRM1 and subsequent nuclear export in response to nutrients. Thus, our study reveals a complex scenario in which TFEB phosphorylation may occur in different subcellular compartments to finely tune its nucleo-to-cytoplasm shuttling. This model may unveil new pharmacological strategies aimed to control TFEB localization and activity by modulating its nuclear import and nuclear export in human diseases associated with autophagy or lysosomal defects, such as neurodegenerative and lysosomal storage disorders.

INTRODUCTION

1. THE LYSOSOME AS A SIGNALING HUB

1.1 The lysosome

Lysosomes were first discovered as intracellular vesicles in the early 50's by Christian de Duve (de Duve, 2005). They are membrane-enclosed cytoplasmic organelles specialized in the breakdown and recycling of complex cellular components, containing over 60 luminal hydrolases with specificity for different substrates, including lipids, polysaccharides and proteins (Xu and Ren, 2015). Most lysosomal hydrolases require an acidic lumen to function; the presence of the vacuolar (H⁺)-ATPases complex (v-ATPase) on the lysosomal membrane serves to pump protons into the lumen and maintain the acidic environment (pH 4.5-5) required for hydrolytic activity (Lim and Zoncu, 2016). In addition, together with the v-ATPases, other ion channels (Na⁺, K⁺, Ca²⁺, Cl⁻) cooperate to regulate the lumen homeostasis by generating an ionic gradient and a membrane potential important for lysosomal acidification, catabolite transporters and lysosomal trafficking (Xu and Ren, 2015). Ultimately, the end products of lysosome-mediated digestion are actively or passively transported by integral membrane proteins of the lysosomal membrane to the cytoplasm, where they can be reused in anabolic processes (Perera and Zoncu, 2016). Lysosomes can also function as a cellular storage site, where catabolic intermediates are exchanged with the cytoplasm in a regulated manner in response to changing cellular needs (Perera and Zoncu, 2016).

1.2 Lysosomal degradation and secretion

These essential organelles are primarily involved in several degradative and recycling processes, including endocytosis and autophagy (Fig. 1), in which extracellular or intracellular material, respectively, is delivered to the lysosome for degradation by lysosomal hydrolases (Ballabio, 2016). Endocytosis starts with the formation of endocytic vesicles from the plasma membrane that subsequently mature into early and late endosomes, which finally fuse with lysosomes forming endolysosomes where all the materials transported are degraded (Xu and Ren, 2015). On the contrary, during the autophagy process, autophagosomes directly fuse with lysosomes, where delivered organelles and long lived proteins are broken down into building-block molecules (Settembre et al., 2013b).

In addition, lysosomes can also fuse to the plasma membrane in a process known as lysosomal exocytosis (Perera and Zoncu, 2016), which plays important roles in several physiological processes such as degranulation, bone resorption, pigmentation, coagulation and hydrolase release during fertilization (Settembre et al., 2013b).

1.3 Lysosomal signaling

In addition to the “old” view of the lysosome as a degradative organelle, recent studies highlighted additional roles of the lysosome that make this organelle a central signaling hub (Fig. 1) responsible for nutrient sensing, gene regulation, secretion, plasma membrane repair, metal ion homeostasis, cholesterol transport and immune response (Saftig and Klumperman, 2009; Lim and Zoncu, 2016; Perera and Zoncu, 2016). In particular, following the discovery that a key regulator of cell growth and metabolism, the mechanistic target of rapamycin complex 1 (mTORC1), is localized to the lysosomal surface, the lysosome is now indicated as a platform for metabolic signaling that integrates different environmental signals to regulate

anabolic and catabolic pathways important for cellular homeostasis (Lamming and Bar-Peled, 2019). In addition, opposite to the traditional view of the lysosome as a static organelle, recent discoveries also showed that the number and composition of lysosomes within a cell is highly dynamic and subject to transcriptional modulation (Sardiello et al., 2009).

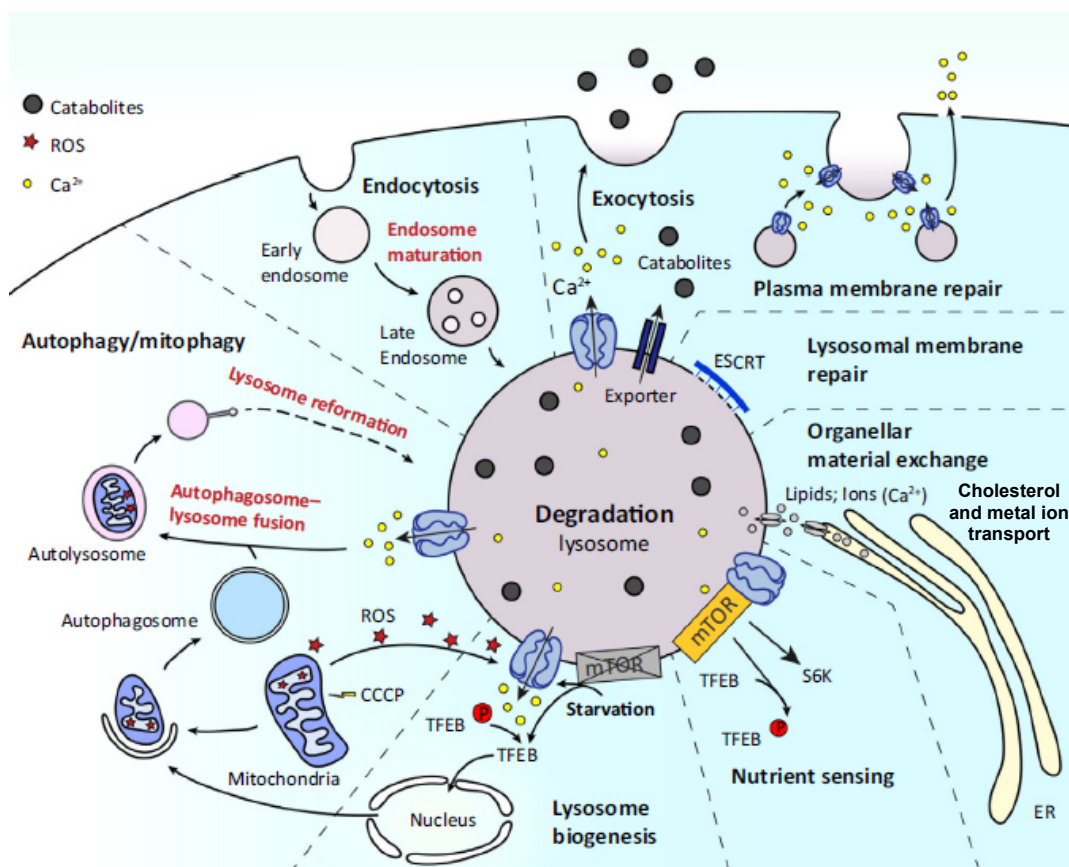


Figure 1. Function and regulation of lysosomes (adapted from Li et al., Trends Biochem. Sci., 2019). Lysosomes are the degradation center in the cell, receiving inputs from both endocytic and autophagic pathways. The degradation products are released through exporters, vesicular trafficking, lysosomal exocytosis or membrane contact sites. Lysosomal ion channels, by mediating signal-dependent lysosomal ion flux, participate in various lysosomal functions, including lysosomal membrane trafficking, catabolite export, nutrient sensing, mTOR signaling. autophagy and mitophagy, plasma membrane and lysosomal membrane repair, TFEB nuclear translocation and lysosome biogenesis.

2. MECHANISTIC TARGET OF RAPAMYCIN (mTOR)

2.1 The mechanistic target of rapamycin (mTOR) complexes

The mechanistic target of rapamycin (mTOR) was identified in mammals as a target of rapamycin, an inhibitor of cell growth and proliferation (Sabatini et al., 1994).

mTOR is a serine/threonine kinase belonging to the PI3K-related kinase family (PIKK) and serves as a core component for two distinct protein complexes that regulate different cellular processes: mTOR Complex 1 (mTORC1) and mTOR Complex 2 (mTORC2). Besides the catalytic mTOR subunit, mTORC1 is composed by: the regulatory-associated protein of mammalian target of rapamycin (Raptor), a specific subunit required for mTORC1 subcellular localization, activation and substrates recruitment (Kim et al., 2002); the proline-rich Akt substrate 40 kDa (PRAS40), a specific inhibitor subunit (Sancak et al., 2007); the mammalian lethal with sec-13 protein 8 (mLST8, also known as GβL) (Jacinto et al., 2004; Kim et al., 2003), which interacts with the catalytic domain of mTOR and stabilizes the kinase activation loop (Yang et al., 2013); the DEP domain containing mTOR-interacting protein (DEPTOR), which also appears to have inhibitory functions (Peterson et al., 2009); Similar to mTORC1, the mTORC2 complex contains the mTOR subunit as well as mLST8 and DEPTOR; however, mTORC2 specifically contains three additional subunits: the rapamycin-insensitive companion of mTOR (Rictor), which, similar to Raptor, also appears to act as an adaptor and have regulatory functions (Sarbasov et al., 2004); the mammalian stress-activated map kinase-interacting protein 1 (mSin1) (Jacinto et al., 2006); the protein observed with Rictor 1 and 2 (protor1/2) (Pearce et al., 2007), both with regulatory functions.

The cellular functions of mTORC1 have been extensively studied and are well-defined. mTORC1 activity is modulated in response to changes in the levels of

amino acids, oxygen, energy, growth factors, as well as stress conditions, thus modulating cell growth, cell cycle progression, metabolism, macromolecule biosynthesis and autophagy (Laplante and Sabatini, 2012). Conversely, mTORC2 responds to growth factors and regulates cell survival and metabolism, as well as the cytoskeleton organization (Laplante and Sabatini, 2012).

In addition to their distinct functions, the two mTOR complexes also differ in their sensitivity to drug inhibitors. For instance, while catalytic inhibitors of mTOR (e.g. Torin1) completely inhibit both complexes, only mTORC1 is sensitive to short-term treatments with rapamycin (Laplante and Sabatini, 2012). Rapamycin binds the cytosolic 12-kDa FK506-binding protein (FKBP12) (Sabatini et al., 1994), which in turn interacts with the FKBP12/rapamycin-binding domain (FRB) of mTOR contained in mTORC1, but not mTORC2, thus masking the mTOR catalytic domain and blocking its kinase activity (Yang et al., 2013). Rapamycin was also proposed to disrupt the interaction of mTOR with Raptor, thus resulting in complex disassembling (Kim et al., 2002). On the other hand, mTORC2 activity is insensitive to acute rapamycin treatment, probably because of a strong interaction between Rictor and mTOR that does not allow FKBP12 accessibility and mTORC2 allosteric inhibition (Gaubitz et al., 2015). Nonetheless, prolonged rapamycin treatment abolishes mTORC2 signaling, due to the ability of rapamycin to bind to newly synthesized mTOR, thus preventing the formation of a new mTORC2 complex (Sarbasov et al., 2006).

2.2 Downstream targets of mTORC1

mTORC1 activity is crucial to ensure a proper balance between anabolism and catabolism during cell growth and division. mTORC1 activates anabolic processes, including protein, lipid and nucleotide synthesis, whereas it inhibits catabolic

pathways, such as autophagy, proteasomal degradation and lysosomal biogenesis (Laplante and Sabatini, 2012; Saxton and Sabatini, 2017).

mTORC1 promotes protein synthesis mainly through the phosphorylation of two key substrates, p70S6 Kinase 1 (S6K1) and eIF4E Binding Protein 1 (4E-BP1), referred to as the mTORC1 canonical substrates. Both contain a five-amino acid conserved TOR-signaling motif (TOS motif) that allows their recruitment by the mTORC1 subunit Raptor; point mutations within the TOS motif, specifically mutations F5A in S6K1 and F114A in 4E-BP1, abolish the interaction with Raptor and abrogate the mTOR-mediated phosphorylation of these substrates (Schalm and Blenis, 2002; Nojima et al., 2003). S6K1 is directly phosphorylated by mTORC1 at Thr389 (Isotani et al., 1999), which triggers its subsequent phosphorylation and activation by PDK1 (Dennis et al. 1998). Next, activated S6K1 modulates several substrates involved in mRNA translation initiation, such as eIF4B which is an important factor required for the 5' cap binding eIF4F complex (Holz et al., 2005). S6K1 also induces the degradation of PDCD4, an inhibitor of eIF4A (Dorrello et al., 2006), and enhances mRNA splicing through the interaction with SKAR, a component of exon-junction complexes (Ma et al., 2008). 4E-BP1 is also involved in protein translation by preventing the formation of the eIF4F complex through the sequestration of the subunit eIF4E, thus blocking the translational process. mTORC1-mediated phosphorylation of 4E-BP1 causes its dissociation from eIF4E thus promoting the initiation of the cap-dependent translation (Gingras et al., 1999).

mTORC1 is also involved in lipid synthesis necessary to generate new membranes in proliferating cells. In particular, mTORC1 controls the sterol regulatory element-binding protein 1/2 (SREBP1/2) transcription factors, which are important for the expression of genes required in fatty acid and cholesterol production (Espenshade and Hughes, 2007). Inactive SREBPs are normally localized on the endoplasmic reticulum (ER); upon sterol depletion, mTORC1 promotes the processing of SREBP

precursors through S6K and 4E-BP1 activity, and once activated, SREBPs translocate to the nucleus where they regulate the transcription of genes important for lipogenesis (Düvel et al., 2010; Wang et al., 2011). Recently, mTORC1 has been shown to be involved in nucleotide synthesis, which is required for DNA replication and ribosome biogenesis: mTORC1 increases purine synthesis by regulating the expression of a crucial component of the mitochondrial tetrahydrofolate cycle, namely MTHFD2 (Ben-Sahra et al., 2016); in addition, mTORC1 is also involved in pyrimidine synthesis by inducing the S6K-dependent phosphorylation of CAD, an enzyme that catalyses the first three steps of *de novo* pyrimidine synthesis (Ben-Shara et al., 2013; Robitaille et al., 2013). Finally, it enhances ATP production through the activation of the hypoxia inducible factor 1 α (HIF1 α), a positive regulator of glycolysis (Brugarolas et al., 2004; Düvel et al., 2010).

Concomitantly with the activation of anabolic mechanisms, mTORC1 also suppresses catabolic processes, such as the autophagy pathway. In particular, mTORC1 is known to phosphorylate the kinase ULK1, which is involved in the early stages of autophagosome formation by recruiting a VPS34 kinase complex responsible for the production of the phospholipid phosphatidylinositol 3-phosphate (PI3P) at the autophagy initiation site (Zachari and Ganley, 2017), thus blocking its AMPK-dependent activation and autophagy initiation (Kim et al., 2011). In addition, mTORC1 exerts a negative effect on autophagy via the downregulation of the transcription factor EB (TFEB), member of the microphthalmia family of transcription factors (MiT/TFE), which is responsible for autophagic gene expression (Martina et al., 2012; Roczniak-Ferguson et al., 2012; Settembre et al., 2012).

Besides autophagy, mTORC1 activity is also involved in the modulation of the proteasome activity, another degradative system specific for protein turnover (Zhang et al., 2014; Zhao et al., 2015; Rousseau and Bertolotti, 2016). However, it is unclear whether it is the activation (Zhang et al., 2014) or inhibition (Zhao et al.,

2015; Rousseau and Bertolotti, 2016) of mTORC1 that increases proteasome-mediated protein degradation.

2.3 mTORC1 response to growth factors and stress

mTORC1 has long been known as a downstream mediator of growth factor and mitogenic signaling pathways. For instance, the insulin/insulin-like growth factor-1 (IGF-1) pathway (Inoki et al., 2002), as well as receptor tyrosine kinase-dependent Ras signaling (Roux et al., 2004), modulate mTORC1 activity by inhibiting the Tuberous Sclerosis Complex (TSC). TSC is a heterotrimeric complex composed of the subunits TSC1, TSC2 and TBC1D7 (Dibble et al., 2012), which acts as a GTPase activating protein (GAP) for Rheb, a small GTPase that resides at the lysosomal surface and activates mTORC1 (Inoki et al., 2003; Long et al., 2005). TSC2 inhibition, induced by its phosphorylation by AKT and other mitogen-activated kinases, including ERK, MAPKAPK2 and RSK1 (Huang and Manning, 2008), causes the dissociation of the TSC complex from the lysosomes, allowing Rheb to activate mTORC1 (Inoki et al., 2002; Roux et al., 2004). By contrast, stress conditions, such as hypoxia, low ATP levels, glucose deprivation and DNA damage (Saxton and Sabatini, 2017), inhibit mTORC1 by activating the stress responsive metabolic regulator 5' AMP-activated protein kinase (AMPK), which indirectly activates TSC2 and promotes mTORC1 inhibition (Gwinn et al., 2008).

2.4 mTORC1 response to amino acids

Amino acid levels are essential for mTORC1 activation and represent one of the most conserved growth signals to this pathway (Bar-Peled and Sabatini, 2014).

Recent work has shown that amino acids modulate mTORC1 recruitment to the lysosomal surface (Fig. 2) (Sancak et al., 2010), an essential step for mTORC1 activation which occurs through the modulation of the GTP/GDP bound state of the

Rag GTPases (Kim et al., 2008; Sancak et al., 2008). In mammals, there are 4 Rag GTPases that work as heterodimers composed of RagA or RagB bound with RagC or RagD. In the presence of amino acids, the heterodimer acquires an active conformation in which RagA/B is bound to GTP and RagC/D is bound to GDP. This conformation allows the interaction of Rags with Raptor subunit of mTORC1 (Sancak et al., 2008), thus leading to the recruitment of the complex to the lysosomal surface, where is activated by Rheb (Inoki et al., 2003; Long et al., 2005). On the other hand, the absence of amino acids causes a switch of the Rag dimers into an inactive conformation containing GDP-bound RagA/B and GTP-bound RagC/D (Sancak et al., 2008), thereby releasing mTORC1 from the lysosomal surface and causing its inactivation (Bar-Peled et al., 2013). Rags are anchored to the lysosomal membrane through a pentameric complex called Ragulator (Sancak et al., 2010), which consists of a scaffold protein, namely Lamtor1 (late endosomal/lysosomal adaptor, MAPK and MTOR activator 1), which is bound to two heterodimers composed of Lamtor2–Lamtor3 and Lamtor4–Lamtor5 (Sancak et al., 2010). In particular, the myristoylated N-terminus of Lamtor1 anchors the Ragulator complex to the lysosomal surface (Nada et al., 2009).

The activity of Rag GTPases is modulated by a series of GEFs and GAPs that control the nucleotide-bound state of each Rag within the heterodimer. In particular, the amino acid sensor sodium-coupled neutral amino acid transporter 9 (SLC38A9) has been proposed to act as a GEF for RagA/B (Shen and Sabatini, 2018); Folliculin (FLCN), together with its partners folliculin-interacting protein 1/2 (FNIP1/2), acts as a GAP for RagC/D, promoting the hydrolysis of inactive GTP form into active GDP form (Tsun et al., 2013); another important player is the octameric complex GAP activity toward Rags (GATOR), which is composed by two sub-complexes called GATOR1 and GATOR2: GATOR1 works as a GAP for RagA/B, whereas GATOR2 is an inhibitor of GATOR1 (Bar-Peled et al., 2013). Notably, it has been recently

identified a feedback mechanism by which MiT/TFE transcription factors, downstream targets of mTORC1 signaling, control mTORC1 lysosomal recruitment and activity by directly regulating the expression of RagD and, at lower levels, other components such as RagC and FLCN (Di Malta et al., 2017).

mTORC1 senses, via two distinct mechanisms, both intra-lysosomal and cytosolic amino acids. The lysosomal v-ATPase pump communicates the luminal amino acids abundance to Ragulator and the arginine sensor SLC38A9 (Zoncu et al., 2011, Shen and Sabatini, 2018; Wang et al., 2015). A specific leucine-binding protein, Sestrin2 (SESN2), senses and signals cytosolic leucine levels via modulation of GATOR2 (Chantranupong et al., 2014; Wolfson et al., 2016). Cytosolic arginine abundance is detected through the sensor CASTOR1, which also acts on GATOR2 inhibitory activity in the absence of arginine (Chantranupong et al., 2016). Finally, glutamine promotes mTORC1 lysosomal recruitment via an unconventional Ragulator/Rags-independent mechanism that involves the v-ATPase and ADP-ribosylation factor 1 (ARF1) (Jewell et al., 2015).

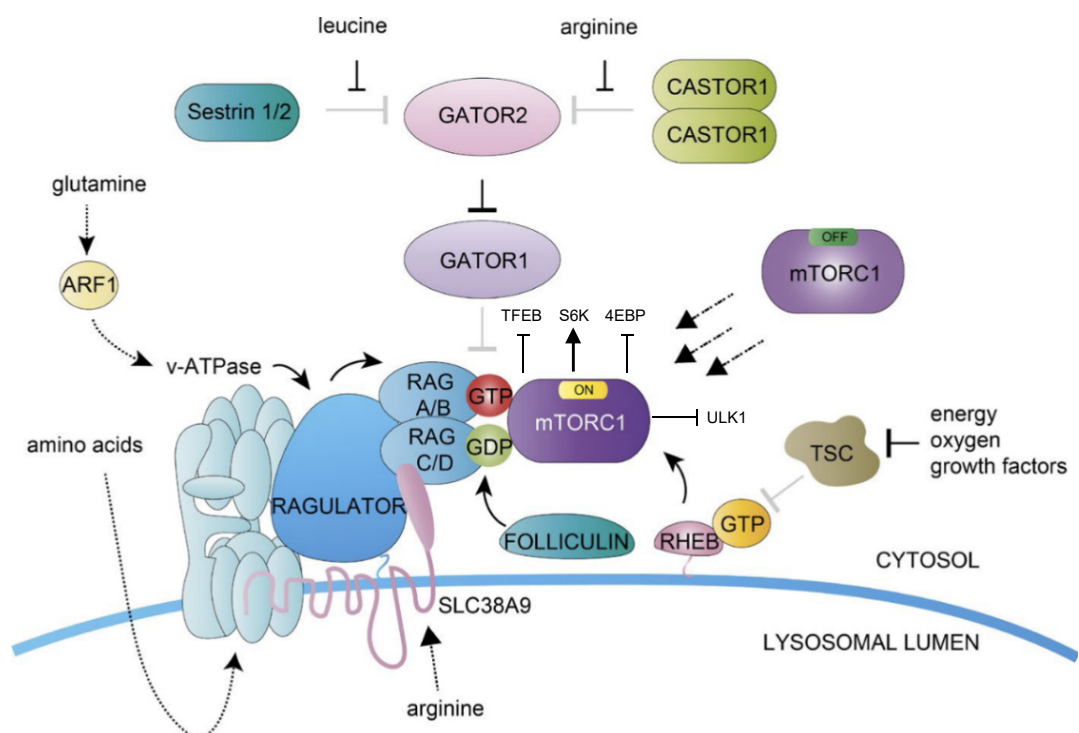


Figure 2. The nutrient sensing machinery that controls mTORC1 activity (adapted from Lim and Zoncu, J. Cell Biol., 2016). Schematic model that shows the main cellular components involved in amino acid sensing and response to external stimuli such as energy, oxygen and growth factors. Different signals are integrated upstream to coordinate the lysosomal recruitment of mTORC1 and activation.

3. MiT/TFE TRANSCRIPTION FACTORS

3.1 MiT/TFE family of transcription factors

In mammals, the microphthalmia family of transcription factors (MiT/TFE family) are involved in several developmental and differentiation processes. Over the years, four MiT members have been identified: the microphthalmia-associated transcription factor (MITF), the transcription factor EB (TFEB), the transcription factor E3 (TFE3) and the transcription factor C (TFEC).

MiT proteins are a subgroup of basic helix-loop-helix leucine-zipper (bHLH-Zip) transcription factors, as they share an identical DNA-binding region and similar HLH and Zip regions important for homo- or hetero- dimerization (Fig. 3) (Steingrímsson et al., 2004). Most of the bHLH-Zip factors, including MiT proteins, bind an hexameric CACGTG sequence, called E-box, in the proximal promoter of target genes. However, MiT factors can also recognize a particular CATGTG-type E-box, called M-box (Hemesath et al., 1994; Aksan and Goding, 1998). bHLH-Zip factors bind to DNA in the form of homo- or hetero- dimers; interestingly, however, MiT proteins can only heterodimerize with one another but cannot interact with other bHLH-Zip transcription factors (Hemesath et al., 1994). Nevertheless, whether MiT homo- versus hetero-dimers are functionally different remains currently unknown.

Proteins of the MiT/TFE family largely overlap in terms of their function and regulatory mechanisms. MITF is predominantly active in mast-cells, osteoclasts,

melanocytes and retinal pigmented epithelium (RPE) (Steingrímsson et al., 2004). It is considered a crucial regulator of melanosomal differentiation and development, with an important role during the generation of action potentials in the inner ear (Hodgkinson et al, 1993; Hemesath et al., 1994). Accordingly, mice carrying mutations in the MITF gene exhibit a white coat and eye developmental defects, due to MITF deficiency in melanocytes and the RPE (Steingrímsson et al., 2004). In humans, MITF mutations are responsible for Waardenbrug Syndrome type 2, a dominantly inherited syndrome characterized by hearing loss and pigmentation alterations (Tassabehji et al, 1994).

In the last decade, TFEB was identified as the main transcription factor involved in the regulation of lysosomal genes (Sardiello et al., 2009). Subsequent studies demonstrated that TFEB controls not only lysosome biogenesis and function, but also autophagic genes involved in autophagosome and autolysosome formation (Settembre et al., 2011), and lysosomal exocytosis (Medina et al., 2011). Moreover, it was found that TFE3 and some MITF isoforms are able to bind the same regulatory sequences upstream these genes, thus showing redundant functions of these transcription factors (Martina et al., 2014). Indeed, TFEB and TFE3 are ubiquitously expressed and control the same processes such as humoral immunity (Huan et al., 2006) and glucose and lipid metabolism (Pastore et al., 2017). However, their roles in gene expression do not overlap completely, since *Tfeb*-null mice are embryonic lethal (Steingrímsson et al., 1998) whereas *Tfe3* knock-out mice apparently do not show developmental defects (Steingrímsson et al., 2002).

Finally, TFEC is mainly expressed in monocytes and macrophages (Rehli et al., 1999) and is reported to share less common features with the other members (Zhao et al., 1993).

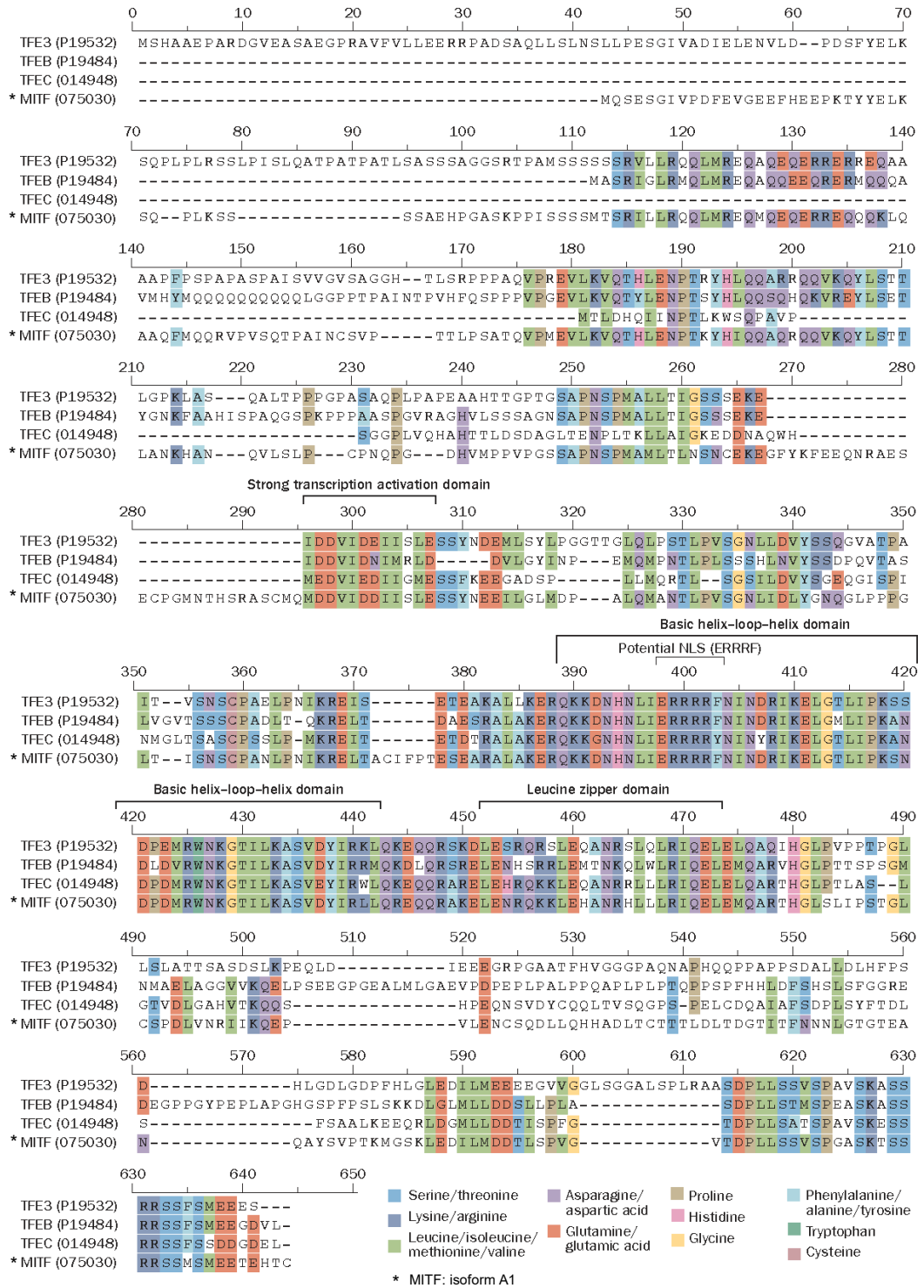


Figure 3. The microphthalmia family of transcription factors (adapted from Kauffman et al., Nat. Rev. Urol., 2014). Multiple sequence alignment created with the protein sequence of the four human genes of the microphthalmia transcription factor (MIT) family (TFE3, TFEB, TFEC, and MITF). The alignment highlights all the conserved regions and shows all the shared functional domains (activation domain, HLH domain, LZ domain).

3.2 Role of MiT/TFE transcription factors in cancer

MiT/TFE transcription factors are known oncogenes and their upregulation is associated with several human tumours in different tissues (Haq and Fisher, 2011). For example, MITF amplification is reported in 20% of melanomas (Garraway et al., 2005) and single-nucleotide mutations of MITF have been frequently found in melanoma cells (Cronin et al., 2009). In addition, oncogenic MITF dysregulation has been found also in clear cell sarcoma (Davis et al., 2006).

Other tumours associated to MiT proteins are the so-called TFE-fusion renal cell carcinomas (TFE-fusion RCCs, namely also tRCCs), a kidney-specific type of cancer caused by chromosomal translocation of TFEB, TFE3 and MITF (Kauffman et al., 2014). These fusions preserve the TFEB/TFE3 open reading frame and include the DNA-binding domains. An example, is the rare case of 6p21/11q13 translocation resulting in a fusion between TFEB gene and the promoter region of the non-coding MALAT1 gene; as a consequence of the stronger efficiency of this promoter, a massive increase in the expression levels of a full-length TFEB protein occurs in this RCCs (Kuiper et al., 2003). TFE3, which is the most common gene translocated in tRCC, is often translocated also in a particular type of sarcoma called alveolar soft part sarcoma (Goodwin et al., 2014).

In terms of molecular mechanisms, a recent study revealed that in kidney-specific TFEB overexpressing transgenic mice, the transcriptional induction of the tumorigenic WNT β -catenin signaling pathway is responsible for tumour development (Calcagni et al., 2016). It has been shown that also the induction of MITF expression in a melanoma model enhances WNT signaling, generating a positive-feedback loop that may function during the proliferative stages of the tumour (Ploper et al., 2015). Moreover, cytoplasmic accumulation of β -catenin was observed in patients with TFE3-tRCC, suggesting the presence of a possible link between TFE-factors and WNT-signaling components (Bruder et al., 2007). More

recently, xenograft experiments using melanoma cell lines highlighted the existence of a TFEB-RagD-mTORC1 axis that causes an hyperactivation of mTORC1, a key regulator of cell growth and metabolism, responsible for subsequent oncogenesis (Di Malta et al., 2017). Additionally, it has been found that several genes encoding anti-apoptotic proteins, for example Bcl-2 and HIF-1 α , are direct targets of MITF in melanoma cells, indicating a role in both tumour progression and survival (Hartman and Czyz, 2015).

4. TRANSCRIPTION FACTOR EB (TFEB)

4.1 TFEB and TFE3 as master regulators of lysosomal function and autophagy

Recent work demonstrated that lysosomal genes are co-expressed in various cell types and that their expression is globally modulated in response to specific environmental cues (Sardiello et al., 2009), revealing how actually lysosomal biogenesis and function are dynamic and subjected to transcriptional regulation. Promoter analysis of lysosomal genes then identified a conserved 10 base-pairs long E-box-like palindromic sequence (GTCACGTGAC), which was named “coordinated lysosomal expression and regulation” (CLEAR) motif, typically recognized by bHLH-LZ transcription factors (Sardiello et al., 2009). Next, it was demonstrated that TFEB can directly bind to CLEAR sequences, promoting the expression of target genes containing a CLEAR regulatory element within the promoter, such as lysosomal transmembrane proteins, lysosomal enzymes and some subunits of the V-ATPase system, which are part of the CLEAR network (Sardiello et al., 2009; Palmieri et al., 2011). Accordingly, overexpression of TFEB

was shown to induce an increase in lysosome number and enhance lysosomal catabolic activity (Sardiello et al., 2009).

Subsequent studies revealed that TFEB coordinates the expression of genes not only related to lysosomal biogenesis and activity, but also involved in autophagy, by regulating the expression of autophagy genes, which also contained the CLEAR elements in their promoters (Settembre et al., 2011; Palmieri et al., 2011). Specifically, TFEB overexpression induced autophagosome formation and autophagosome-lysosome fusion, resulting in an increased degradation of canonical autophagic substrates such as long-lived proteins (Settembre et al., 2011) as well as selective cargos like lipid droplets or damaged mitochondria (Settembre et al., 2013a; Nezich et al., 2015). Finally, TFEB was shown to regulate lysosomal exocytosis by increasing the release of lysosomal Ca^{2+} and the number of lysosomes in proximity to the plasma membrane (Medina et al., 2011). Therefore, TFEB coordinates a complex transcriptional program that promotes intracellular clearance by modulating different degradative pathways in response to environmental signals (Fig. 4). Interestingly, TFE3 was also found to control lysosomal biogenesis and autophagy by regulating a gene network that largely overlaps with the one regulated by TFEB (Martina et al., 2014).

More recently, TFEB has been found to play a role also in lysosomal positioning, by inducing the movement of lysosomes toward the center of the cell upon nutrient deprivation (Willett et al., 2017), and in endocytic gene expression, thus increasing cellular endocytosis and leading to activation of autophagic functions (Nnah et al., 2019). In addition, TFEB and TFE3 were recently shown to be involved in ER stress response (Martina et al., 2016), by promoting apoptosis, and in DNA damages response, by increasing p53-dependent transcription of genes implicated in DNA repair, cell cycle arrest and apoptosis (Brady et al., 2018).

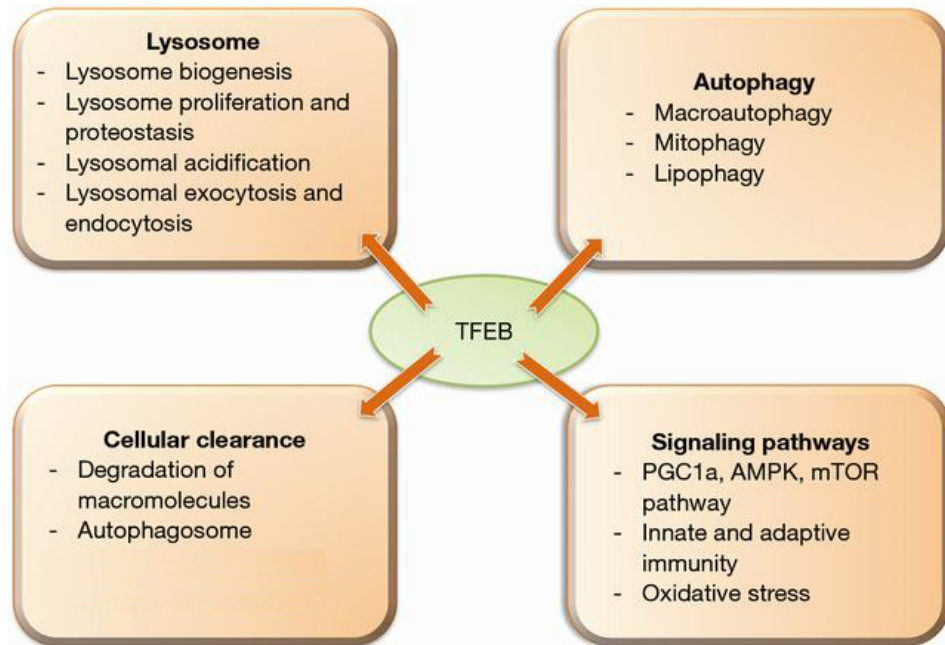


Figure 4. Overview of TFEB roles in cellular processes (adapted from Bala and Szabo, *Dig. Med. Res.*, 2018). The diagram shows most of the cellular processes regulated by TFEB activity, including lysosome function and biogenesis, autophagy, mitophagy, lipophagy, lysosomal exocytosis, endocytosis and several signaling pathways.

4.2 Physiological roles of TFEB *in vivo*

TFEB-null mice die at embryonic day (E)9.5–10.5 because of defective placental vascularization (Steingrímsson et al., 1998). Thus, the generation of tissue-specific conditional knock-out mouse models has been extremely beneficial to understand the function of TFEB in different tissues and organs.

In the liver, TFEB deletion alters lipid metabolism, resulting in severe obesity (Settembre et al., 2013a, Pastore et al., 2017). In particular, TFEB was shown to control the expression of genes involved in lipid catabolic pathways, such as fatty acid oxidation and lipophagy (Settembre et al., 2013b). In the liver, TFEB was also shown to control the peroxisome proliferator-activated receptor- γ coactivator 1 α gene (*Pgc1 α*) (Settembre et al., 2013a), an important player in the maintenance of glucose, lipid and energy homeostasis (Lin et al., 2005), giving an additional evidence of TFEB involvement in liver lipid catabolism.

The role of TFEB in the liver is different, however, from its role in skeletal muscle, where TFEB was shown to modulate glucose uptake and energy balance, during physical exercise, through the activation of genes related to glucose homeostasis and mitochondrial biogenesis, independently from PGC1 α (Mansueto et al., 2017). In osteoclasts, TFEB controls bone resorption, and TFEB depletion was shown to impair osteoclast functionality and increase bone mass (Ferron, et al., 2013).

In macrophages, loss of both TFEB and TFE3 impairs the production and secretion of several pro-inflammatory cytokines and chemokines (Pastore et al., 2016), highlighting that TFEB plays an important role in the inflammatory and immune responses. It was also shown that TFEB, during infection, is activated by protein kinase D (PKD) (Najibi et al., 2016) and promotes the expression of several antimicrobial and autophagy genes that are essential for host tolerance of infection (Visvikis et al., 2014). In the immune system, TFEB depletion was also shown to affect T-cell-dependent antibody response (Huan et al., 2006) and antigen presentation by dendritic cells (Samie and Cresswell, 2015), further supporting a role for TFEB in the immune response.

In addition, specific deletion in the intestinal epithelium leads to increase epithelial cells injury and colitis (Murano et al., 2017), revealing a TFEB role also in defence against injury. Moreover, TFEB loss of function in endothelial cells showed that TFEB positively regulates angiogenesis via activation of AMPK and autophagy (Fan et al., 2018).

Interestingly, TFEB and TFE3 were also shown to control the expression of Rev-erba (NR1D1), a transcriptional repressor of the circadian clock machinery involved in the regulation of whole-body metabolism and autophagy during the diurnal light, further revealing a crosstalk between nutrients and circadian cycles (Pastore et al., 2019).

4.3 TFEB as a therapeutic target

Due to its ability to promote intracellular clearance, TFEB has emerged as an appealing therapeutic target for many human diseases associated with autophagy or lysosomal defects.

Recent studies have shown that induction of TFEB activity in cellular or mouse models of Lysosomal Storage Disorders (LSDs), a class of diseases caused by genetic defects in specific lysosomal proteins that lead to the accumulation of toxic aggregates inside the lysosomal lumen (Parenti et al., 2015), ameliorates the pathological phenotype of the diseases (Palmieri et al., 2017; Lotfi et al., 2018). Accordingly, TFEB overexpression in models of multiple sulfatase deficiency, mucopolysaccharidosis type IIIA, Batten disease, Pompe disease, Gaucher disease, Tay-Sachs disease and cystinosis, showed a beneficial effect as it promoted a strong reduction of undigested material, thus resulting in improved lysosomal function and autophagy (Medina et al., 2011; Rega et al., 2016; Song et al., 2013; Spampanato et al., 2013).

In addition to LSDs, induction of TFEB activity was also shown to be beneficial in neurodegenerative diseases, such as Parkinson's, Huntington's and Alzheimer's disease. Such diseases are characterized by toxic protein aggregation, which is often caused by or associated with autophagy or lysosomal dysfunctions (Menzies et al., 2015). In Parkinson's disease, genetic or pharmacological induction of TFEB reduces the accumulation of α -synuclein aggregates and restores proper lysosome function (Decressac et al., 2013; Dehay et al., 2010; Kilpatrick et al., 2015). Similarly, in Huntington's disease models, TFEB activation decreases protein aggregation and improves the neurological phenotype (Sardiello et al., 2009; Tsunemi et al., 2012). Finally, overexpression or activation of TFEB limits aggregation and neurodegeneration in cellular and mouse models Alzheimer's disease (Chauhan et al., 2015; Polito et al., 2014; Xiao et al., 2014, 2015).

Furthermore, other liver pathologies, such as α 1-antitrypsin deficiency and obesity, were also shown to benefit from TFEB upregulation, which resulted in enhanced autophagy (Pastore et al., 2013) or lipophagy (Settembre et al., 2013a), respectively.

Therefore, novel strategies such as pharmacological or genetic modulation of TFEB activity represent an appealing and potential therapeutic tool for a broad variety of diseases; however, due to the role of TFEB and MiT proteins in carcinogenesis, the long-term effects of such treatments require further investigation.

4.4 Regulation of TFEB activity

TFEB activity is modulated via the control of its subcellular localization. In resting conditions, TFEB is predominantly inactive and localized in the cytosol, whereas specific stimuli rapidly induce TFEB nuclear translocation and subsequent transcription of its target genes (Sardiello et al., 2009; Settembre et al., 2011).

The first evidence of stimulus-induced TFEB nucleo-cytoplasmic shuttling was obtained in cells treated with sucrose, which accumulates in lysosomes and mimics the lysosomal overload observed in lysosomal storage disorders (Sardiello et al., 2009). Other pharmacological treatments that result in lysosomal stress, such as chloroquine, bafilomycin or trehalose, also cause TFEB nuclear translocation (Roczniak-Ferguson et al., 2012; Settembre et al., 2012; Palmieri et al., 2017).

In addition to lysosomal stress, TFEB localization was shown to be highly sensitive to nutrient levels. Accordingly, nutrient deprivation causes a rapid and strong TFEB nuclear translocation, which is maximal approximately 1 h after amino acid and serum removal. In addition, nutrient refeeding of starved cells is sufficient to induce TFEB nucleus-to-cytoplasm relocalization within minutes (Settembre et al., 2011, 2012; Martina et al., 2012; Roczniak-Ferguson et al., 2012). This observation was also supported by *in vivo* studies, in which TFEB was shown to be predominantly

localized in the nucleus when mice were deprived of food for approximately 16 hours (Settembre et al., 2011; Chen et al., 2017). In addition to lysosomal stress and starvation, many other conditions have been shown to promote TFEB translocation, including infection (Visvikis et al., 2014; Campbell et al., 2015; Pastore et al., 2016), bacterial phagocytosis (Gray et al., 2016), inflammation (Pastore et al., 2016), physical exercise (Mansueto et al., 2017), mitochondrial damage (Nezich et al., 2015) and ER stress (Martina et al., 2016).

The primary mechanism by which TFEB subcellular localization is modulated within the cell is protein phosphorylation. In particular, the phosphorylation of two serine residues is crucial to determine the cytosolic localization of TFEB: when S142 (Settembre et al., 2011, 2012) and S211 (Martina et al., 2012; Roczniak-Ferguson et al., 2012; Settembre et al., 2012) are phosphorylated, TFEB is retained inactive in the cytosol. Thus, phosphorylation of S211 has been demonstrated to be responsible for the interaction with the chaperone 14-3-3, resulting in TFEB cytosolic sequestration (Martina et al., 2012; Roczniak-Ferguson et al., 2012). In particular, 14-3-3 binding has been proposed to mask the nuclear localization signal (NLS) of TFEB, thus preventing nuclear translocation (Roczniak-Ferguson et al., 2012). Accordingly, serine-to-alanine mutations of either S142 and S211 result in a constitutive nuclear and active form of TFEB (Martina et al., 2012; Roczniak-Ferguson et al., 2012; Settembre et al., 2011, 2012). A recent study also showed that phosphorylation of S142 and S211 targets TFEB to the proteasome system via the binding to the E3 ubiquitin ligase STUB1, suggesting that phosphorylation may regulate TFEB activity also by modulating its stability (Sha et al., 2017).

The main protein kinase involved in TFEB phosphorylation on S142 and S211 is mTORC1 (Martina et al., 2012; Roczniak-Ferguson et al., 2012; Settembre et al., 2012). In the presence of nutrients, mTORC1 is recruited to the lysosomal surface, where it phosphorylates TFEB and keeps it cytosolic and inactive (Fig. 4). Upon

starvation or lysosomal stress, mTORC1 is inactivated and released from the lysosomal surface to the cytosol (Sancak et al., 2010). Concomitantly, lysosomal Ca^{2+} is pumped out through the Ca^{2+} channel mucolipin 1 (MCOLN1, also known as TRPML1) and activates the calcium-dependent phosphatase calcineurin, which in turn dephosphorylates TFEB and promotes its nuclear translocation and activation (Fig. 5) (Medina et al., 2015).

The signaling pathway previously described highlights the lysosome as a central machinery that senses nutrient availability and finely coordinates the transcription of several genes important for cellular response to metabolic changes. Interestingly, there is a self-sustaining feedback mechanism by which TFEB auto-regulates many factors important for its own activity, such as v-ATPase subunits (Peña-Llopis et al., 2011) and MCOLN1 (Palmieri et al., 2011). In addition, TFEB also promotes its own transcription through a retroactive loop that recognizes the CLEAR sequences located in its promoter (Settembre et al., 2013a).

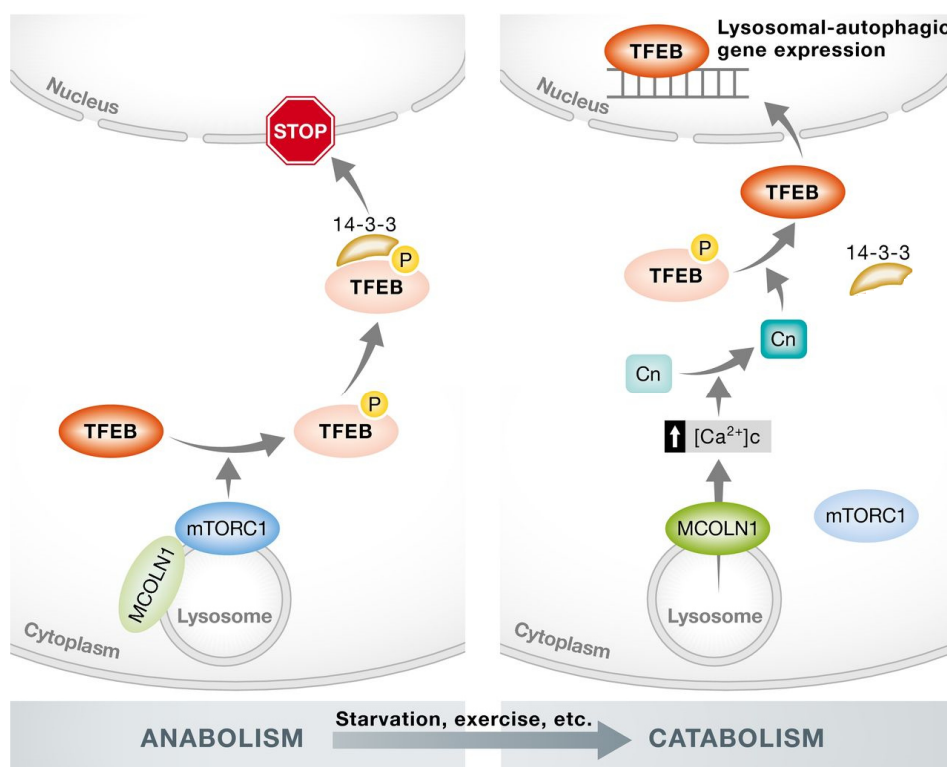


Figure 5. Model of TFEB regulation in response to nutrient availability (adapted from Ballabio, EMBO Mol. Med., 2016). In the presence of nutrients (anabolism), mTORC1 is recruited on the lysosomal membrane and mediates the phosphorylation of TFEB on S211, responsible for the binding to 14-3-3 chaperone and subsequent sequestration in the cytoplasm. During starvation or lysosomal stress or exercise (catabolism), mTORC1 is inactivated and diffused in the cytosol, whereas Ca^{2+} is released from the lysosomal lumen through MCOLN1 and activates calcineurin which in turn dephosphorylates TFEB, which is able to translocate to the nucleus where activates the transcription of lysosomal and autophagic genes.

More recently, it has been found that additional phosphorylation events play a role in the modulation of TFEB localization and other protein kinases are implicated (Fig. 6). For instance, similar to mTORC1, extracellular signal-regulated kinase 2 (ERK2) is another kinase important in cell growth that has been shown to phosphorylate TFEB on S142 (Settembre et al., 2011). Another study demonstrated that an mTOR-dependent phosphorylation occurs on S122 (Vega-Rubin-de-Celis et al., 2017). Moreover, another work showed that GSK3 β -dependent phosphorylation on S134 and S138 is also important for TFEB lysosomal localization (Li et al., 2016), although the mechanism by which these two phosphorylation sites contributed in the modulation of TFEB subcellular localization has not been elucidated. In osteoclasts, it has also been shown that upon stimulation with receptor activator of nuclear factor κB ligand (RANKL), TFEB is phosphorylated in its C-terminal region (S462, S463, S466, S467, S469) by protein kinase C β (PKC β) and this leads to stabilization and nuclear accumulation of the protein (Ferron et al., 2013). Furthermore, when amino acids are plentiful, the mitogen-activated protein kinase MAP4K3 physically interacts with TFEB and phosphorylates residue S3 (Hsu et al., 2018), which was proposed to be required for mTORC1-dependent phosphorylation on S211 (Martina and Puertollano, 2013). Finally, a recent study showed that TFEB is phosphorylated also by AKT at S467 (Palmieri et al., 2017).

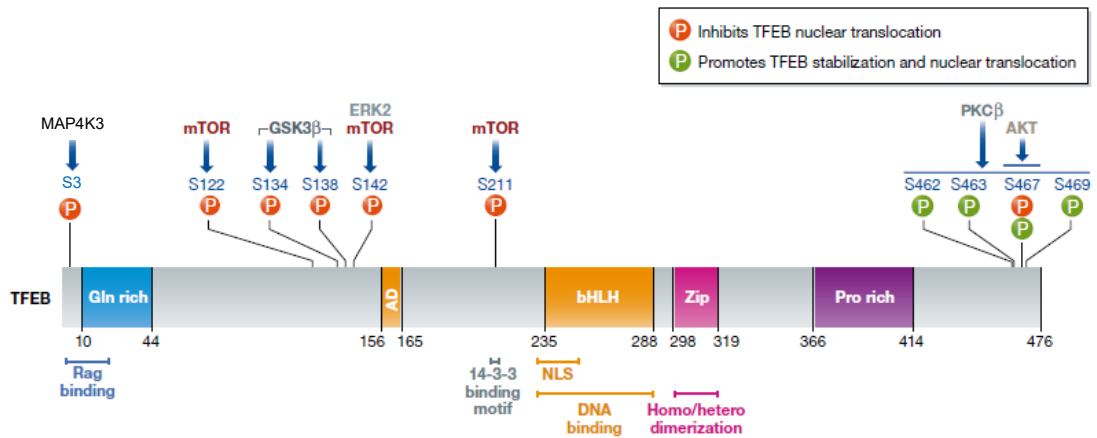


Figure 6. Relevant TFEB phosphorylation sites and their regulatory effects (adapted from Puertollano et al., EMBO J., 2018). Schematic representation of TFEB structural domains in which are indicated the most relevant phosphorylation sites and the major kinases involved. In red, phosphorylation sites that prevent TFEB nuclear translocation; in green, phosphorylation sites that control TFEB stabilization and promote its translocation.

Interestingly, other MiT/TFE proteins have been shown to be modulated similarly to TFEB. For example, TFE3 subcellular localization is controlled by mTORC1-dependent phosphorylation and 14-3-3-mediated cytosolic sequestration (Martina et al., 2014). Similarly, mTORC1 activity also regulates the localization of various MITF isoforms (Martina and Puertollano, 2013).

5. NUCLEO-CYTOPLASMIC SHUTTLING PROTEINS

5.1 The mechanism of nucleo-cytoplasmic shuttling

The first observations indicating that proteins can shuttle continuously between the nucleus and the cytoplasm date back to the 1950s (Goldstein et al., 1958).

Transport between the nucleus and the cytoplasm occurs through the nuclear pore complex (NPC). Small molecules or proteins with a mass smaller than 40 kDa passively diffuse across the NPS; on the contrary, macromolecules require an active

transport accompanied by energy consumption (Fried and Kutay, 2003). In this case, in general the cargo protein has to contain specific signal sequences recognized by two classes of transport receptors that rapidly move the molecule across the NPC, namely importins (import receptors) and exportins (export receptors). Importin- β proteins belong to the karyopherins family and regulate, directly or through the mediation of the adaptor importin- α , the nuclear import of cargos containing a Nuclear Localization Signal (NLS). On the contrary, Exportin 1/CRM1 is a member of karyopherin- β family that specifically recognizes a leucine-rich Nuclear Export Signal (NES) and drives the exit of the cargo out of the nucleus (Sorokin et al., 2007).

NLSs can be classified into: monopartite NLSs, containing seven amino acids PKKKRKV abundant in Lys and Arg, that have been found for example in the MYC proto-oncogene (c-Myc) and nuclear factor kappa B (NF- κ B) transcription factors (Dang and Lee, 1988; Chen et al., 2007); bipartite NLSs, comprised of two clusters of basic amino acids separated by 10-12 non-conservative amino acids (Lange et al., 2010); non-classical NLSs, without any conserved amino acid disposition (Xu et al., 2010). Leucine-rich NESs have been first identified in human immunodeficiency virus (HIV) Rev protein and in cAMP-dependent protein kinase inhibitor (PKI) (Fischer et al., 1995; Wen et al., 1995). They typically contain large hydrophobic conserved residues separated by a variable number of amino acids, given by the consensus sequence L-X(2,3)-[LIVFM]-X(2,3)-L-X-[LI], where X(2,3) represents any two or three amino acids that allow to classify all the NESs into six different patterns, depending not only on the hydrophobicity of the amino acid side chain but also on the size and shape of the side chain (Kosugi et al., 2008).

The small Ras-like GTPase Ran is a crucial element in nucleo-cytoplasmic transport: it can switch between a GDP- and GTP-bound state and be recognized by importin-related family proteins, thus driving the selective binding of substrates

to the transport receptors (Sorokin et al., 2007). In fact, importins preferentially bind their cargo at low RanGTP levels, whereas exportins recruit their cargo at high RanGTP levels. To ensure an efficient transport and correct recycling of the components involved, Ran-GDP and Ran-GTP pools are asymmetrically distributed in the two compartments, respectively in the nucleus and in the cytoplasm; this gradient is maintained by the RanGTPase activating protein (RanGAP), higher in the cytoplasm, and the guanidine nucleotide exchange factor RCC1 (RanGEF), more concentrated in the nucleus (Görlich et al., 1996; Cook et al., 2007).

Thus, the canonical nucleo-cytoplasmic shuttling consists of different crucial steps (Fig. 7): first, importin- α recognizes the NLS-containing cargo protein and then dimerizes with importin- β , which in turn interacts with nucleoporins and mediates the translocation of the complex; once in the nucleus, RanGDP is converted into RanGTP by RanGEF and binds importin- β , inducing the dissociation of the complex and release of the cargo protein. During the nuclear export process, CRM1 binds RanGTP and then the NES-containing cargo, which is consequently exported through the NPC; once in the cytoplasm, RanGTP is hydrolysed into RanGDP by RanGAP and this event is responsible for the detachment of the complex and the release of the cargo (Cautain et al., 2015).

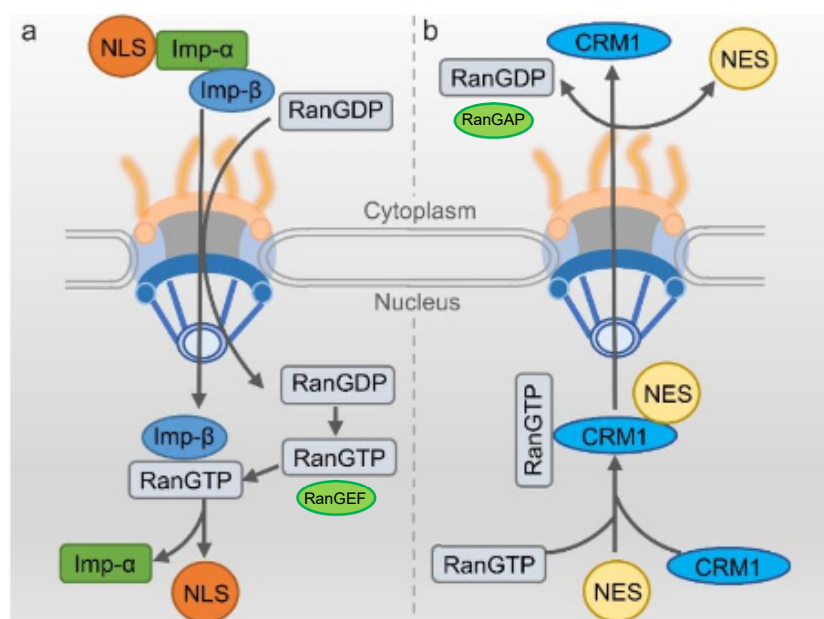


Figure 7. Classic protein nuclear transport mediated by NLS and NES sequences (adapted from Fu et al., *Int. J. Mol. Sci.*, 2018). Schematic representation of protein nucleo-cytoplasmic shuttling across the NPC. a) Importin- α binds to the NLS motif of cargo protein, and then associates with importin- β . This complex passes through the NPC and dissociates following Ran-GTP binding. The cargo is retained in the nucleus whereas importins cycle back to the cytoplasm. b) The NES sequence of the cargo protein is recognized by CRM1 which facilitates nuclear export together with Ran-GTP. Once in the cytosol, Ran-GTP is hydrolysed into Ran-GDP and the cargo is released.

AIMS OF THE STUDY

For its role in the regulation of catabolic processes, such as autophagy and lysosomal degradation, thus inducing intracellular clearance, TFEB is nowadays considered a potential therapeutic target for many human diseases. For this purpose, considerable efforts have been invested in understanding the molecular mechanism by which cytosolic TFEB undergoes nuclear translocation and activation in response to environmental stimuli. However, how TFEB is inactivated within the nucleus and relocalized to the cytoplasm remains poorly understood. In this context, the main objective of this study is to investigate the dynamics and kinetics of TFEB shuttling between the nucleus and the cytoplasm in response to different stimuli. To achieve this goal several unanswered questions have to be addressed. In particular, it would be important to uncover the mechanisms that drive TFEB nuclear export in response to nutrient availability, and to identify the regulatory sites in TFEB protein that are involved in this process. Moreover, we would like to understand how phosphorylation may contribute to the modulation of TFEB nuclear export and determine which protein kinases may support this activity. Finally, since both TFEB and mTOR functions are closely associated with lysosomes, we would like to explore whether and how lysosomal activities of mTOR impact activation and compartmentalization of TFEB.

MATERIALS AND METHODS

Cell culture conditions

HeLa cells stably expressing TFEB-GFP were previously described (Settembre et al., 2012). HEK293A and RagA/B KO HEK293A cell lines were generated by Kun-Liang Guan's laboratory (Jewell et al., 2015). Cells were cultured in the following media: HeLa (ATCC) in MEM (Cat# ECB2071L, Euroclone); HEK293A, RagA/B KO HEK293A and HeLa stably expressing TFEB-GFP in DMEM high glucose (Cat# ECM0728L, Euroclone). All media were supplemented with 10% inactivated FBS (Cat# ECS0186L, Euroclone), 2 mM glutamine (Cat# ECB3000D, Euroclone), penicillin (100 IU/mL) and streptomycin (100 µg/mL) (Cat# ECB3001D, Euroclone). All cell lines were maintained at 37 °C and 5% CO₂, tested and validated for the absence of mycoplasma.

Materials

Primary antibodies were obtained from the following sources: antibodies to human TFEB (Cat# 4240) (1:1000), Phospho-p70 S6 Kinase Thr389 (1A5) (Cat# 9206) (1:1000), p70 S6 Kinase (Cat# 9202) (1:1000), 4E-BP1 (Cat# 9644) (1:1000), Phospho-4E-BP1 Ser65 (Cat# 9456) (1:1000), mTOR (7C10) (Cat# 2983) (1:1000), Raptor (24C12) (Cat# 2280) (1:1000), were from Cell Signaling Technology; antibodies to GAPDH (6C5) (Cat# sc-32233) (1:3000), LAMP1 (H4A3) mouse (Cat# sc-20011) (1:500), were from Santa Cruz; antibody to FLAG M2 (Cat# F1804) (1:1000), CRM1 (Cat# AV40465) (1:1000), were from Sigma Aldrich; antibody to LAMP1 rabbit (Cat# ab24170) was from Abcam; antibody to TFEB-pSer142 (Cat# ABE1971) (1:15000) was from EMD-Millipore; antibodies to TFEB-pS138 (1:15000) and TFEB-pS211 (1:1000) were custom generated in collaboration with Bethyl

Laboratories. TFEB-pSer142, TFEB-pS138 and TFEB-p211 antibodies were tested for their specificity and showed marginal cross-reactivity with non-phosphorylated TFEB. These antibodies were used to study specific TFEB phosphorylation in cells overexpressing or stably-expressing TFEB, in which protein levels are sufficiently high to detect the specific signal.

Secondary antibodies were obtained from the following sources: antibodies to Mouse (Cat# 401215) and Rabbit (Cat# 401315) IgGs were from Calbiochem; Donkey anti-Rabbit IgG (H+L) Alexa Fluor 568 (Cat# A-10042), Donkey anti-Rabbit IgG (H+L) Alexa Fluor 594 (Cat# A-21207), Donkey anti-mouse IgG (H+L) Alexa Fluor 568 Alexa Fluor 647 (Cat# A-31571), Donkey anti-mouse IgG (H+L) Alexa Fluor 594 (Cat# A-21203), Donkey anti-mouse IgG (H+L) Alexa Fluor 488 (Cat# A-21202) were from Thermo Fisher Scientific.

Chemicals were obtained from the following sources: Torin1 (Cat# 4247) was from Tocris; Leptomycin B (Cat# L2913) and Protease Inhibitor Cocktail (Cat# P8340) were from Sigma-Aldrich; PhosSTOP phosphatase inhibitor cocktail tablets (Cat# 04906837001) was from Roche.

Plasmids

Human full-length pEGFPN1-TFEB-GFP WT plasmid was previously described (Settembre et al., 2011). Human TFEB S138A-GFP was a kind gift of Chonglin Yang (Chinese Academy of Sciences, China). The lentiviral plasmid pLJM60-S6K1 (wt) barcoded (here reported as wt S6K) was purchased from Addgene (Cat# 48801). The human LAMP1-mGFP plasmid was purchased from Addgene (Cat# 34831). Human TFEB S142A-GFP, TFEB S211A-GFP, TFEB S142A/211A-GFP, TFEB M144A-GFP, TFEB L147A-GFP, and TFEB I149A-GFP were generated using QuikChange II-XL Site-Directed Mutagenesis Kit (Cat# 200522, Agilent Technologies).

To generate Lamtor1(1-39)-TFEB-GFP (Lys-TFEB) and Lamtor1(1-39)-FLAG-S6K (Lys-S6K) fusion constructs, we used a cloning strategy previously described to anchor proteins at the lysosomal membrane (Amick et al., 2018). The fragment containing the first 39 amino acids of Lamtor1 was amplified by PCR and fused to the N-terminus of linearized TFEB-GFP WT and pLJM60-S6K wt vectors, respectively, by using In-Fusion HD Cloning Plus Kit (Cat# 638911, Takara). Lys-S6K TOS-mutant (F5A) was mutagenized by using QuikChange II-XL Site-Directed Mutagenesis Kit. Oligonucleotide primer sequences used to generate these plasmids were designed by using the SnapGene software version 4.1.3. Insert primers were created with 18-bp extensions at their ends complementary to the linearized vector ends.

For Lys-TFEB: pEGFPN1-LAMTOR1_fw (ATTAAGCTTGCGGCCGCGATGGGGT GCTGCTACAGC), linker-LAMTOR1_rv (GACCGGTCCAGACCCTGAGTTGGGCT CGGCTCC), pEGFPN1_rv (CGCGGCCGCAAGC), linker-pEGFPN1_fw (TCAGGG TCTGGACCGGTCTG).

For Lys-S6K: pLJM60-LAMTOR1_fw (CCTTTCTCTCCACAGGTGATGGGGTGCT GCTACAGC), FLAG-linker_rv (ATCGTCATCCTTGTA GTCGGTGGCGACCGGT), pLJM60_rv (CACCTGTGGAGAGAAAGGCAAAG), FLAG-S6K_fw (GACTACAAG GATGACGATGACAAGGG).

PCR products were purified by gel extraction in 1-3% agarose gels (Cat# AS-101, Fisher Molecular Biology) using QIAquick Gel Extraction Kit (Cat# 28704, Qiagen). Plasmid DNA for transfection was isolated by using ZymoPURE II Plasmid Maxiprep Kit (Cat# D4203, Zymo Research). All the resulting plasmid DNA were verified for their sequence by Sanger sequencing.

Transfection

Cells were transfected in 10 cm dishes, 6-well dishes or 35 mm glass bottom dishes (Cat# 81156, Ibidi) using Fugene® HD Transfection Reagent (Cat# E2312, Promega). For 10 cm dishes, the following concentrations were used: 1 µg TFEB WT-GFP, 1 µg TFEB S138A-GFP, 2 µg TFEB S142A-GFP, 2.5 µg TFEB S211A-GFP, 1 µg TFEB S142/211A-GFP, 1.5 µg TFEB-M144A-GFP, 1.5 µg TFEB-L147A-GFP, 1.5 µg TFEB-I149A-GFP, 1 µg LYS-TFEB-GFP, 2 µg FLAG-S6K WT, 2 µg LYS-FLAG-S6K WT and 2 µg LYS-FLAG-S6K F5A. The total amount of transfected plasmid DNA in each transfection was normalized to 3 µg using an empty plasmid. For the other cell culture supports, transfection reactions were prepared respecting the proportions of each reagent according to Fugene protocol. Cells were analysed 24 h after transfection.

For siRNA-based experiments, cells were transfected using Lipofectamine® RNAiMAX Transfection Reagent (Cat# 13778, Invitrogen) with the indicated siRNAs (20 nM) mixed in OptiMEM (Cat# 31985062, Thermo Fischer Scientific), and analysed after 72 h. The following siRNA were used: control non-targeting siRNA Pool (Cat# D-001810-10-05), siRNA Human RPTOR (Cat# L-004107-00-0005) and siRNA Human CRM1 (#Cat L-003030-00-0005) were from Dharmacon.

Cell treatments

For amino acid starvation, cell culture plates were washed twice with PBS (Cat# ECB4004L, Euroclone) and incubated in amino acid-free RPMI (Cat# R9010-01, USBiological) supplemented with 10% dialyzed FBS (Cat# 26400044, Gibco) for 1 h. Cells were then restimulated for 30 min with 1x MEM Amino Acids Solution (50X) (Cat# 11130036, Thermo Fisher Scientific), 1x MEM Non-Essential Amino Acids Solution (100X) (Cat# 11140035, Thermo Fisher Scientific) and 2 mM glutamine resuspended in amino acid-free RPMI. Where reported, cells were

incubated with 5 nM leptomycin B or 250 nM Torin1 during amino acid restimulation. For evaluation of TFEB nuclear phosphorylation, leptomycin B (5 nM) was also used during starvation as a pre-treatment to maximize TFEB nuclear retention.

High-content analysis

HeLa TFEB-GFP cells were seeded in 96-well plates and incubated for 24 h. After incubation, cells were treated as described above, rinsed with PBS once, fixed for 10 min with 4% paraformaldehyde and stained 15 min with DAPI. At least, 10 image fields were acquired per each well of the 96-well plate by using confocal automated microscopy (Opera high content system; Perkin-Elmer). A dedicated script was developed to perform the analysis of TFEB localization on the images (Harmony and Acapella software; Perkin-Elmer). The script calculates the ratio value resulting from the average intensity of nuclear TFEB-GFP fluorescence divided by the average of the cytosolic intensity of TFEB-GFP fluorescence.

Cell lysis and western blotting

Cells were rinsed once with PBS and lysed in ice cold lysis buffer (250 mM NaCl, 1% Triton, 25 mM Hepes pH 7.4) supplemented with protease and phosphatase inhibitors. Total lysates were passed ten times through a 25-gauge needle with syringe, kept on ice for 10 min and then cleared by centrifugation at 21,000 x g at 4 °C for 10 min. Protein concentration was measured by the Bradford assay. 5-20 µg of protein samples were denatured with the addition of 6x laemmli buffer at 80° for 10 min, then resolved in MOPS buffer (50 mM MOPS, 50 mM Tris-Base, 0,1% SDS, 1 mM EDTA) by SDS-polyacrylamide gel electrophoresis on 4-12% Bis-Tris gradient gels (Cat# NP0323PK2 NuPage, Thermo Fischer Scientific) and transferred to PVDF membranes (Cat# IPVH00010, Millipore). Membranes were blocked in 5% milk (Cat#70166, Sigma-Aldrich) diluted in PBS-Tween (1X Phosphate-Buffered

Saline, 0.1% Tween[®] 20) for 1 h and hybridized overnight with the indicated primary antibodies diluted in 5% milk and PBS-T. After three washes with PBS-T of 10 min each, filters were hybridized with secondary antibodies for 1 h, then washed three times and finally analysed by immunoblotting using the ECL method with WESTAR ETA C ULTRA 2.0 (Cat# XLS075,0100, Cyanagen).

Co-immunoprecipitation assay

Transfected ATCC HeLa cells were lysed in lysis buffer (20 mM Tris-HCl pH 7.4, 150 mM NaCl, 1 mM EDTA, 1% Triton X-100) supplemented with protease and phosphatase inhibitors. Total lysates were passed ten times through a 25-gauge needle with syringe, kept on ice for 10 min and then cleared by centrifugation at 21,000 x g at 4 °C for 10 min. 1 mg of cleared HeLa extracts were incubated with 20 µl of specific anti-CRM1 antibody in a total volume of 1 ml lysis buffer in rotation at 4 °C for 1 h. Then, samples were incubated with 20 µl of Protein G-Sepharose (Cat# 101243, Thermo Fisher) in rotation at 4 °C for 30 min. Then, the resins were washed four times in PBS with 1 % Triton X-100 before the protein complexes were eluted by 10 min boiling in 6x laemmli buffer.

RNA extraction and real-time PCR

Total RNA was extracted from cellular lysates using the RNeasy Mini kit (Cat# 74104, Qiagen). cDNA was synthesized by reverse transcription of total RNA (500 ng per sample) using QuantiTect Reverse Transcription kit (Cat# 205311, Qiagen). The generated cDNA was diluted six-fold and used as a template for real-time quantitative PCR, which was performed with the LightCycler 480 SYBR Green I mix (Cat# 04 887 352 001, Roche) using the Light Cycler 96 detection system (Roche). Melting curve analyses were performed to verify the amplification specificity. The housekeeping gene HPRT1 was used as an internal control to normalize the

variability in expression levels. Relative quantification of gene expression was performed according to the $2^{-\Delta\Delta CT}$ method. The forward and reverse primers for HPRT1 were 5'-TGGCGTCGTGATTAGTGATG-3' and 5'-AACACCCTTTCCAAA TCCTCA-3' and for CRM1 were 5'-AGCAAAGAATGGCTCAAGAAGT-3' and 5'-TATTCCTTCGCACTGGTTCCT-3'.

Immunofluorescence and confocal microscopy

For HEK293A cell lines, glass coverslips were treated in advance with fibronectin bovine plasma (Cat# F1141, Sigma-Aldrich) diluted in PBS for 30 min to increase their adhesion to the surface. Cells seeded on coverslips were fixed with 4% paraformaldehyde for 10 min at room temperature, then rinsed once with PBS and mounted using VECTASHIELD® mounting medium (Cat# H-1200, Vector Laboratories) with DAPI.

When indicated, the coverslips were incubated in blocking buffer (3 % Bovine Serum Albumin and 0,02% saponin in PBS) for 45 min at room temperature, then incubated for 24 h at 4 °C with primary antibodies diluted in blocking buffer: FLAG M2 (1:500), LAMP1 mouse (1:500), LAMP1 rabbit (1:200), mTOR (1:100). Subsequently, the coverslips were washed three times with blocking buffer and incubated with Alexa-Fluor conjugated secondary antibodies diluted in blocking buffer (1:500) for 1 h at room temperature in the dark. Finally, the coverslips were washed three times with blocking buffer and mounted.

Images were analysed using LSM 700 or LSM 800 with a Plan-Apochromat ×63/1.4 NA M27 objective using immersion oil (Cat# 518F, Carl Zeiss) at room temperature. The microscopes were operated on the ZEN 2013 software platform (Carl Zeiss). Images were processed with ImageJ software (National Institute of Health). For the mTOR/LAMP1 and mTOR/Lys-S6K co-localization analysis, Mander's co-localization coefficients (MCC) were calculated using JACoP ImageJ Plugin. The

program quantifies the fraction of lysosomal puncta (LAMP1, Lys-S6K) overlapping the fraction of mTOR puncta.

FRAP, FLIP and live cell imaging experiments

For time-lapse imaging, HeLa cells stably expressing TFEB-GFP were seeded on 35 mm glass bottom dishes, starved of amino acids and then treated with complete medium until TFEB was completely cytosolic. Cells were imaged every 2 min using a LSM 880 + Airyscan systems (Carl Zeiss).

Fluorescence recovery after photobleaching (FRAP) is a technique suitable to study protein diffusion: fluorescent molecules are irreversibly photobleached in a small area of the cell, then diffusion of the surrounding non-bleached fluorescent molecules into the bleached area leads to fluorescence recovery, which is recorded during frames acquisition at low laser power. Fluorescence loss in photobleaching (FLIP) differs from FRAP for the repetitive bleaching that prevents fluorescence recovery; it is used in combination with FRAP experiments to obtain combined information regarding active or passive transport and fluxes between different compartments (Ishikawa-Ankerhold et al., 2012).

For FRAP experiments, HeLa cells stably expressing TFEB-GFP were seeded on 35 mm glass bottom dishes and starved for 1 h in HBSS (Cat# 14025092, Gibco) and 10 mM Hepes (Cat# ECM0180D, Euroclone), then medium was replaced with either starvation medium or with complete DMEM in the presence or absence of either 250 nM Torin1 or 5 nM leptomycin B for 30 min. Cells were imaged using a LSM 880 + Airyscan systems (Carl Zeiss) or a LSM 800 (Carl Zeiss) equipped with an objective heater (Okolab), detected with a 488 nm laser through a 63x oil immersion objective at 37 °C and 5% CO₂, conditions that are essential to prevent TFEB nuclear translocation induced by environmental stress. A selected region (ROI) comprising the whole cytosol was drawn and a movie was acquired. After 10

frames, cells were photobleached with three consecutive intense 488 nm pulses, each separated by three acquisition frames, and then imaged for 15 min. For FLIP experiments, the whole cytosol of the selected cell was photobleached every frame until the end of the imaging. In our short-time movies (15 min), loss of signal caused by protein degradation was excluded since it has been reported that TFEB degradation by proteasome pathway occurs with a half-life of 4-6 h in HeLa cells (Sha et al., 2017). Stress response caused by photo-toxicity was also excluded using TFEB nuclear translocation as a stress indicator (Martina et al., 2016; Brady et al., 2018): no TFEB nuclear translocation was observed in cells exposed to confocal laser light using image acquisition parameters that have been reported to produce minimal light-induced damage (Boudreau et al., 2016). Fluorescence signal associated to new TFEB protein synthesis was also excluded by observing the absence of GFP signal reappearing over time in previously photobleached cells.

For FRAP experiments with TFEB mutants, HeLa ATCC cells were transfected using a Fugene HD transfection reaction containing the following plasmids: 200 ng TFEB WT-GFP, 200 ng TFEB S138A-GFP, 400 ng TFEB S142A-GFP, 500 ng TFEB 211A-GFP, 200 ng TFEB M144A-GFP, 200 ng TFEB L147A-GFP, and 200 ng TFEB I149A-GFP, which were normalized to 1 μ g total DNA using an empty plasmid. Half of each transfection mixture was used for reverse transfection and cells were analysed 24 h after transfection.

FRAP and FLIP experiments were analysed using the ImageJ software to calculate nuclear and cytosolic intensity of TFEB-GFP signal, then the decay of nuclear intensity was calculated by dividing the nuclear intensity for the total cell fluorescence intensity (cytosolic + nuclear intensity) in each frame, starting from the first frame after photobleaching to the end of the acquisition. Then, these parameters were processed to generate a kinetic plot of photobleaching; from these data curves was possible to extract information about changes in the mobile fraction.

Statistical analysis

Data were analysed and plotted using GraphPad Prism 6.0 software. ANOVA was used when comparing more than two groups. ANOVA assumes that the data are normally distributed and the variances across groups are homogeneous: we used the Levene's test to check the homogeneity of variances and we applied the Shapiro-Wilk test on the ANOVA residuals to verify that normality is not violated. A non-parametric alternative to ANOVA test was used when data were not normally distributed. For co-localization analysis, after the ANOVA test, error bars and mean comparison p -values were calculated by using a t-test method (or Wilcoxon test method for non-parametric data). We used the following convention for symbols indicating statistical significance: * $p \leq 0.05$, ** $p \leq 0.01$, *** $p \leq 0.001$, **** $p \leq 0.0001$.

RESULTS

1. TFEB continuously shuttles between the cytosol and the nucleus through the activity of exportin CRM1

Nutrient deprivation is known to induce TFEB nuclear translocation and consequent transcriptional activation (Medina et al., 2015). However, how TFEB is inactivated upon nutrient refeeding and the mechanism of TFEB cytosolic redistribution remained unclear. By monitoring TFEB cellular distribution in time-lapse imaging experiments of cells stably expressing TFEB-GFP, we observed that during nutrient refeeding TFEB rapidly redistributed from the nucleus to the cytoplasm within 20 min (Fig. 8), suggesting an active nuclear export in response to nutrient stimulation.

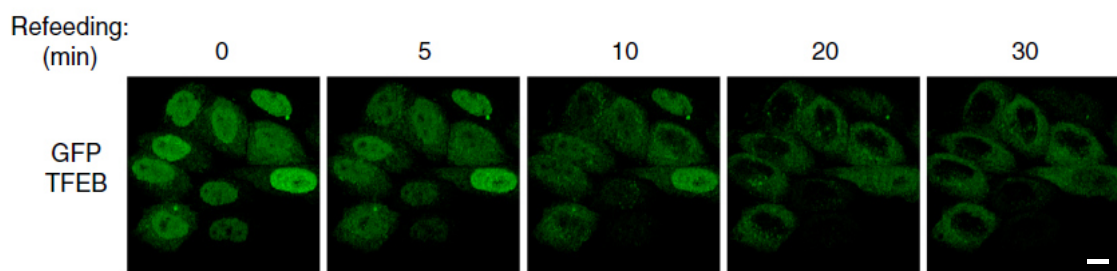


Figure 8. Time-lapse imaging of TFEB localization upon nutrient refeeding. Time-lapse analysis of HeLa cells stably expressing TFEB-GFP. Cells were starved for 1 h and then restimulated with nutrients until TFEB was completely cytosolic. Each panel represents a selected frame at the indicated time points using the ImageJ software. Scale bar: 10 μ m.

Interestingly, a recent interactome analysis identified TFEB as a strong interacting protein of the exportin CRM1 (Kirli et al., 2015). In order to investigate the involvement of CRM1 during TFEB nuclear export, we treated cells with leptomycin B (LMB), a specific CRM1 inhibitor that competes for the interaction between the cargo protein and CRM1, thus blocking the nuclear export mechanism

(Fukuda et al., 1997). Interestingly, LMB caused an impairment in TFEB nuclear export even under nutrient replenishment, showing a predominant nuclear localization similarly to starved conditions (Fig. 9). We also measured the ratio between nuclear and cytosolic TFEB fluorescence intensity in TFEB-GFP-expressing HeLa cells analysed by automated high-content imaging, resulting in a strong impairment in TFEB nuclear export following LMB treatment compared to control cells (Fig. 10). These data suggest that TFEB nuclear export is mediated by CRM1 activity.

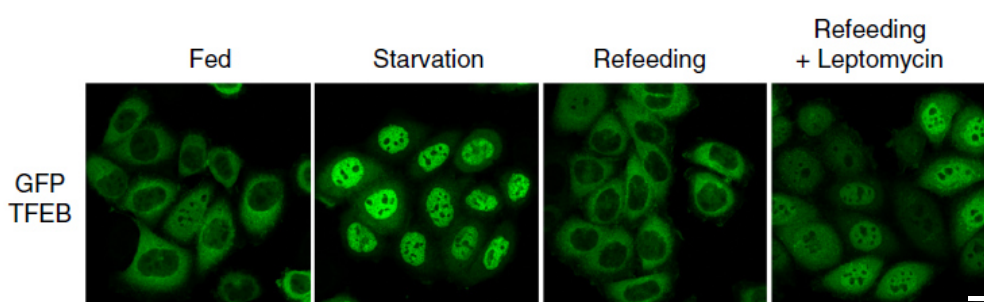


Figure 9. TFEB nuclear export impairment following leptomycin B treatment. HeLa cells stably expressing TFEB-GFP were left untreated (fed), starved for amino acids for 1 h (starvation), restimulated with amino acids for 30 min in the absence of drugs (refeeding) or in the presence of the CRM1 inhibitor leptomycin B (5 nM). Cells were analysed by confocal microscopy. Scale bar: 10 μ m.

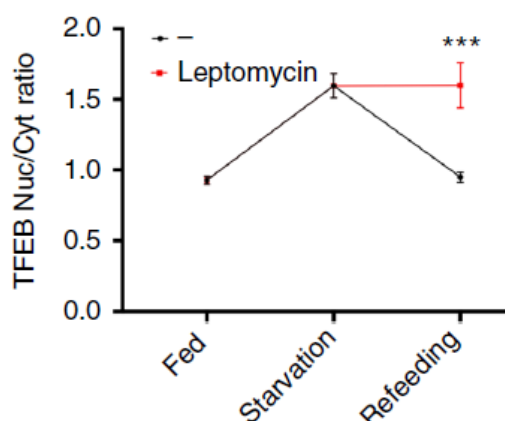


Figure 10. TFEB nucleo/cytoplasmic ratio in cells analysed by high-content imaging. HeLa cells stably expressing TFEB-GFP were plated in 96-well plate and left untreated (fed), starved for 1 h (starvation) or restimulated for 30 min (refeeding) in the absence or presence of leptomycin B

(5 nM). Cells were analysed by automated high-content imaging and calculated for the ratio between nuclear/cytosolic TFEB. Each dot represents the average of nucleo/cytoplasmic TFEB fluorescence intensity ratio analysed in several hundred cells from three different wells. Results are mean \pm SEM. $n > 1500$ cells per condition. *** $P \leq 0.001$, two-way ANOVA.

Accordingly, silencing of CRM1 in HeLa cells (Fig. 11) was able to affect TFEB cytosolic relocalization upon nutrient refeeding (Fig. 12), supporting the importance of this transporter during TFEB nuclear export.

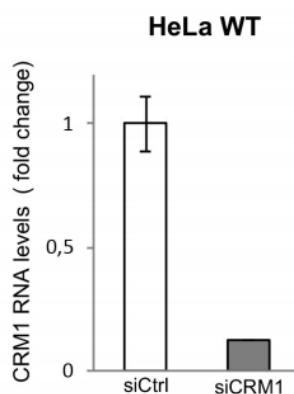


Figure 11. CRM1 RNA expression levels in silenced HeLa cells. RT-qPCR showing CRM1 knockdown efficiency in HeLa cells. HeLa cells were transfected with a siRNA specific for CRM1 (siCRM1) or with a control siRNA (siCtrl), both at 10 nM concentration. Gene expression was normalized relative to housekeeping gene HPRT1. Results are mean \pm SEM.

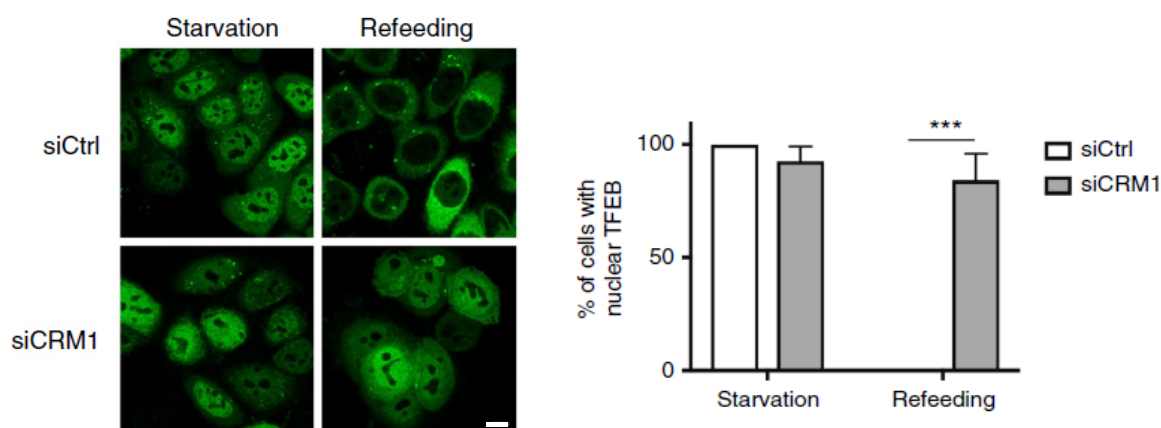


Figure 12. CRM1 depletion impairs TFEB nuclear export. HeLa cells stably expressing TFEB-GFP were transfected with a siRNA specific for CRM1 (siCRM1) or with a control siRNA (siCtrl), both at 10 nM concentration. Cells were either starved for 1 h or restimulated after starvation with amino acids for 30 min. Images were collected by confocal microscopy analysis (on the left). Then, we

calculated the percentage of cells showing nuclear TFEB localization (on the right). $n > 30$ cells per condition. Results are mean \pm SEM. *** $P \leq 0.001$, two-way ANOVA. Scale bar: 10 μ m.

Unexpectedly, leptomycin B treatment in fed cells, which show a predominant cytosolic TFEB localization (Martina et al., 2012, Settembre et al., 2012), was sufficient to promote a progressive TFEB nuclear accumulation within 30 min (Fig. 13), indicating a continuous shuttling between the cytosol and the nucleus for TFEB, even in basal conditions. Hence, TFEB distribution is more dynamic than what was commonly believed.

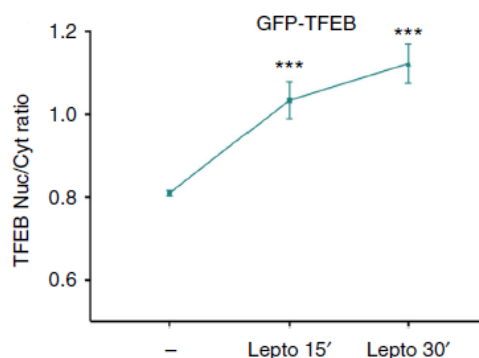


Figure 13. TFEB nuclear accumulation induced by leptomycin B treatment. In fed condition, HeLa cells stably expressing TFEB-GFP were treated with leptomycin B (5 nM) for the indicated time points and analysed for TFEB subcellular localization (nucleus/cytoplasm ratio) by high-content imaging. Results are mean \pm SEM. $n > 1200$ cells per condition. *** $P \leq 0.001$, one-way ANOVA.

2. TFEB cytosolic relocation is controlled by a nuclear export signal

Next, we decided to investigate the presence of a nuclear export signal (NES) in TFEB that could explain its recognition by the CRM1 transport system.

By a comparative analysis of intra-family (Fig. 14) and cross-species (Fig. 15) sequence alignments, we found the presence of four highly conserved hydrophobic residues in the N-terminal portion of TFEB, namely P140, M144, L147 and I149, which resembled class 1a of NES consensus patterns $\Phi 1X_3\Phi 2X_2\Phi 3X_1\Phi 4$ (Kosugi

et al., 2008), thus indicating the presence of a NES signal in TFEB, which was evolutionary conserved among the MiT/TFE transcription factors, except for TFEC which did not show in the alignment the same conserved residues.

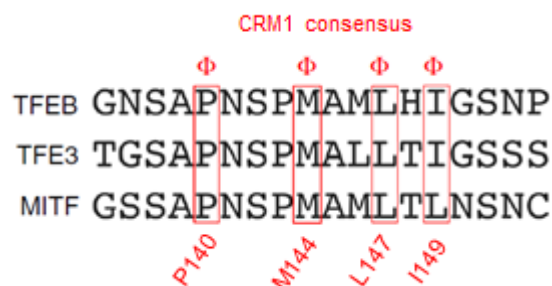


Figure 14. CRM1 consensus motif conserved among MiT/TFE members. Intra-family sequence alignment, elaborated with Clustal Omega online tool, highlighting in red four hydrophobic residues highly conserved in TFEB, TFE3 and MITF transcription factors, representing a conserved nuclear export signal (NES).

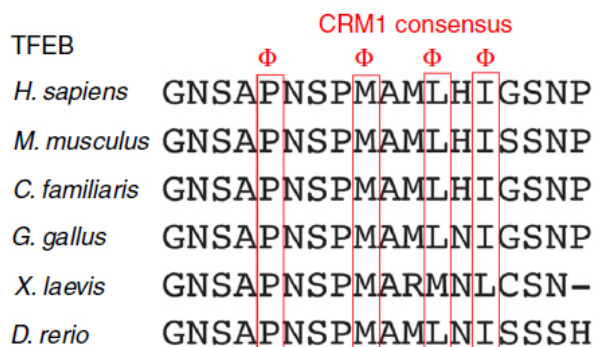


Figure 15. TFEB CRM1 consensus motif conserved among different species. Cross-species sequence alignment, elaborated with Clustal Omega online tool, showing similarities in the N-terminus of TFEB protein from different species. In red, are highlighted conserved hydrophobic residues conform to the consensus NES sequence.

To verify the role of the putative NES consensus sequence identified, we mutagenized the key residues M144, L147, and I149 into alanine and tested their effect on TFEB localization. Strikingly, each of the mutants generated, namely TFEB-M144A, TFEB-I146A and TFEB-L147A, showed severely impaired nuclear export kinetics of TFEB upon nutrient refeeding (Fig. 16), supporting a role for the CRM1 consensus sequence in TFEB nuclear export.

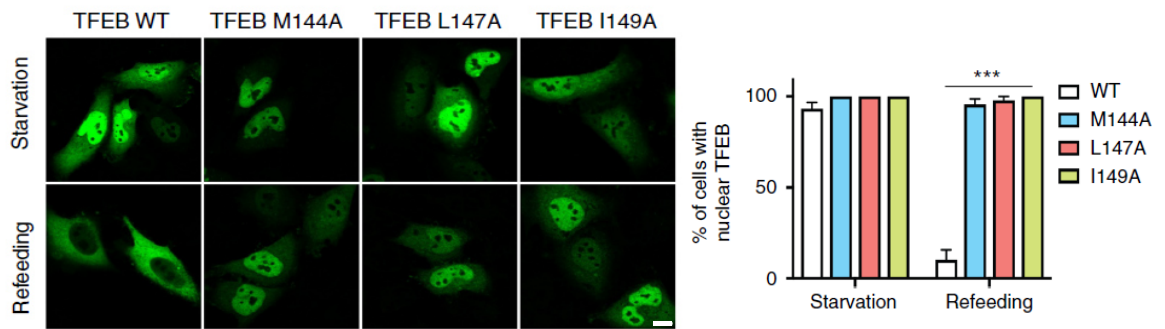


Figure 16. TFEB distribution in nuclear export signal (NES) mutants. HeLa cells were transfected with 200 ng of TFEB-GFP WT or TFEB-GFP NES-mutants (M144A, L147A, I149A) for 24 h. Then cells were treated with amino acid starvation (1 h) or starvation followed by 30 min of refeeding, and analysed by confocal microscopy (on the left). Then, we calculated the percentage of cells showing nuclear TFEB localization (on the right). $n > 20$ cells per condition. Results are mean \pm SEM. *** $P \leq 0.001$, two-way ANOVA. Scale bar: 10 μ m.

In order to assess the nucleo-cytoplasmic shuttling dynamics of these mutants and further validate this point, we performed fluorescence recovery after photobleaching (FRAP) experiments, a live imaging technique that allows monitoring of the mobility of GFP-tagged proteins within selected cells by measuring the fluorescence recovery rate of the tagged protein into a previously bleached region of interest. In our experiments, conducted under experimental conditions that mostly exclude variations due to protein degradation, protein synthesis and photobleaching-induced stress (see Materials and Methods), we measured the intensity of cytosolic/nuclear TFEB-GFP signal after cytosolic photobleaching over time (Fig. 17), in cells transfected with wild-type or NES-mutants TFEB-GFP.

Fluorescence recovery after photobleaching (FRAP)

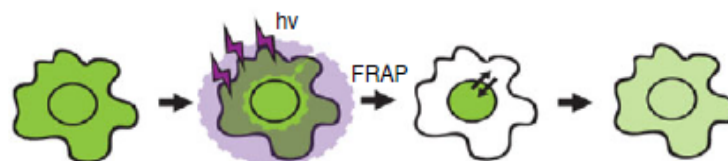


Figure 17. Fluorescence recovery after photobleaching (FRAP). Schematic experimental model that shows the FRAP technique applied to HeLa cells expressing GFP-tagged TFEB.

Consistently, we found that the nuclear export kinetics of M144A-, I146A- and L147A-TFEB-GFP mutants were drastically impaired compared to the wild-type protein, showing a permanent nuclear TFEB localization over time (Fig. 18). These data further indicated that NES-mediated CRM1-dependent nuclear export of TFEB is essential for its proper cytosolic relocalization in response to nutrient availability.

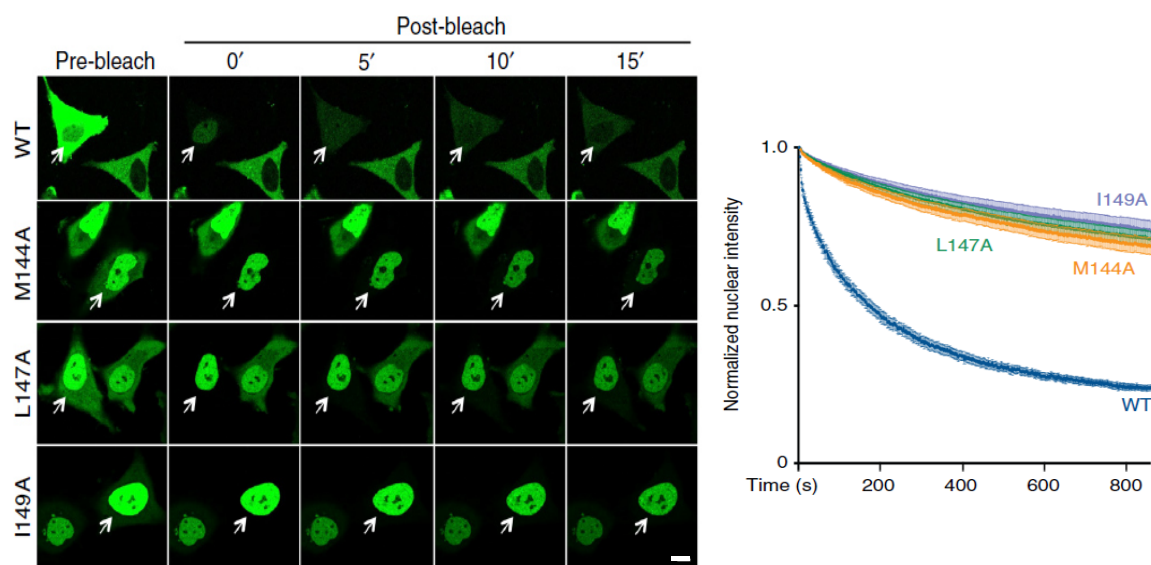


Figure 18. Analysis of TFEB NES-mutants export kinetics by FRAP. Representative time-lapse images, selected at the indicated time points by using ImageJ software, of HeLa cells transfected with wild-type TFEB-GFP or with TFEB-GFP mutants M144A, L147A, and I149A. 24 h after transfection, cells were imaged upon cytosolic photobleaching (on the left). Cells were then analysed and plotted for the decay in TFEB nuclear fluorescence (on the right). Results are mean \pm SEM. $n > 12$ cells per condition. Scale bar: 10 μ m.

3. TFEB nuclear export kinetics are modulated by nutrients

Next, in order to analyse TFEB export kinetics in response to nutrient availability, we performed FRAP experiments by photobleaching the cytosolic GFP signal in HeLa cells stably expressing TFEB-GFP under different nutrient conditions.

Under refeeding conditions, as expected, we observed a significant loss of TFEB nuclear signal and a rapid recovery of the cytosolic signal in response to amino acids supply (Fig. 19). Interestingly, under starvation conditions, upon photobleaching of cytosolic TFEB-GFP signal, a consistent fraction of nuclear TFEB relocalized to the cytosol as well (Fig. 20), supporting the idea of a continuous TFEB nucleo-cytoplasmic shuttling both in the presence or absence of nutrients. Notably, in both experimental conditions, the treatment with Torin1, a potent and selective ATP-competitive inhibitor of mTOR (Liu et al., 2010), was able to block TFEB nucleus-to-cytoplasm shuttling similarly to leptomycin B treatment, suggesting an mTOR activity during TFEB nuclear export (Fig. 19, Fig. 20). These results indicated a highly dynamic subcellular distribution of TFEB and suggested that the nuclear or cytosolic detection of TFEB is actually determined by both nuclear import and export rates, whose kinetics are influenced by nutrient levels and mTOR activity.

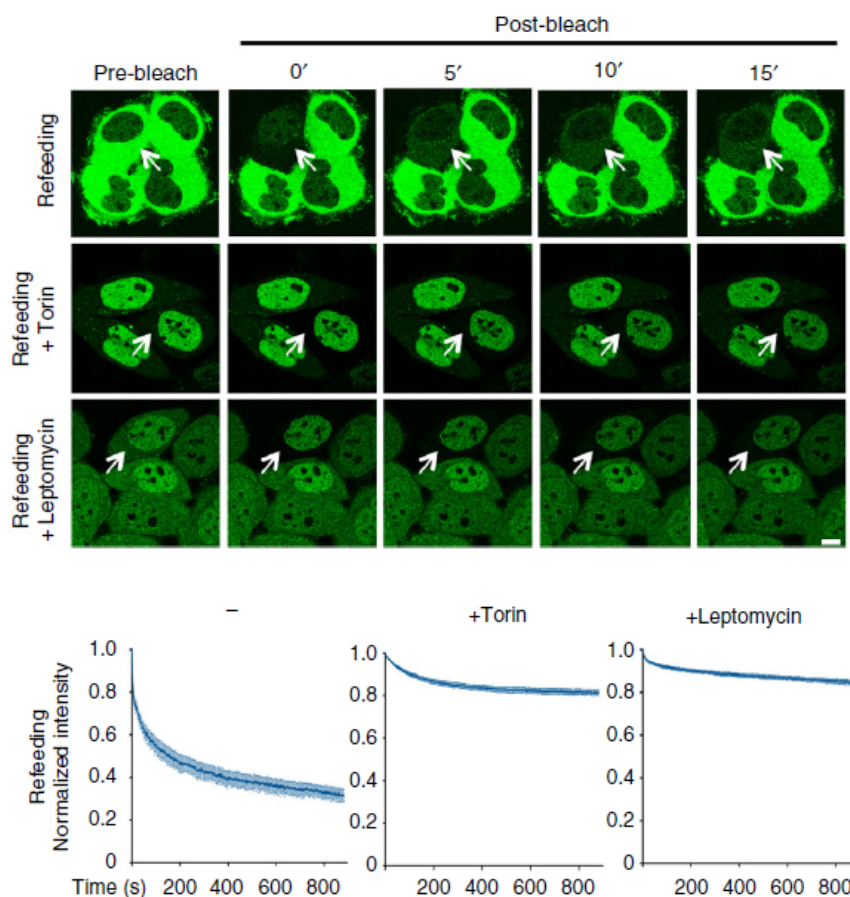


Figure 19. Analysis of TFEB export kinetics in the presence of nutrients by FRAP.

Representative time-lapse images, selected at the indicated time points by using ImageJ software, of HeLa cells stably expressing TFEB-GFP upon cytosol photobleaching (on the top). Cells were starved for 1 h and treated in refeeding condition in the absence or presence of Torin1 (250 nM) or leptomycin B (5 nM). Cells were analysed and plotted for the decay of TFEB nuclear fluorescence using ImageJ software (on the bottom). $n > 6$ cells per condition. Results are mean \pm SEM.

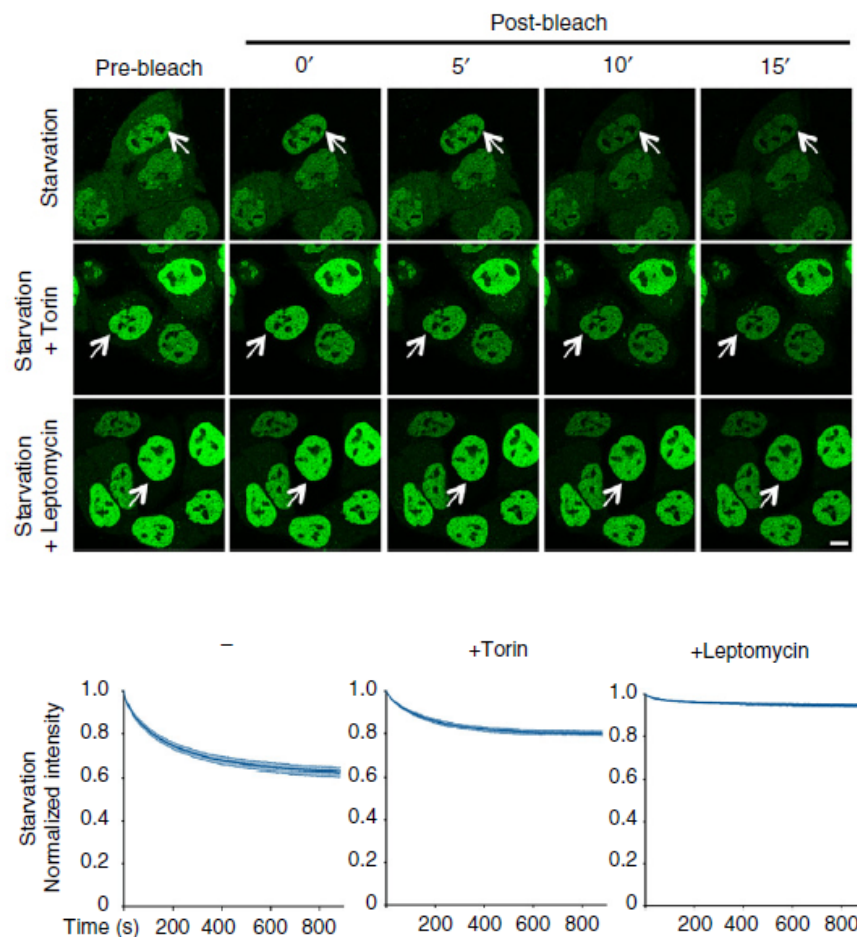


Figure 20. Analysis of TFEB export kinetics in the absence of nutrients by FRAP.

Representative time-lapse images, selected at the indicated time points by using ImageJ software, of HeLa cells stably expressing TFEB-GFP upon cytosol photobleaching (on the top). Cells were starved for 1 h and treated in the absence or presence of Torin1 (250 nM) or leptomycin B (5 nM). Cells were analysed and plotted for the decay of TFEB nuclear fluorescence using ImageJ software (on the bottom). $n > 6$ cells per condition. Results are mean \pm SEM. Scale bars: 10 μ m.

To directly estimate the nuclear export kinetics in response to nutrient availability, we performed fluorescence loss in photobleaching (FLIP) experiments in which

HeLa cells stably expressing GFP-tagged TFEB were continuously photobleached in the cytosolic fraction (Fig. 21) and then, the loss of nuclear signal was quantified over time as a measure of the relative nuclear export rate in the presence or absence of nutrients.

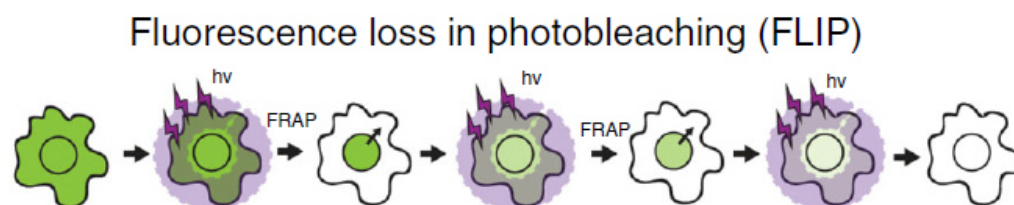


Figure 21. Fluorescence loss in photobleaching (FLIP). Schematic experimental model that shows the FLIP technique applied to TFEB-GFP-expressing HeLa cells.

In line with FRAP experiments, we observed that TFEB is rapidly exported during refeeding condition, as indicated by the faster loss of nuclear signal within 5 min, whereas during starvation the decay in nuclear fluorescence occurs with slower dynamics (Fig. 22).

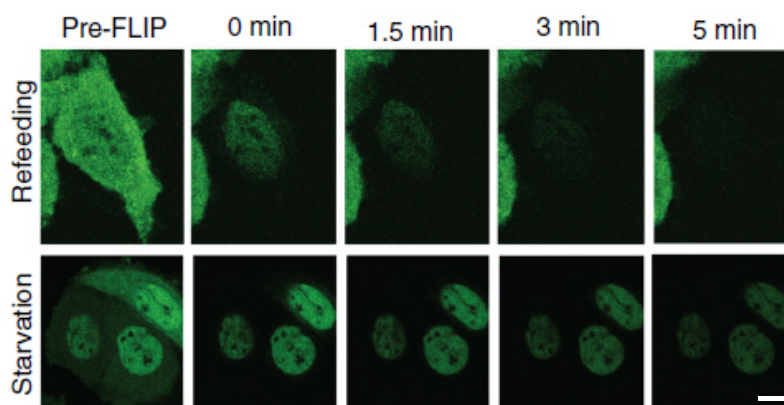


Figure 22. Analysis of nuclear export kinetics in response to nutrient availability by FLIP. Representative time-lapse images, selected at the indicated time points by using ImageJ software, of HeLa cells stably expressing TFEB-GFP upon multiple cytosolic photobleaching events. Cells were treated in starvation or refeeding conditions and images were acquired until the fluorescence signal was completely lost. Scale bar: 10 μ m.

Interestingly, our measurements followed a bi-exponential fitting, indicating the presence of two different nuclear pools of TFEB that are exported at different rates. In particular, the decay curve showed specific time constants of the two pools that were $T_{\text{slow}} = 216$ s and $T_{\text{fast}} = 70$ s. These constants did not change during starvation and refeeding, however the relative amounts of slow and fast populations in each condition were different: under refeeding 80% of nuclear TFEB consisted of fast population and only 20% of slow population, whereas under starvation 35% of nuclear TFEB comprised the fast population and 65% the slow population (Fig. 23). These results indicated that nutrients promote faster TFEB export kinetics, responsible for the predominant cytosolic detection of TFEB, and suggested that the two different pools exported at different rates may represent the two phosphorylated and non-phosphorylated forms of TFEB.

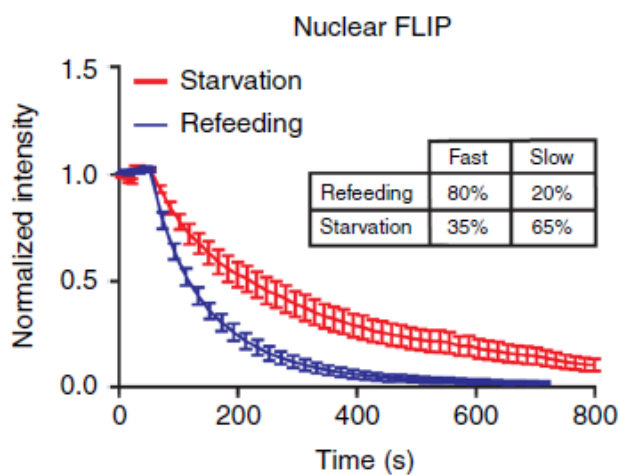


Figure 23. TFEB nuclear fluorescence decay measured by FLIP in response to nutrients. Cells treated and imaged by FLIP (Fig. 22) were analysed and plotted for decay in TFEB nuclear fluorescence. The intensity values were normalized by dividing each measurement for the starting nuclear fluorescence value before the first photobleaching event. The table shows the percentages in fast and slow TFEB populations for each condition. Results are mean \pm SEM.

4. TFEB nuclear export is controlled by hierarchical phosphorylation

The newly identified TFEB NES sequence is located in close proximity to the phosphorylation residues S142 and S138 (Fig. 14, Fig. 15), which are important for TFEB cytosolic localization (Settembre et al., 2011; Li et al., 2016), but whose functional role was still unknown and to be defined.

Hence, we hypothesized that phosphorylation on these residues could be important for proper TFEB nuclear export. To test this, we decided to analyse the nucleocytoplasmic shuttling dynamics of TFEB mutants in which residues S142 and S138 were mutated into alanine (S142A and S138A), which show a predominantly nuclear localization (Settembre et al., 2011; Li et al., 2016). In addition, we also used a serine-to-alanine TFEB mutant of the S211 phosphorylation site (S211A), which was proposed to serve as a 14-3-3 binding site responsible for TFEB cytosolic retention (Martina et al., 2012; Roczniak-Ferguson et al., 2012; Settembre et al., 2012). Thus, we performed FRAP experiments to monitor nuclear export rates of wild-type or mutant TFEB. Remarkably, TFEB mutants S142A and S138A showed a drastic impairment in TFEB cytosolic redistribution, as only 20% and 30% of the TFEB-GFP phosphorylation mutants redistributed to the cytosol, respectively. By contrast, the mutant S211A was exported out from the nucleus much more efficiently than S142A and S138A (60-70% of S211A-TFEB redistributed to the cytosol), showing only a marginal impairment compared to wild-type TFEB (Fig. 24), which was consistent with a role of this phosphorylation site in TFEB cytosolic retention (Martina et al., 2012; Roczniak-Ferguson et al., 2012). In summary, this experiment suggested that phosphorylation of S142 and S138 is necessary for TFEB nuclear export.

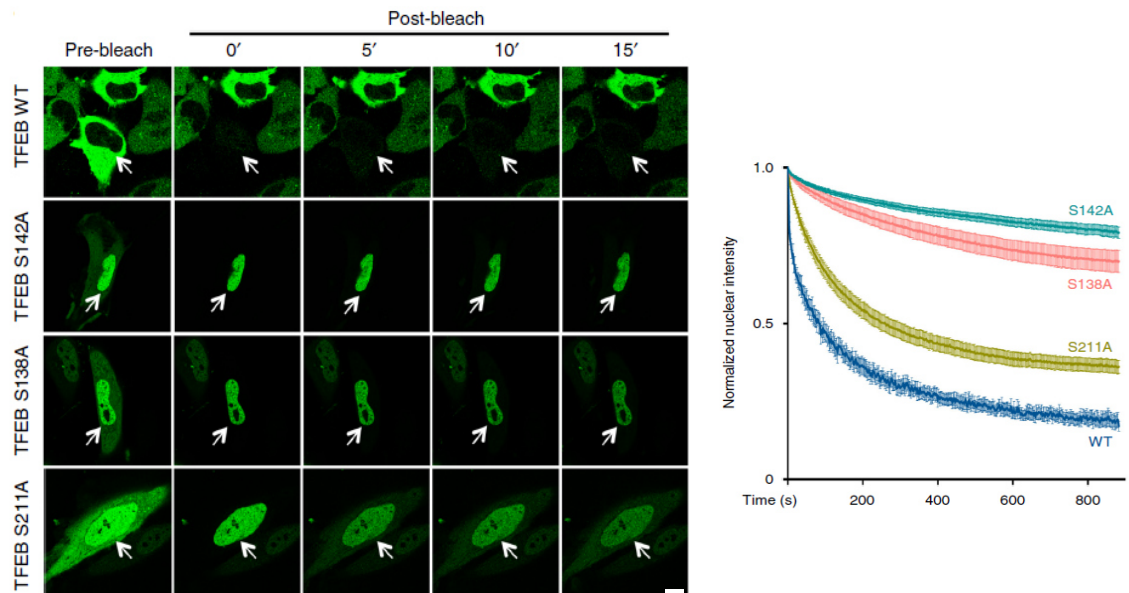


Figure 24. Nuclear export kinetics of constitutive nuclear TFEB forms analysed by FRAP.

Representative time-lapse images, selected at the indicated time points by using ImageJ software, of HeLa cells transfected with wild-type TFEB-GFP or with constitutive nuclear TFEB mutants S142A, S138A and S211A. 24 h after transfection, cells were imaged by FRAP (on the left). Cells were then analysed and plotted for the decay in TFEB nuclear fluorescence (on the right). Results are mean \pm SEM. $n > 7$ cells per condition. Scale bar: 10 μ m.

Next, in order to study the phosphorylation status of these TFEB mutants, we used specific phospho-antibodies that recognize phospho-S142, phospho-S138 and phospho-S211 residues. Interestingly, we found that TFEB S142A mutant was strongly dephosphorylated on all the residues tested. Moreover, the S138A mutant was phosphorylated only on S142, whereas S211 phosphorylation was impaired. Finally, TFEB S211A, the only mutant that can be exported out of the nucleus (Fig. 24), was normally phosphorylated on both S142 and S138 residues, whereas the phosphorylation on mutated S211 was impaired, as expected (Fig. 25). These data suggested that TFEB is finely regulated by a hierarchical phosphorylation pattern in which phosphorylation of S142 acts as a priming event for subsequent S138 phosphorylation, required then for S211 phosphorylation, necessary for TFEB cytosolic sequestration.

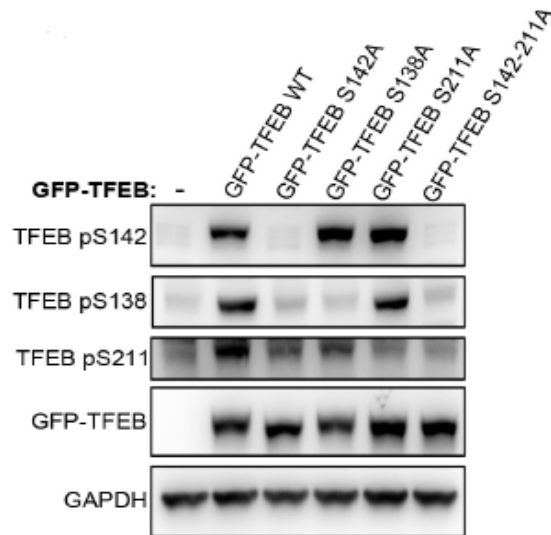


Figure 25. Hierarchical phosphorylation pattern of TFEB analysed with specific phospho-antibodies. Immuno-blotting analysis of HeLa cells transfected with either wild-type or serine-to-alanine TFEB mutants (S142A, S138A, S211A). Double mutant S142-211A was used as a negative control as a completely TFEB dephosphorylated form. After 24 h, lysates were evaluated for TFEB phosphorylation by using the specific phospho-antibodies indicated in the blot. The blot is representative of three independent experiments.

5. TFEB undergoes mTOR-dependent nuclear phosphorylation

It was described that, in response to starvation or stress conditions, TFEB is dephosphorylated by calcineurin and imported into the nucleus (Medina et al., 2015). Interestingly, we demonstrated that phosphorylation, specifically on S138 and S142, is also important to induce TFEB nuclear export (Fig. 24). These observations suggested the possibility that phosphorylation on these residues could occur in the nucleus. Moreover, our data showing that TFEB nuclear export is inhibited by Torin1 treatment (Fig. 19, Fig. 20) suggested that mTOR activity is required for TFEB nuclear phosphorylation.

To test this hypothesis, we treated TFEB-GFP-expressing HeLa cells with leptomycin B, which causes TFEB retention in the nucleus (Fig. 26), and then analysed the phosphorylation status of nuclear TFEB with specific phospho-antibodies. As expected, TFEB was strongly dephosphorylated in starved cells

(Fig. 27). Strikingly, amino acid replenishment caused a rapid TFEB S138 and S142 re-phosphorylation, both in the presence or absence of leptomycin B (Fig. 27), indicating that phosphorylation of these residues occurs in the nucleus. Interestingly, the addition of Torin1 to LMB-treated cells strongly abolished the phosphorylation on these residues (Fig. 27), indicating that mTOR activity is required for TFEB nuclear phosphorylation.

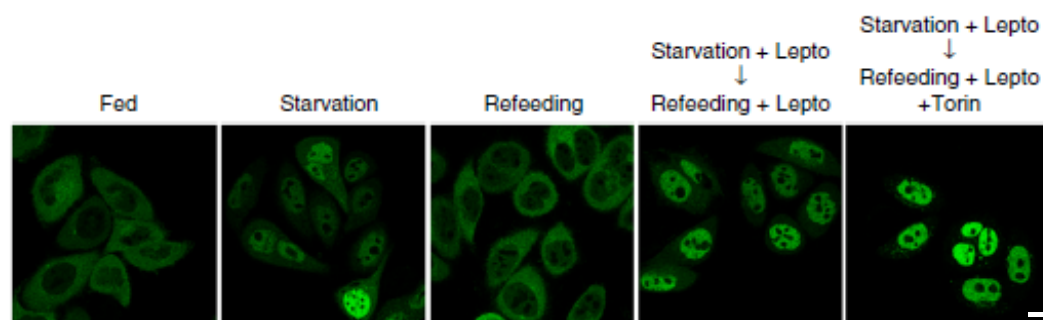


Figure 26. TFEB localization under leptomycin B and Torin1 treatment. Representative immunofluorescence images analysed by confocal microscopy showing TFEB localization in HeLa cells stably expressing TFEB-GFP that were left untreated, starved for 1 h or fed again with amino acids for 30 min. When indicated, cells were pre-treated with leptomycin B (5 nM) during starvation, prior to refeeding with or without the addition of leptomycin B or Torin1 (250 nM). Scale bar: 10 μ m.

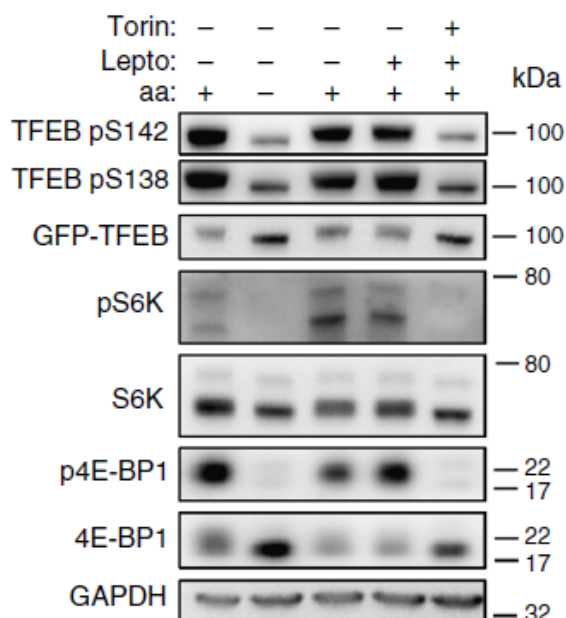


Figure 27. TFEB phosphorylation under leptomycin B and Torin1 treatment. Representative blot of three independent experiments showing the western blotting analysis of HeLa cells stably expressing TFEB-GFP treated as reported in Fig. 26. They were evaluated for TFEB phosphorylation

on S142 and S138 by using specific phospho-antibodies. pS6K and p4E-BP1 canonical targets were used as a control for mTOR activity. GAPDH was used as a loading control.

Consistently, the TFEB NES-mutant M144A, which showed a constitutively nuclear localization under starvation and refeeding conditions (Fig. 16), showed an efficient nutrient-dependent phosphorylation of S142 and S138 (Fig. 28), similarly to wild-type protein, supporting the notion that these residues are phosphorylated in the nuclear compartment.

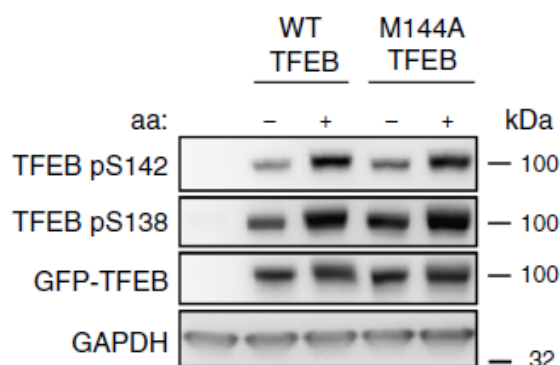


Figure 28. Nutrient-dependent phosphorylation of TFEB NES-mutant M144A. HeLa cells were transfected with wild-type TFEB or M144A mutant for 24 h. Cells were then starved for 1 h or starved and restimulated with nutrients for 30 min. Then, cell extracts were analysed by western blotting with the indicated antibodies. The blot is representative of three independent experiments.

6. Phosphorylation on S142 and S138 is crucial for the interaction between TFEB and CRM1

Next, we sought to identify the mechanism by which phosphorylation on S142 and S138 promotes TFEB nuclear export. Therefore, considering that fall within a CRM1 consensus sequence (Fig. 14, Fig. 15), we decided to verify whether S142 and S138 phosphorylation could influence the interaction between TFEB and CRM1.

Thus, in collaboration with Antoni Wiedlocha from University of Oslo, we performed co-IP experiments to pull down CRM1 in cells transfected with the different TFEB mutants described above. Importantly, we found that CRM1 interacted with wild-

type TFEB, as previously observed (Kirli et al., 2015), in a leptomycin-sensitive manner (Fig. 29). Strikingly, however, S142A and S138A mutations drastically affected such binding (Fig. 29), suggesting that phosphorylation of these residues is required for TFEB interaction with CRM1. In addition, the mutant S211A, which showed efficient S142 and S138 phosphorylation (Fig. 25), still retained its ability to interact with CRM1 (Fig. 29). Finally, consistent with our previous observations showing that TFEB nuclear export was affected by mTOR inhibition (Fig. 19, Fig. 20), the interaction between wild-type TFEB and CRM1 was heavily impaired upon Torin1 treatment (Fig. 29). These data, together with other data showing an mTOR- and nutrient-dependent TFEB nucleo-cytoplasmic shuttling, supported the hypothesis that the mTOR-dependent S142 and S138 TFEB phosphorylation induces nuclear export of TFEB by promoting its interaction with the transporter CRM1.

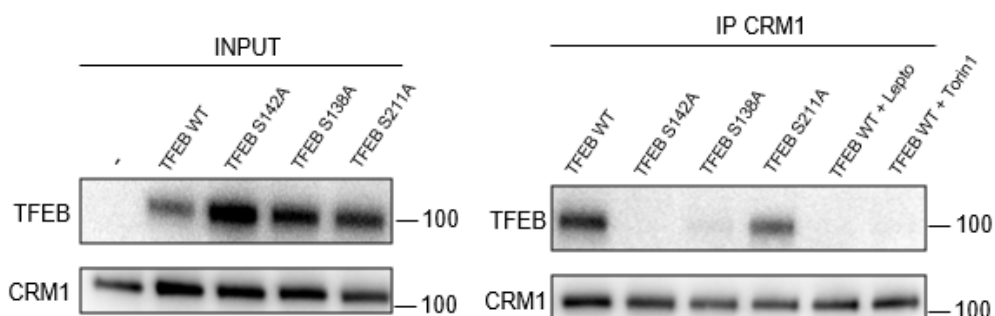


Figure 29. Immunoblotting analysis of CRM1 interaction with wild-type TFEB or constitutive nuclear TFEB mutants. Immunoprecipitation of CRM1 in HeLa cells transfected for 24 h with TFEB wild-type protein or nuclear TFEB mutants such as TFEB S142A, S138A and S211A. 1 mg of protein samples were pulled-down with 20 μ l of a specific anti-CRM1 antibody for 1 h. Then samples were analysed by western blotting for the indicated proteins.

7. Analysis of lysosomal TFEB phosphorylation

Our data on TFEB nuclear phosphorylation revealed a complicated scenario in which TFEB phosphorylation may occur in different subcellular compartments, namely the lysosomes and the nucleus, to finely tune its nucleo-cytoplasmic

shuttling dynamics. However, which of these two compartments represents the main subcellular localization where TFEB phosphorylation occurs remained to be determined. In order to address this point, we decided to generate an engineered TFEB construct to constitutively target TFEB to the lysosomal compartment.

This construct (Lys-TFEB) was obtained by fusing the first 39 amino acids (aa) of Lamtor1, a component of the Ragulator complex (Sancak et al., 2010), at the N-terminus of the GFP-tagged protein; this 39 aa sequence consists of a lipidated tail (Nada et al., 2009) that allows TFEB to be anchored on the lysosomal membrane (Fig. 30).

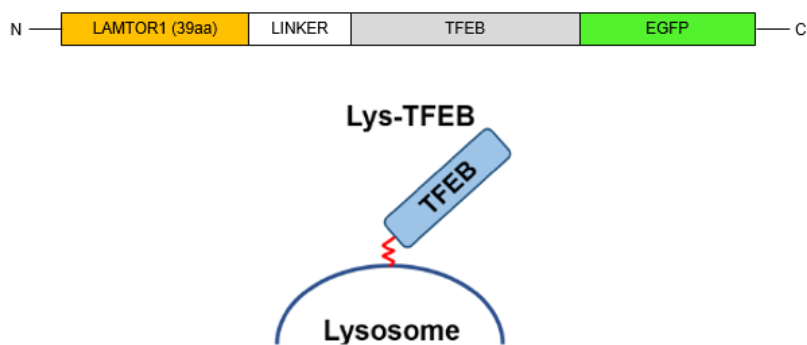


Figure 30. Schematic representation of the constitutive Lys-TFEB construct. Scheme of a constitutive lysosomal TFEB construct. TFEB was anchored to the lysosomal membrane by fusing the first 39 amino acids of Lamtor1 to the N-terminus of TFEB followed by a C-terminal GFP tag.

Accordingly, Lys-TFEB transfected in HeLa cells showed a constitutive lysosomal localization, independently from nutrient availability, as assessed by its strong co-localization with the lysosomal marker LAMP1 both during starvation and refeeding (Fig. 31).

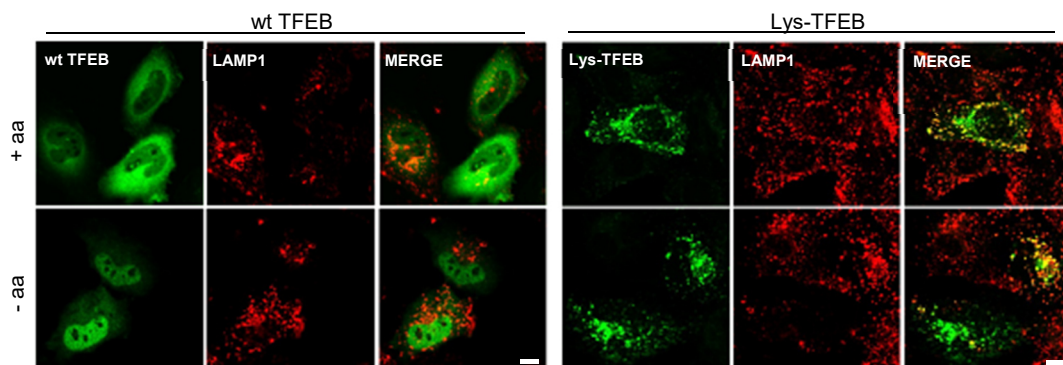


Figure 31. Lys-TFEB localization in response to nutrient availability. Representative images analysed by confocal microscopy showing the co-localization of TFEB (green) with lysosomal marker LAMP1 (red). HeLa cells were transfected with TFEB wild-type or Lys-TFEB for 24 h, then they were left untreated (+ aa) or starved for 1 h in a medium without amino acids (- aa). Scale bars: 10 μ m.

Then, we evaluated the phosphorylation status of TFEB, by using specific phospho-antibodies, when trapped on the lysosomal surface. Surprisingly, we found that Lys-TFEB was strongly dephosphorylated both during starvation and refeeding, although the other canonical mTOR substrates S6K and 4E-BP1 were normally phosphorylated in the same cells (Fig. 32). In addition, IF analysis showed that mTOR was efficiently recruited to the lysosomal surface in cells expressing Lys-TFEB (Fig. 33), as assessed by its co-localization with LAMP1 (Fig. 34), thus excluding an impaired activation of mTOR caused by the expression of TFEB at the lysosomal surface. These results suggested that, despite the lysosomal recruitment of mTORC1 is not altered, TFEB shows impaired phosphorylation when directly anchored to the lysosomes bypassing the nuclear compartment.

In order to exclude technical problems and stoichiometric impediments that may interfere with TFEB re-phosphorylation, we decided to replace the linker sequence between the 39 aa of Lamtor1 and TFEB with a longer sequence (5xGGGS), thus increasing the distance of TFEB from the lysosomal membrane and facilitate the accessibility to the mTORC1 complex. Also in this case, we found that Lys-TFEB was dephosphorylated both during starvation and refeeding (data are not shown). Thus, these results indicated an impairment in the mTOR-dependent mechanism that specifically regulates TFEB phosphorylation when targeted to the lysosomes. However, we cannot formally exclude technical issues that may alter the result we observed for Lys-TFEB phosphorylation.

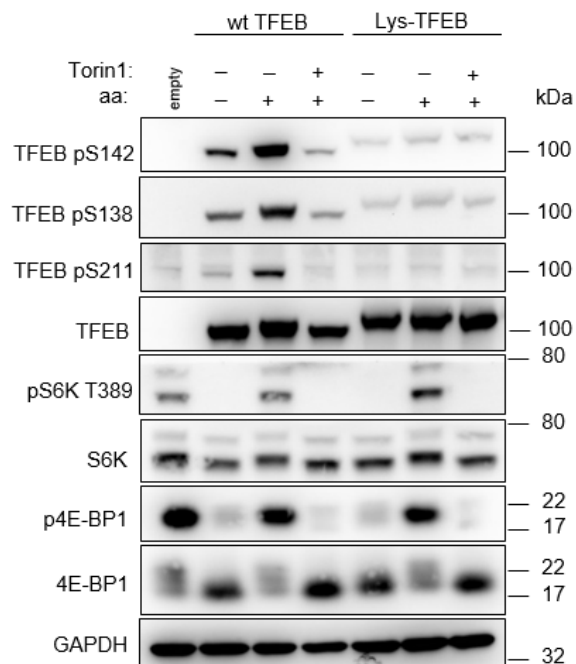


Figure 32. Lys-TFEB phosphorylation analysis in response to nutrient availability. HeLa cells were transfected with wild-type TFEB or Lys-TFEB for 24 h, then starved for 1 h or starved and restimulated with amino acids for 30 min in the presence or absence of Torin1 (250 nM). Cell lysates were analysed by western blotting with the indicated antibodies. The blot is representative of three independent experiments.

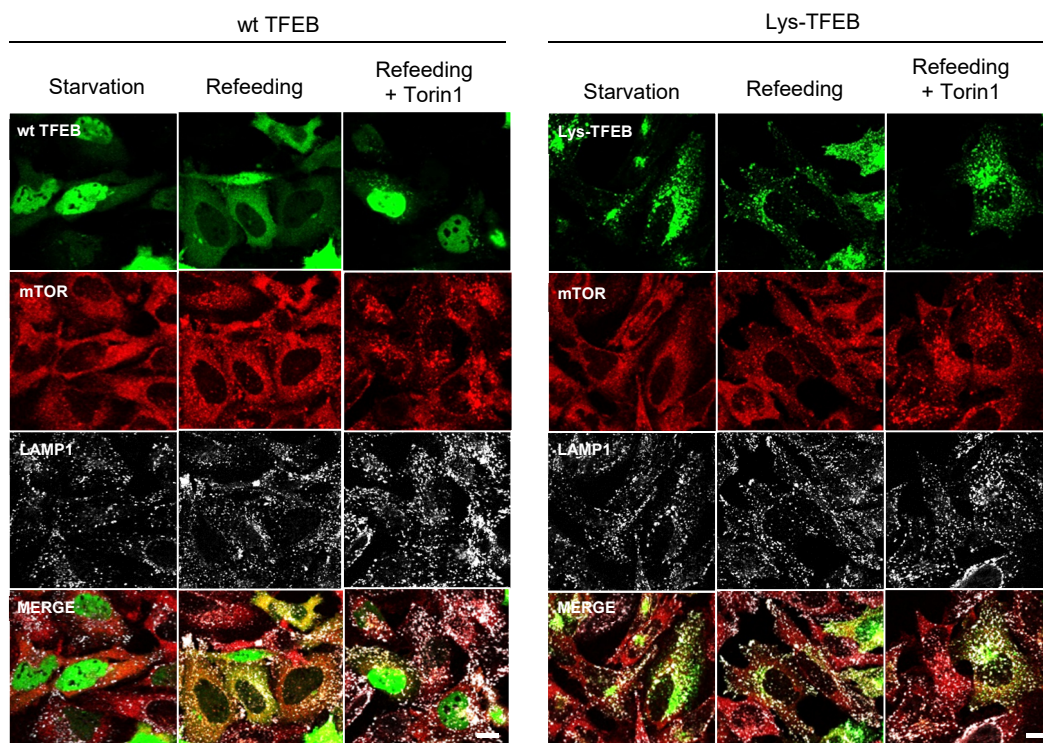


Figure 33. mTOR localization in HeLa cells expressing Lys-TFEB. Representative immunofluorescence images analysed by confocal microscopy, showing TFEB (green), mTOR (red) and LAMP1 (grey). HeLa cells were transfected with wild-type TFEB or Lys-TFEB for 24 h, then

starved for 1 h (starvation) or starved and refeed with amino acids for 30 min (refeeding) in the presence or absence of Torin1 (250 nM). Scale bars: 10 μ m.

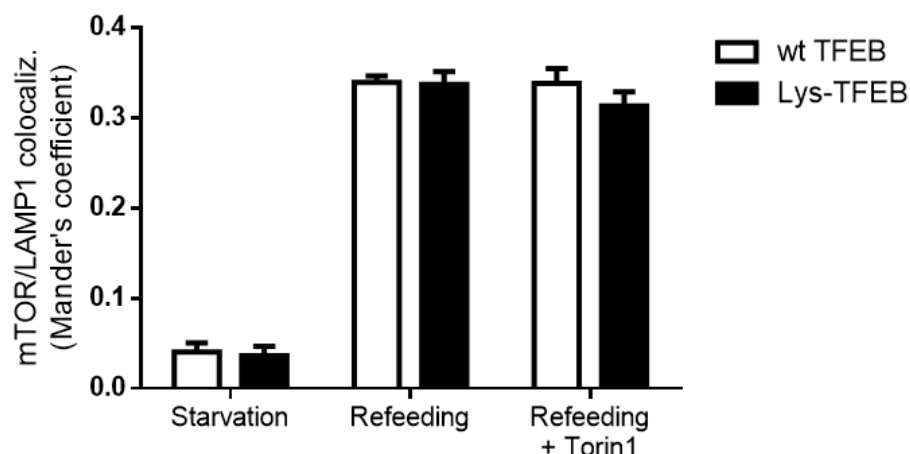


Figure 34. Analysis of mTOR co-localization with LAMP1 in cells expressing Lys-TFEB. Cells treated and stained as indicated in Fig. 33 were analysed for mTOR-LAMP1 co-localization. The plot is representative of three independent experiments and shows mTOR-LAMP1 co-localization values calculated with ImageJ software. $n \geq 5$ cells per condition. Results are mean + SEM, t-test method.

Hence, in order to verify the reliability of our approach, we designed the same strategy for the canonical mTORC1 substrate S6K (Fig. 35).

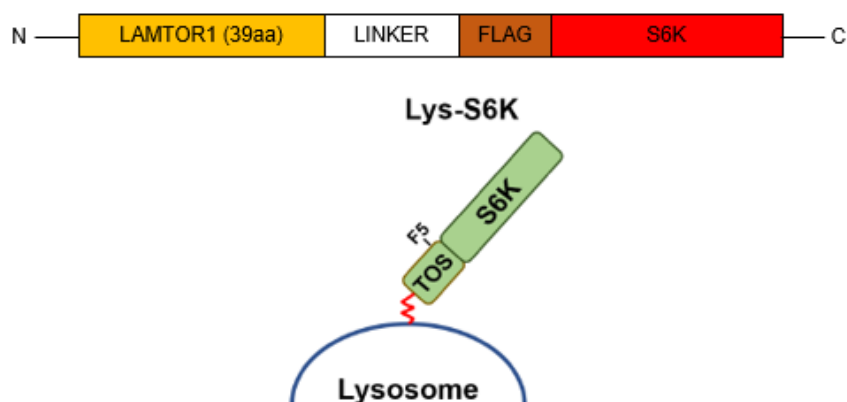


Figure 35. Schematic diagram of the constitutive Lys-S6K construct. Scheme of a constitutive lysosomal S6K construct. The first 39 amino acids of Lamtor1 were fused to the N-terminus portion of a FLAG-tagged S6K protein.

S6K wild-type protein is generally distributed in the cytosol but, similarly to TFEB, Lys-S6K predominantly showed a lysosomal localization, as shown by its striking

co-localization with lysosomal LAMP1 (Fig. 36).

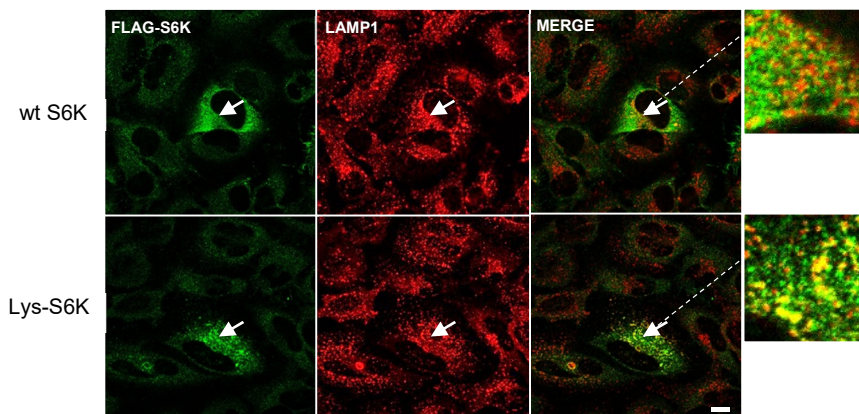


Figure 36. Lys-S6K localization in HeLa cells. Representative images showing the co-localization of S6K (green) with lysosomal marker LAMP1 (red). HeLa cells were transfected with wild-type S6K or Lys-S6K for 24 h, then analysed by confocal microscopy in fed condition. Scale bar: 10 μ m.

Then, we transfected Lys-S6K in HeLa cells to assess its phosphorylation status in the presence or absence of nutrients. Surprisingly, lysosomal-S6K was strongly phosphorylated on T389 both in starvation and refeeding conditions in an mTOR-dependent manner, since Torin1 treatment strongly abrogated the phosphorylation (Fig. 37). On the contrary, transfected wild-type S6K, as well as endogenous mTORC1 substrates, were normally phosphorylated only after amino acids restimulation (Fig. 37) This experiment indicated a nutrient-independent activation of mTOR in cells expressing constitutive lysosomal S6K.

To further analyse this point, we assessed mTOR subcellular localization in cells transfected with Lys-S6K. Strikingly, expression of Lys-S6K induced mTOR lysosomal localization not only under refeeding condition, when Rags are activated in response to nutrients and mediate mTORC1 lysosomal recruitment (Kim et al., 2008; Sancak et al., 2008), but also during starvation, when Rag GTPases are inactive and mTOR shows a diffuse cytosolic localization (Fig. 38). In particular, during nutrient deprivation we measured a three-fold increase in mTOR lysosomal localization when S6K is targeted to lysosomes compared to cells expressing wild-

type S6K (Fig. 39). These data suggested that S6K, unlike TFEB, has the intrinsic ability to bind and recruit mTOR to the lysosomal surface, independently of Rag GTPases.

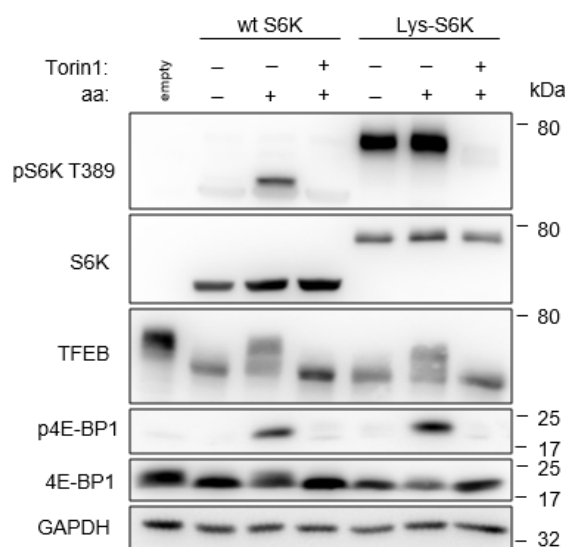


Figure 37. Lys-S6K phosphorylation analysis in response to nutrient availability. HeLa cells were transfected for 24 h with wild-type S6K or Lys-S6K, then treated with starvation for 1 h and refeeding after starvation for 30 min in the absence or presence of Torin1 (250 nM). Lysates were analysed by western blotting for S6K phosphorylation and other common mTORC1 substrates. The blot is representative of three independent experiments.

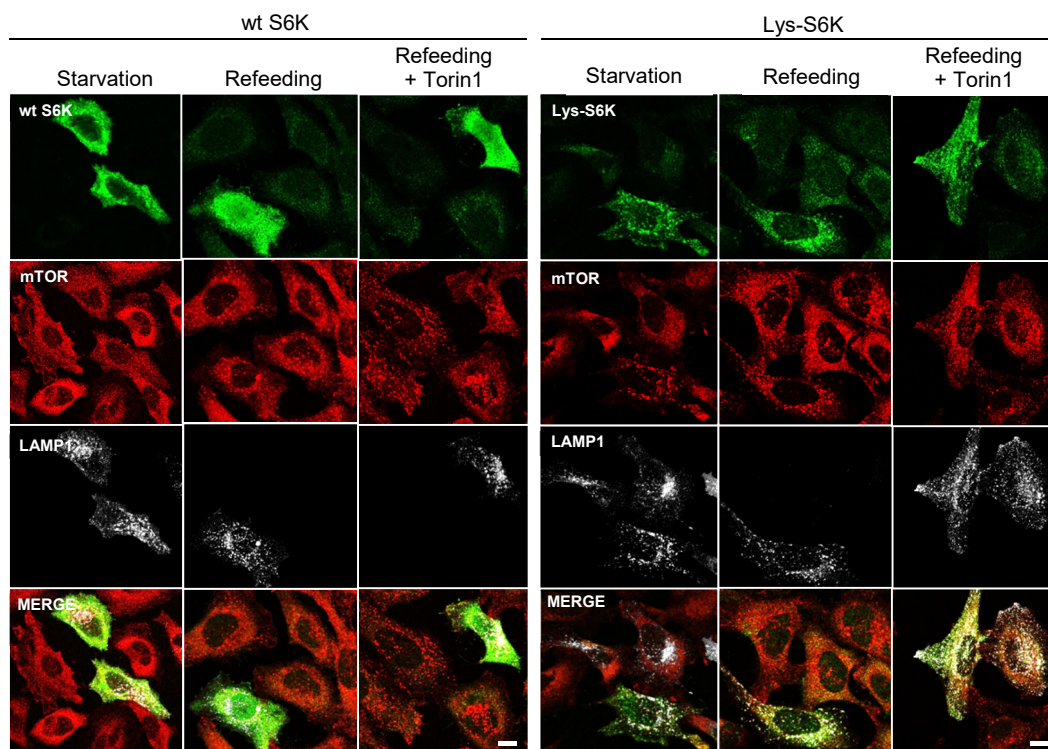


Figure 38. mTOR localization in HeLa cells expressing lysosomal S6K. Representative immunofluorescence images analysed by confocal microscopy showing S6K (red), mTOR (grey) and LAMP1 (green). HeLa cells were co-transfected for 24 h with wild-type S6K or Lys-S6K together with GFP-LAMP1 as a lysosomal marker. Then, cells were starved for 1 h (starvation) or starved and refed with amino acids for 30 min (refeeding) in the presence or absence of Torin1 (250 nM). Scale bars: 10 μ m.

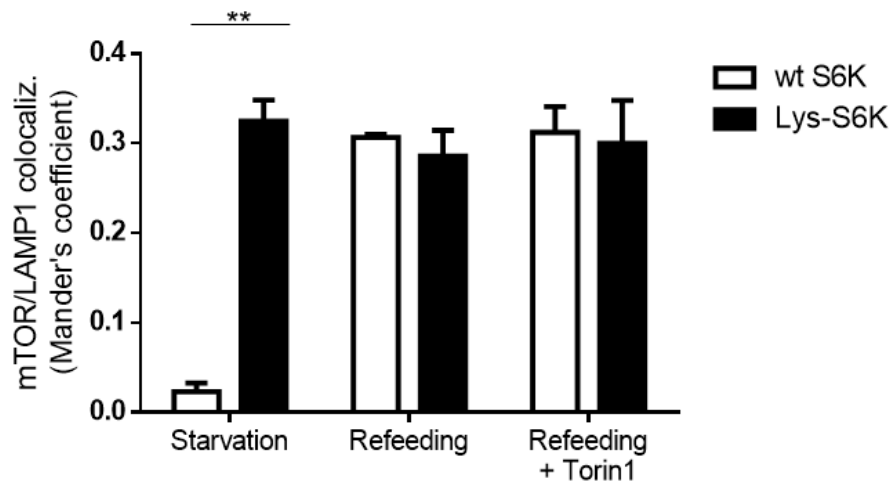


Figure 39. Analysis of mTOR co-localization with LAMP1 in cells expressing Lys-S6K. The plot is representative of two independent experiments, showing mTOR co-localization with GFP-LAMP1 in cells treated and stained as indicated in Fig. 38. Co-localization coefficients were calculated with ImageJ software. $n \geq 5$ cells per condition. Results are mean + SEM. ** $P \leq 0.01$, Wilcoxon test method.

To test this, we used HEK293A cells in which RagA and RagB genes are inactivated by genome editing (CRISPR/Cas9) (RagA/B KO HEK293A, Jewell et al., 2015). In these cells, deletion of RagA/B destabilizes also RagC and RagD, thus destroying the recruitment machinery; as a consequence, mTOR lysosomal localization is strongly impaired even when nutrients are available (Jewell et al., 2015). In line with our hypothesis, the absence of Rag GTPases did not affect Lys-S6K-mediated mTOR recruitment, as shown by immunofluorescence images showing a constitutive mTOR lysosomal localization independently from nutrient availability (Fig. 40). Our observations were confirmed also by the co-localization analysis of lysosomal mTOR with lysosomal S6K, used here as a lysosomal marker due to its

co-localization with LAMP1 (Fig. 36), showing no differences in mTOR recruitment both in the presence or absence of Rags, independently from nutrients (Fig. 41).

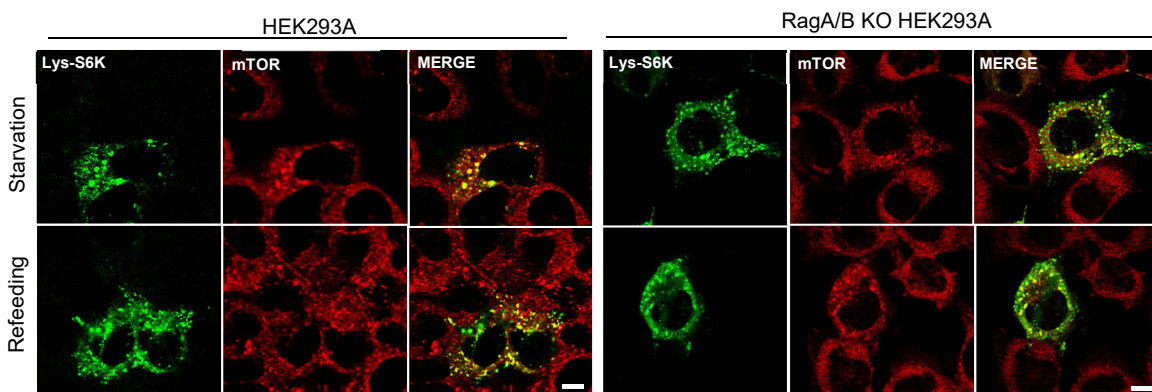


Figure 40. mTOR localization in RagA/B KO HEK293A cells expressing Lys-S6K. HEK293A control cells and RagA/B KO HEK293A cells were transfected for 24 h with Lys-S6K, then treated with starvation (1 h) and refeeding (30 min). Images are analysed by confocal microscopy and show mTOR localization (red) related to lysosomal-S6K localization (green). Scale bars: 10 μ m.

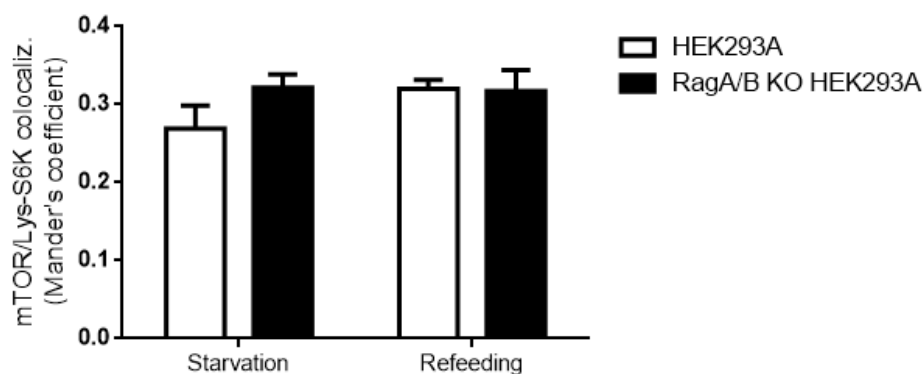


Figure 41. mTOR and Lys-S6K co-localization analysis in RagA/B KO HEK293A cells. Cells transfected with Lys-S6K for 24 h, treated and stained as indicated in Fig. 40, were analysed for mTOR co-localization with lysosomal-S6K. Co-localization coefficients were calculated with ImageJ software. The bar plot is representative of two independent experiments. $n \geq 5$ cells per condition. Results are mean + SEM, t-test method.

In addition, Lys-S6K was however phosphorylated in both starved and fed cells despite the canonical mTORC1 recruitment machinery not working in RagA/B KO HEK293A cells and other substrates such as 4E-BP1 not being regulated (Fig. 42).

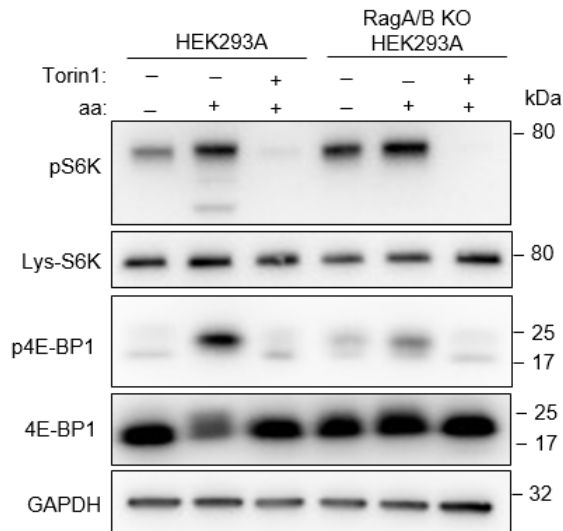


Figure 42. Lys-S6K phosphorylation analysis in RagA/B KO HEK293A cells. HEK293A control cells and RagA/B KO HEK293A cells were transfected for 24 h with Lys-S6K, then treated with starvation (1 h) and refeeding after starvation (30 min) in the absence or presence of Torin1 (250 nM). Lysates were analysed by western blotting for S6K phosphorylation and 4E-BP1 phosphorylation as a control for mTORC1 activity. The blot is representative of two independent experiments.

It is well-known that S6K directly interacts with the mTORC1 subunit Raptor through a region defined “TOS motif”, localized at the N-terminus of S6K (Schalm and Blenis, 2002; Nojima et al., 2003). Accordingly, Lys-S6K phosphorylation, as well as mTOR lysosomal localization in Lys-S6K-expressing cells, were both impaired upon Raptor silencing (Fig. 43, Fig. 44). Thus, we postulated that the mTOR lysosomal recruitment caused by expression of Lys-S6K was mediated by its binding with Raptor.

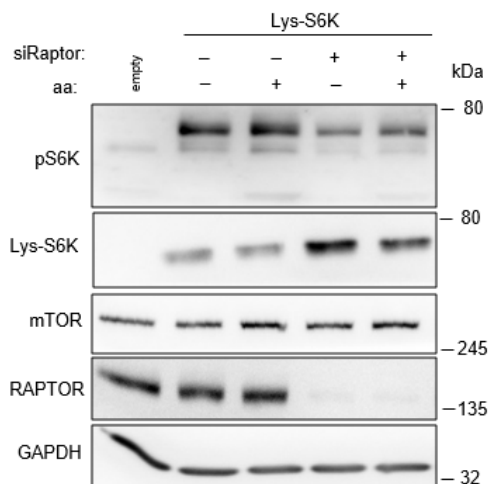


Figure 43. Lysosomal-S6K phosphorylation after Raptor silencing. HeLa cells were transfected with siCtr or siRaptor (10 nM) for 72 h. After 48 h, 500 ng of Lys-S6K were used to transfect control cells and 1 μ g for Raptor-silenced cells. At the end of 72 h treatment, cells were treated with starvation (1 h) and refeeding (30 min) conditions and then analysed for S6K phosphorylation by western blotting. The blot is representative of two independent experiments.

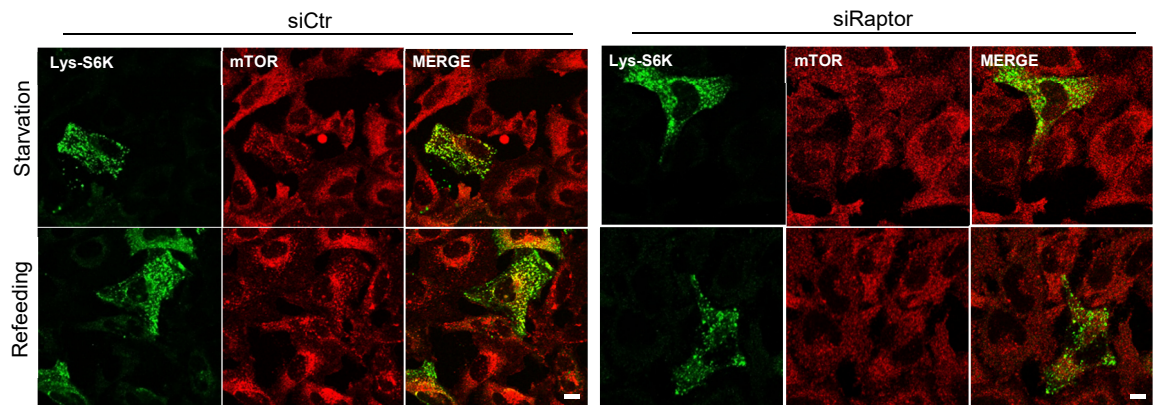


Figure 44. mTOR recruitment in cells expressing Lys-S6K after Raptor silencing. Representative images by confocal microscopy showing the co-localization of mTOR (red) with S6K (green). HeLa cells were silenced with siCtr or siRaptor (10 nM) for 72 h. After 48 h, cells were transfected with 200 ng Lys-S6K for 24 h. Then, cells were starved for 1 h or starved and refed for 30 min. The panel represents a single experiment. Scale bars: 10 μ m.

To demonstrate our hypothesis, we inserted a phenylalanine-to-alanine mutation (F5A) within the TOS domain of S6K, known to prevent the interaction of S6K with Raptor (Schalm and Blenis, 2002). Importantly, immunofluorescence analysis showed that the F5A TOS mutation abrogated the ability of Lys-S6K to induce mTOR lysosomal recruitment during starvation. Indeed, mTOR distribution appeared similar to control cells, with predominant diffused cytosolic localization in starved cells and spotted lysosomal accumulation during refeeding (Fig. 45). Accordingly, quantification of mTOR co-localization with Lys-S6K, used here as a lysosomal marker, confirmed a drastic reduction of mTOR lysosomal localization in starved cells expressing Lys-S6K-F5A compared to cells expressing wild-type Lys-S6K (Fig. 46).

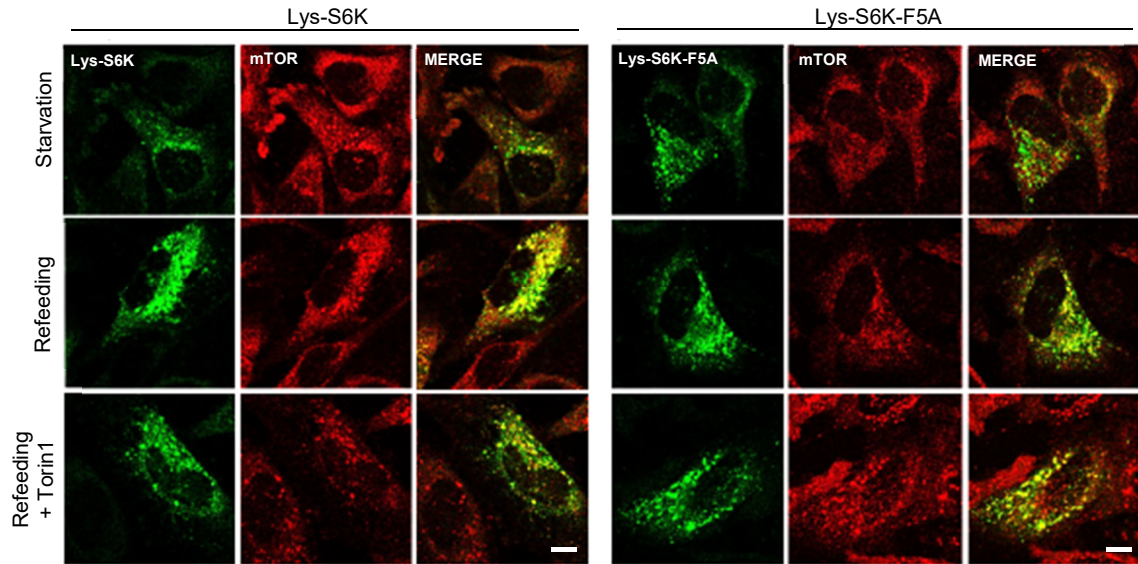


Figure 45. mTOR localization in HeLa cells expressing Lys-S6K TOS-mutant. Representative immunofluorescence images analysed by confocal microscopy, showing S6K (green) and mTOR (red). HeLa cells were transfected with Lys-S6K or Lys-S6K-F5A for 24 h, then starved for 1 h (starvation) or starved and refed with amino acids for 30 min (refeeding) in the presence or absence of Torin1 (250 nM). Scale bars: 10 μ m.

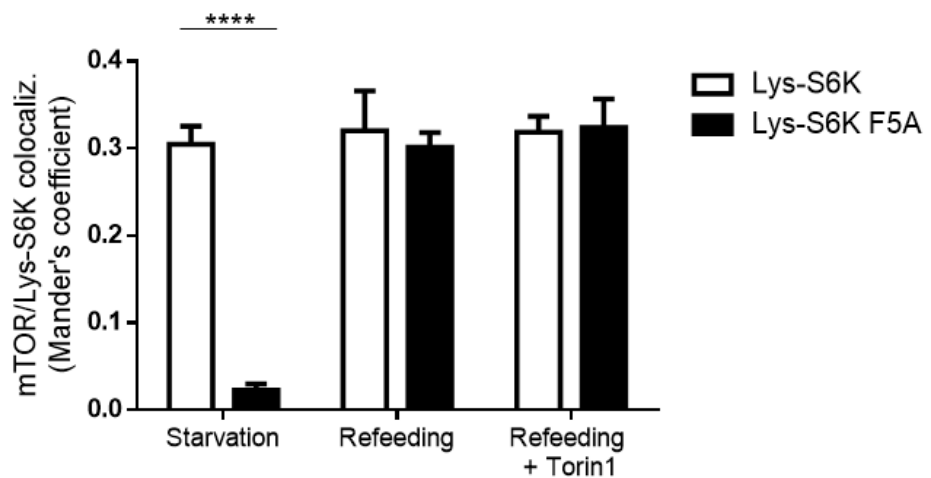


Figure 46. Analysis of mTOR co-localization with Lys-S6K wild-type or TOS-mutant protein. Cells treated and stained as indicated in Fig. 45 were analysed for mTOR co-localization with lysosomal-S6K. Co-localization coefficients were calculated with ImageJ software. The plot is representative of three independent experiments. $n \geq 5$ cells per condition. Results are mean + SEM. **** $P \leq 0.0001$, t-test method.

Strikingly, western blotting analysis showed that the mTOR-dependent phosphorylation of TOS-mutant F5A-Lys-S6K lysosomal S6K during starvation was

strongly impaired both during starvation and refeeding (Fig. 47), confirming that this interaction is essential for the correct substrate modulation by mTOR (Schalm and Blenis, 2002).

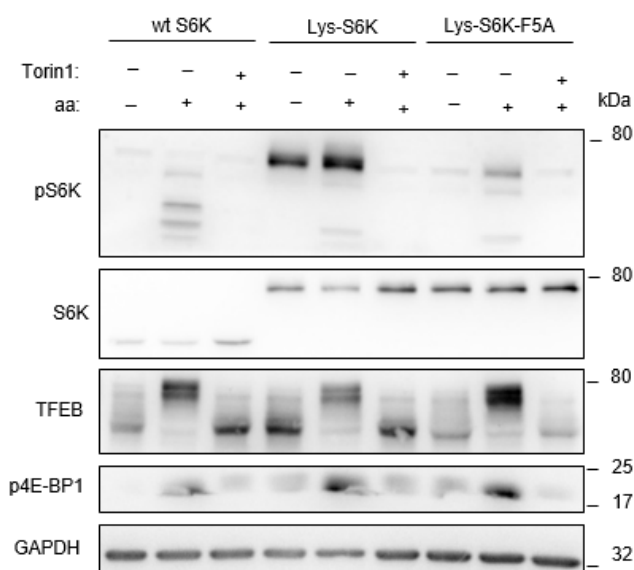


Figure 47. S6K phosphorylation analysis in cells expressing lysosomal-S6K TOS-mutant.

HeLa cells were transfected with wild-type S6K, Lys-S6K or Lys-S6K TOS-mutant (F5A) for 24 h. After, cells were starved for 1 h or starved and refed with amino acids for 30 min in the absence or presence of Torin1 (250 nM). The western blotting analysis shows the mTOR-dependent phosphorylation of transfected S6K and other specific substrates. The blot is representative of three independent experiments.

To summarize, all these data support the idea of a regulatory mechanism in which the mediation of Raptor, but not the Rag complex, is sufficient to induce mTOR-dependent phosphorylation of the canonical substrate S6K at the lysosomes. By contrast, we were not able to identify, by anchoring TFEB protein on the lysosomal membrane, phosphorylation events that specifically occur at the lysosomal compartment. Hence, different approaches are required to discern nuclear phosphorylation mechanisms, important for TFEB nuclear export, from cytosolic phosphorylation mechanisms, important for TFEB nuclear import.

DISCUSSION

In the last decade, TFEB has emerged as an appealing therapeutic target for diseases characterized by the accumulation of intracellular undigested material, such as lysosomal storage disorders and neurodegenerative diseases (Napolitano and Ballabio, 2016). Accordingly, due to the role of this transcription factor as a global modulator of lysosomal biogenesis, autophagy and lysosomal exocytosis (Sardiello et al., 2009; Settembre et al., 2011; Palmieri et al., 2011), during the years several studies have demonstrated that TFEB overexpression or activation in cellular and murine disease models induces the intracellular clearance of pathogenic aggregates and toxic undigested material, thus ameliorating the pathological signs of various pathologies (Sardiello et al., 2009; Dehay et al., 2010; Medina et al., 2011; Tsunemi et al., 2012; Settembre et al., 2013a; Pastore et al., 2013; Spampinato et al., 2013; Decressac et al., 2013; Song et al., 2013; Polito et al., 2014; Xiao et al., 2014, 2015; Kilpatrick et al., 2015; Chauhan et al., 2015; Rega et al., 2016).

For this reason, considerable progresses have been made in the study of the signaling pathways that regulate TFEB nucleo-cytoplasmic shuttling and activity. Although the efforts led to define a model that well describes the mechanism how cytosolic TFEB undergoes nuclear translocation and activation in response to amino acid limitation (Ballabio, 2016), all the studies published in the field were so far limited to the comprehension of the cytosolic events that regulate TFEB. However, how TFEB, once in the nucleus, is inactivated and relocalized to the cytoplasm was unknown and only recently elucidated. Indeed, we and others have recently published (Napolitano et al., 2018; Li et al., 2018, Silvestrini et al., 2018) that TFEB nuclear export represents a major and limiting step in the modulation of its nucleo-

cytoplasmic shuttling and activity, thus uncovering a new mechanism by which nutrient availability controls TFEB localization and activity.

In particular, our data indicate that TFEB continuously shuttles between the cytosol and the nucleus (Fig. 13, Fig. 19, Fig. 20), suggesting a highly dynamic intracellular distribution of TFEB in which the net localization results from the relative contribution of its import and export rates. Based on leptomycin B treatment and CRM1 silencing experiments, we pointed out that TFEB undergoes a CRM1-dependent nuclear export (Fig. 9, Fig. 10, Fig. 12). This is consistent with the results of a recent proteomic analysis aimed at the identification of all CRM1-interacting proteins. Strikingly, TFEB ranked as the second highest-scoring protein for its ability to bind CRM1 (Kirli et al., 2015). The role of CRM1 in the export of TFEB was further confirmed by the identification of a consensus hydrophobic NES sequence located at the N-terminal portion of TFEB (Fig. 14, Fig. 15), whose integrity is essential to promote an efficient CRM1-mediated active export (Fig. 16, Fig. 18).

Our data also show that TFEB nucleo-cytoplasmic shuttling is regulated through hierarchical phosphorylation of specific serine residues (Fig. 25) that are proximal to the NES sequence. In particular, we discovered a functional role for S142 and S138 phosphorylation, which act as a priming event to induce an efficient nuclear export. Indeed, TFEB S142A and S138A mutants show highly impaired export kinetics (Fig. 24), whereas the S211A mutant, which is efficiently phosphorylated on S142 and S138 (Fig. 25), retains, by and large, its ability to be exported (Fig. 24). It is known that phosphorylation can mediate the induction of CRM1-dependent nuclear export of several transcription factors, including for example the group of NFAT proteins, in which phosphorylation is necessary to unmask a NES sequence and allow its export (Xu and Massagué, 2004). This mechanism may be extremely similar to the one here observed for TFEB, as suggested by the finding that S142A and S138A TFEB mutants were unable to interact with CRM1 (Fig. 28).

Importantly, similar findings on the role of CRM1 in the modulation of TFEB have been also described in two recently published manuscripts (Silvestrini et al., 2018; Li et al., 2018): an unbiased genome-wide RNAi approach in *C. elegans* selected CRM1 as a potent regulator of TFEB localization whose inhibition enhances TFEB nuclear accumulation and consequent autophagy and lysosome biogenesis (Silvestrini et al., 2018), thus indicating that CRM1-mediated nuclear export is an evolutionary conserved process. Moreover, another work also found CRM1 as a main modulator of TFEB nuclear export and identified the same NES consensus sequence described in Fig. 14 as an important region for CRM1-mediated nuclear export of TFEB (Li et al., 2018). Strikingly, the same manuscript also found S142 and S138 phosphorylation as a key mechanism that allows TFEB nuclear export (Li et al., 2018), thus corroborating the robustness of our findings.

S142 and S138 are phosphorylated in a nutrient-sensitive manner (Fig. 27). These data indicate that nutrient levels finely control TFEB subcellular localization via modulation of its nuclear export, other than its import. Accordingly, analysis of nuclear export kinetics showed that nutrients have a high impact on the cytosolic redistribution of nuclear TFEB (Fig. 22, Fig. 23). Importantly, since nutrient deprivation induces TFEB dephosphorylation, which allows nuclear import, our data imply that, for efficient nuclear export, S142 and S138 phosphorylation needs to occur in the nuclear compartment. This hypothesis is supported by several lines of evidence: first, TFEB is efficiently re-phosphorylated upon refeeding in cells treated with leptomycin B (Fig. 27), in which TFEB is predominantly accumulated in the nucleus due to an impairment in nuclear export (Fig. 26); second, the M144A-TFEB NES-mutant shows efficient re-phosphorylation upon refeeding (Fig. 28), despite the evidence that its nuclear export is dramatically impaired (Fig. 16, Fig. 18); third, the constitutively nuclear TFEB S138A mutant is normally phosphorylated on S142

(Fig. 25). However, an important question that still remains unanswered is the nature of the kinase, in the nucleus, that phosphorylates TFEB on S142 and S138.

Serine residue S142 has been shown to be a phosphorylation site for both ERK and mTOR kinases (Settembre et al., 2011; Settembre et al., 2012), whereas S138 has been proposed as a GSK3-dependent phosphorylation site (Li et al., 2016; Li et al., 2018). In our experiments, Torin1 treatment, which severely inhibits the activity of the mTOR kinase, dramatically impaired both S142 and S138 phosphorylation (Fig. 25). Several studies have proposed a role for mTOR in the nuclear compartment (Zhang et al., 2002; Li et al., 2006; Wu et al., 2016; Kazyken et al., 2014). For instance, it has been proposed that NFAT is phosphorylated by mTOR in the nucleus and de-phosphorylated by calcineurin in the cytosol, in a mechanism extremely similar to the one observed for TFEB (Yang et al., 2008). Therefore, a possible model for our data is that a nuclear pool of mTOR controls the phosphorylation of TFEB in order to allow nuclear export. However, a formal proof for this scenario is currently missing and additional data are required to validate this model. In alternative, it is possible that cytosolic mTOR activity is required for the modulation of one or more nuclear kinases that mediate TFEB nuclear phosphorylation. For instance, it has been recently published that mTORC1 suppression leads to GSK3 accumulation in the nucleus, thereby promoting multiple nuclear protein phosphorylation events (He et al., 2019). Nevertheless, considering that mTOR is the main kinase responsible for S211 phosphorylation and cytosolic retention (Martina et al., 2012; Roczniak-Ferguson et al., 2012; Settembre et al., 2012) and that its activity is required for S142/S138 phosphorylation and nuclear export, our data undoubtedly establish the mTOR kinase as a major modulator of TFEB subcellular localization and activity.

Our data support a model in which TFEB nucleo-cytoplasmic shuttling is finely controlled through different phosphorylation mechanisms, occurring either in the

nucleus to control TFEB nuclear export, as shown here (Fig. 24), or at the lysosomal surface to modulate TFEB nuclear import, as previously proposed (Martina and Puertollano, 2013). However, our attempts to identify TFEB phosphorylation sites specifically regulated at the lysosomal surface did not lead to the expected results, due to the surprising and unexpected lack of phosphorylation of TFEB when this protein is permanently docked at the lysosomal membrane (Fig. 32). These results were particularly surprising due to the fact that cells expressing Lys-TFEB showed no alterations in the canonical mTOR signaling (Fig. 33, Fig. 34), and that the same approach to anchor S6K to the lysosomal surface led to a strong and constitutive phosphorylation of this “canonical” substrate (Fig. 37). Although we cannot exclude that the lack of TFEB phosphorylation is due to technical issues (e.g. steric problems due to membrane proximity, intense activity of calcineurin on the lysosomal membrane, the interruption of the hierarchical phosphorylation cascade due to the lack of nuclear phosphorylation), the difference in the phosphorylation between S6K and TFEB when linked to the lysosomal surface may also be due to the intrinsic properties of the two substrates. Accordingly, S6K was able to recruit, via its TOS motif, the mTORC1 complex to the lysosome (Fig. 38, Fig. 39), which caused Lys-S6K constitutive phosphorylation, whereas mutagenesis in the TOS motif strongly abrogated lysosomal-S6K-induced mTOR translocation to the lysosomes (Fig. 45, Fig. 46) and substrate phosphorylation (Fig. 47). By contrast, TFEB, which does not contain a TOS motif, was unable to recruit mTOR, thus suggesting that different recruitment mechanisms may be responsible for the different behaviour between the two substrates.

In summary, our data show a new mechanism in which phosphorylation regulates a CRM1-mediated nuclear export of TFEB. This may represent a potent strategy to unveil new pharmacological interventions aimed to modulate TFEB subcellular localization. In particular, alteration of TFEB nucleo-cytoplasmic shuttling, for

example via CRM1 inhibition, may be promising to pilot its nuclear localization and activity, thus stimulating autophagy in pathologies characterized by the abnormal accumulation of cellular undigested material, such as LSDs and neurodegenerative diseases.

BIBLIOGRAPHY

Aksan, I. and Goding, C. R. (1998). Targeting the microphthalmia basic helix-loop-helix-leucine zipper transcription factor to a subset of E-box elements in vitro and in vivo. *Mol. Cell. Biol.* 18, 6930-6938.

Amick, J., Tharkeshwar. A. K., Amaya, C. and Ferguson, S. M. (2018). WDR41 supports lysosomal response to changes in amino acid availability. *Mol. Boil. Cell* 29, 2213-2227.

Bala, S. and Szabo, G. (2018). TFEB, a master regulator of lysosome biogenesis and autophagy, is a new player in alcoholic liver disease. *Dig. Med. Res.* 1, 6.

Ballabio, A. (2016). The awesome lysosome. *EMBO Mol. Med.* 8, 73-76.

Bar-Peled, L., Chantranupong, L., Cherniack, A. D., Chen, W. W., Ottina, K. A., Grabiner, B. C., Spear, E. D., Carter, S. L., Meyerson, M. and Sabatini, D. M. (2013). A Tumor suppressor complex with GAP activity for the Rag GTPases that signal amino acid sufficiency to mTORC1. *Science* 340, 1100-1106.

Bar-Peled, L. and Sabatini, D. M. (2014). Regulation of mTORC1 by amino acids. *Trends Cell Biol.* 24, 400-406.

Ben-Sahra, I., Howell, J. J., Asara, J. M. and Manning, B. D. (2013). Stimulation of de novo pyrimidine synthesis by growth signaling through mTOR and S6K1. *Science* 339, 1323-1328.

Ben-Sahra, I., Hoxhaj, G., Ricoult, S. J. H., Asara, J. M. and Manning, B. D. (2016). mTORC1 induces purine synthesis through control of the mitochondrial tetrahydrofolate cycle. *Science* 351, 728-733.

Boudreau, C., Wee, T. S., Duh, Y. R., Couto, M. P., Ardakani, K. H. and Brown, C. M. (2006). Excitation light dose engineering to reduce photo-bleaching and photo-toxicity. *Sci. Rep.* 6, 30892.

Brady, O. A., Jeong, E., Martina, J. A., Pirooznia, M., Tunc, I. and Puertollano, R. (2018). The transcription factors TFE3 and TFEB amplify p53 dependent transcriptional programs in response to DNA damage. *eLife* 7, e40856.

Bruder, E., Moch, H., Ehrlich, D., Leuschner, I., Harms, D., Argani, P., Briner, J., Graf, N., Selle, B., Ruffle, A., Paulussen, M. and Koesters, R. (2007). Wnt signaling pathway analysis in renal cell carcinoma in young patients. *Modern Pathol.* 20, 1217-1229.

Brugarolas, J., Lei, K., Hurley, R. L., Manning, B. D., Reiling, J. H., Hafen, E., Witters, L. A., Ellisen, L. F. and Kaelin Jr., W. G. (2004). Regulation of mTOR function in response to hypoxia by REDD1 and the TSC1/TSC2 tumor suppressor complex. *Genes Dev.* 18, 2893-2904.

Calcagni, A., Kors, L., Verschuren, E., De Cegli, R., Zampelli, N., Nusco, E., Confalonieri, S., Bertalot, G., Pece, S., Settembre, C., Malouf, G. G., Leemans, J. C., Salvatore, M., Peters, D. J. M., Di Fiore, P. P. and Ballabio, A. (2016). Modelling TFE renal cell carcinoma in mice reveals a critical role of WNT signaling. *eLife* 5, e17047.

Campbell, G. R., Rawat, P., Bruckman, R. S. and Spector, S. A. (2015) Human immunodeficiency virus type 1 Nef inhibits autophagy through transcription factor EB sequestration. *PLoS Pathog.* 11, e1005018.

Cautain, B., Hill, R., de Pedro, N. and Link, W. (2015). Components and regulation of nuclear transport processes. *FEBS J.* 282, 445-462.

Chantranupong, L., Wolfson, R. L., Orozco, J. M., Saxton, R. A., Scaria, S. M., Bar-Peled, L., Spooner, E., Isasa, M., Gygi, S. P. and Sabatini, D. M. (2014). The Sestrins interact with GATOR2 to negatively regulate the amino-acid- sensing pathway upstream of mTORC1. *Cell Rep.* 9, 1-8.

Chantranupong, L., Scaria, S. M., Saxton, R. A., Gygi, M. P., Shen, K., Wyant, G. A., Wang, T., Harper, J. W., Gygi, S. P. and Sabatini, D. M. (2016). The CASTOR proteins are arginine sensors for the mTORC1 pathway. *Cell* 165, 153-164.

Chauhan, S., Ahmed, Z., Bradfute, S. B., Arko-Mensah, J., Mandell, M. A., Won Choi, S., Kimura, T., Blanchet, F., Waller, A., Mudd, M. H., Jiang, S., Sklar, L., Timmins, G. S., Maphis, N., Bhaskar, K., Piguet, V. and Deretic, V. (2015). Pharmaceutical screen identifies novel target processes for activation of autophagy with a broad translational potential. *Nat. Commun.* 6, 8620.

Chen, L., Wang, K., Long, A., Jia, L., Zhang, Y., Deng, H., Li, Y., Han, J. and Wang, Y. (2017). Fasting-induced hormonal regulation of lysosomal function. *Cell Res.* 27, 748-763.

Chen, Y., Li, H. H., Fu, J., Wang, X. F., Ren, Y. B., Dong, L. W., Tang, S. H., Liu, S. Q., Wu, M. C. and Wang, H. Y. (2007). Oncoprotein p28 GANK binds to RelA and retains NF- κ B in the cytoplasm through nuclear export. *Cell Res.* 17, 1020-1029.

Cook, A., Bono, F., Jinek, M. and Conti, E. (2007). Structural biology of nucleocytoplasmic transport. *Annu. Rev. Biochem.* 76, 647-671.

Cronin, J. C., Wunderlich, J., Loftus, S. K., Prickett, T. D., Wei, X., Ridd, K., Vemula, S., Burrell, A. S., Agrawal, N. S., Lin, J. C., Banister, C. E., Buckhaults, P., Rosenberg, S.A., Bastian, B. C., Pavan, W. J and Samuels, Y. (2009). Frequent mutations in the MITF pathway in melanoma. *Pigment Cell Melanoma Res.* 22, 435-444.

Dang, C. V. and Lee, W. M. F. (1988). Identification of the human c-myc protein nuclear translocation signal. *Mol. Cell. Biol.* 8, 4048-4054.

Davis, I. J., Kim, J. J., Oszolak, F., Widlund, H. R., Rozenblatt-Rosen, O., Granter, S. R., Du, J., Fletcher, J. A., Denny, C. T., Lessnick, S. L., Linehan, W. M., Kung, A. L. and Fisher, D. A. (2006). Oncogenic MITF dysregulation in clear cell sarcoma: defining the MiT family of human cancers. *Cancer Cell* 9, 473-484.

Decressac, M., Mattsson, B., Weikop, P., Lundblad, M., Jakobsson, J. and Bjorklund, A. (2013). TFEB-mediated autophagy rescues midbrain dopamine neurons from alpha-synuclein toxicity. *Proc. Natl. Acad. Sci. USA* 110, E1817-E1826.

de Duve, C. (2005). The lysosome turns fifty. *Nat. Cell Biol.* 9, 847-849.

Dehay, B., Bove, J., Rodriguez-Muela, N., Perier, C., Recasens, A., Boya, P. and Vila, M. (2010). Pathogenic lysosomal depletion in Parkinson's disease. *J. Neurosci.* 30, 12535-12544.

Dennis, P. B., Pullen, N., Pearson, R. B., Kozma, S. C. and Thomas, G. (1998). Phosphorylation sites in the autoinhibitory domain participate in p70s6k activation loop phosphorylation. *J. Biol. Chem.* 273, 14845-14852.

Dibble, C. C., Elis, W., Menon, S., Qin, W., Klekota, J., Asara, J. M., Finan, P. M., Kwiatkowski, D. J., Murphy, L. O. and Manning, B. D. (2012). TBC1D7 is a third subunit of the TSC1-TSC2 complex upstream of mTORC1. *Mol. Cell* 47, 535-546.

Di Malta, C., Siciliano, D., Calcagni, A., Monfregola, J., Punzi, S., Pastore, N., Eastes, A. N., Davis, O., De Cegli, R., Zampelli, A., Di Giovannantonio, L. G., Nusco, E., Platt, N., Guida, A., Ogmundsdottir, M. H., Lanfrancone, L., Perera, R. M., Zoncu, R., Pelicci, P.G., Settembre, C. and Ballabio, A. (2017). Transcriptional activation of RagD GTPase controls mTORC1 and promotes cancer growth. *Science* 356, 1188-1192.

Dorrello, N. V., Peschiaroli, A., Guardavaccaro, D., Colburn, N. H., Sherman, N. E. and Pagano, M. (2006). S6K1- and betaTRCP-mediated degradation of PDCD4 promotes protein translation and cell growth. *Science* 314, 467-471.

Düvel, K., Yecies, J. L., Menon, S., Raman, P., Lipovsky, A. I., Souza, A. L., Triantafellow, E., Ma, Q., Gorski, R., Cleaver, S., Heiden, M. G. V., MacKeigan, J. P., Finan, P.M., Clish, C. B., Murphy, L. O. and Manning, B. D. (2010). Activation of

a metabolic gene regulatory network downstream of mTOR complex 1. *Mol. Cell* 39, 171-183.

Espenshade, P.J. and Hughes, A.L. (2007). Regulation of sterol synthesis in eukaryotes. *Annu. Rev. Genet.* 41, 401-427.

Fan, Y., Lu, H., Liang, W., Garcia-Barrio, M. T., Guo, Y., Zhang, J., Zhu, T., Hao, Y., Zhang, J. and Chen, Y. E. (2018). Endothelial TFEB (Transcription Factor EB) positively regulates postischemic angiogenesis. *Circ. Res.* 122, 945-957.

Ferron, M., Settembre, C., Shimazu, J., Lacombe, J., Kato, S., Rawlings, D. J., Ballabio, A. and Karsenty, G. (2013). A RANKL-PKC β -TFEB signaling cascade is necessary for lysosomal biogenesis in osteoclasts. *Genes Dev.* 27, 955-969.

Fischer, U., Huber, J., Boelens, W. C., Mattajt, L. W. and Lührmann, R. (1995). The HIV-1 Rev Activation Domain is a nuclear export signal that accesses an export pathway used by specific cellular RNAs. *Cell* 82, 475-483.

Fried, H. and Kutay, U. (2003). Nucleocytoplasmic transport: taking an inventory. *Cell. Mol. Life Sci.* 60, 1659-1688.

Fu, X., Liang, C., Li, F., Wang, L., Wu, X., Lu, A., Xiao, G. and Zhang, G. (2018). The rules and functions of nucleocytoplasmic shuttling proteins. *Int. J. Mol. Sci.* 19, 1445.

Fukuda, M., Asano, S., Nakamura, T., Adachi, M., Yoshida, M., Yanagida, M. and Nishida E. (1997). CRM1 is responsible for intracellular transport mediated by the nuclear export signal. *Nature* 390, 308-311.

Garraway, L. A., Widlund, H. R., Rubin, M. A., Getz, G., Berger, A. J., Ramaswamy, S., Beroukhi, R., Milner, D. A., Granter, S. R., Du, J., Lee, C., Wagner, S. N., Li, C., Golub, T. L., Rimm, D. L., Meyerson, M. L., Fisher, D. E. and Sellers, W. R. (2005). Integrative genomic analyses identify MITF as a lineage survival oncogene amplified in malignant melanoma. *Nature* 436, 117-122.

Gaubitz, C., Oliveira, T. M., Prouteau, M., Leitner, A., Karuppasamy, M., Konstantinidou, G., Rispal, D., Eltschinger, S., Robinson, G. C., Thore, S., Aebersold, R., Schaffitzel, C. and Loewith, R. (2015). Molecular basis of the rapamycin insensitivity of target of rapamycin complex 2. *Mol. Cell* 58, 977-988.

Gingras, A. C., Gygi, S. P., Raught, B., Polakiewicz, R. D., Abraham, R. T., Hoekstra, M. F., Aebersold, R. and Sonenberg, N. (1999). Regulation of 4E-BP1 phosphorylation: a novel two-step mechanism. *Genes Dev.* 13, 1422-1437.

Goldstein, L. (1958). Localization of nucleus-specific protein as shown by transplantation experiments in *Amoeba proteus*. *Exp. Cell Res.* 15, 635-637.

Goodwin, M. L., Jin, H., Straessler, K., Smith-Fry, K, Zhu, J. F., Monument, M. J., Grossmann, A., Randall, R. L., Capecchi, M. R., Jones and K. B. (2014). Modeling alveolar soft part sarcomagenesis in the mouse: a role for lactate in the tumor microenvironment. *Cancer Cell* 26, 851-862.

Görlich, D., Panté, N., Kutay, U., Aebi, U. and Bischoff, F. R. (1996). Identification of different roles for RanGDP and RanGTP in nuclear protein import. *EMBO J.* 15, 5584-5594.

Gray, M. A., Choy, C. H., Dayam, R. M., Ospina-Escobar, E., Somerville, A., Xiao, X., Ferguson, S. M. and Botelho, R. J. (2016). Phagocytosis enhances lysosomal and bactericidal properties by activating the Transcription Factor TFEB. *Curr. Biol.* 26, 1955-1964.

Gwinn, D. M., Shackelford, D. B., Egan, D. F., Mihaylova, M. M., Mery, A., Vasquez, D. S., Turk, B. E., and Shaw, R. J. (2008). AMPK phosphorylation of raptor mediates a metabolic checkpoint. *Mol. Cell* 30, 214-226.

Haq, R. and Fisher, D. E. (2011). Biology and clinical relevance of the microphthalmia family of transcription factors in human cancer. *J. Clin. Oncol.* 29, 3474-3482.

Hartman, M. L. and Czyz, M. (2015). Pro-survival role, of MITF in melanoma. *J. Invest. Dermatol.* 135, 352-358.

He, L., Fei, D. L., Nagiec, M. J., Mutvei, A. P., Lamprakis, A., Kim, B. Y. and Blenis, J. (2019). Regulation of GSK3 cellular location by FRAT modulates mTORC1-dependent cell growth and sensitivity to rapamycin. *PNAS*, doi: 10.1073.

Hemesath, T. J., Steingrímsson, E., McGill, G., Hansen, M. J., Vaught, J., Hodgkinson, C. A., Arnheiter, H., Copeland, N. G., Jenkins, N. A. and Fisher, D. E. (1994). Microphthalmia, a critical factor in melanocyte development, defines a discrete transcription factor family. *Genes Dev.* 8, 2770-2780.

Hodgkinson, C. A., Moore, K. J., Nakayama, A., Steingrímsson, E., Copeland, N. G., Jenkins, N. A. and Arnheiter, H. (1993). Mutations at the mouse microphthalmia locus are associated with defects in a gene encoding a novel basic-helix-loop-helix-zipper protein. *Cell* 74, 395-404.

Holz, M. K., Ballif, B. A., Gygi, S. P. and Blenis, J. (2005). mTOR and S6K1 mediate assembly of the translation preinitiation complex through dynamic protein interchange and ordered phosphorylation events. *Cell* 123, 569-580.

Hsu, C. L., Lee, E. X., Gordon, K. L., Paz, E. A., Shen, W. C., Ohnishi, K., Meisenhelder, J., Hunter, T. and La Spada, A. R. (2018). MAP4K3 mediates amino acid-dependent regulation of autophagy via phosphorylation of TFEB. *Nat. Comm.* 9, 942.

Huan, C., Kelly, M. L., Steele, R., Shapira, I., Gottesman, S. R. and Roman, C. A. J. (2006). Transcription factors TFE3 and TFEB are critical for CD40 ligand expression and thymus-dependent humoral immunity. *Nat. Immunol.* 7, 1082-1091.

Huang, J. and Manning, B. D. (2008). The TSC1-TSC2 complex: a molecular switchboard controlling cell growth. *Biochem. J.* 412, 179-190.

Inoki, K., Li, Y., Zhu, T., Wu, J. and Guan, K. L. (2002). TSC2 is phosphorylated and inhibited by Akt and suppresses mTOR signalling. *Nat. Cell Biol.* 4, 648-657.

Inoki, K., Li, Y., Xu, T. and Guan, K. L. (2003). Rheb GTPase is a direct target of TSC2 GAP activity and regulates mTOR signaling. *Genes Dev.* 17, 1829-1834.

Ishikawa-Ankerhold, H. C., Ankerhold, R. and Drummen, G. P. C. (2012). Advanced fluorescence microscopy techniques - FRAP, FLIP, FLAP, FRET and FLIM. *Molecules* 17, 4047-4132.

Isotani, S., Hara, K., Tokunaga, C., Inoue, H., Avruch, J. and Yonezawa, K. (1999). Immunopurified mammalian target of rapamycin phosphorylates and activates p70 S6 kinase alpha in vitro. *J. Biol. Chem.* 274, 34493-34498.

Jacinto, E., Loewith, R., Schmidt, A., Lin, S., Rüegg, M. A., Hall, A. and Hall, M. N. (2004). Mammalian TOR complex 2 controls the actin cytoskeleton and is rapamycin insensitive. *Nat. Cell Biol.* 6, 1122-1128.

Jacinto, E., Facchinetti V., Liu, D., Soto, N., Jung, S. Y., Huang, Q., Qin, J. and Su, B. (2006). SIN1/MIP1 maintains rictor-mTOR complex integrity and regulates Akt phosphorylation and substrate specificity. *Cell.* 1, 125-137.

Jewell, J. L., Kim, Y. C., Russell, R. C., Yu, F. X., Park, H. W., Plouffe, S. W., Tagliabracchi, V. S. and Guan, K. L. (2015). Differential regulation of mTORC1 by leucine and glutamine. *Science* 347, 194-198.

Kauffman, E. C., Ricketts, C. J., Rais-Bahrami, S., Yang, Y., Merino, M. J., Bottaro, D. P., Srinivasan, R. and Linehan, W. M. (2014). Molecular genetics and cellular features of TFE3 and TFEB fusion kidney cancers. *Nat. Rev. Urol.* 11, 465-475.

Kazyken, D., Kaz, Y., Kiyon, V., Zhylybayev, A. A., Chen, C. H., Agarwal, N. K. and Sarbassov, D. D. (2014). The nuclear import of ribosomal proteins is regulated by mTOR. *Oncotarget* 5, 9577-9593.

Kilpatrick, K., Zeng, Y., Hancock, T. and Segatori, L. (2015). Genetic and chemical activation of TFEB mediates clearance of aggregated alpha-synuclein. PLoS ONE 10, e0120819.

Kim, D. H., Sarbassov, D. D., Ali, S. M., King, J. E., Latek, R. R., Erdjument-Bromage, H., Tempst, P. and Sabatini D. M. (2002). mTOR interacts with raptor to form a nutrient-sensitive complex that signals to the cell growth machinery. Cell 2, 163-175.

Kim, D. H., Sarbassov, D. D., Ali, S. M., Latek, R. R., Guntur, K. V. P., Erdjument-Bromage, H., Tempst, P. and Sabatini D. M. (2003). GβL, a positive regulator of the rapamycin-sensitive pathway required for the nutrient-sensitive interaction between raptor and mTOR. Mol. Cell 11, 895-904.

Kim, E., Goraksha-Hicks, P., Li, L., Neufeld, T. P. and Guan, K. L. (2008). Regulation of TORC1 by Rag GTPases in nutrient response. Nat. Cell Biol. 10, 935-945.

Kim, J., Kundu, M., Viollet, B. and Guan, K. L. (2011). AMPK and mTOR regulate autophagy through direct phosphorylation of Ulk1. Nat. Cell Biol. 13, 132-141.

Kirli, K., Karaca, S., Dehne, H. J., Samwer, M., Pan, K. T., Lenz, C., Urlaub, H. and Görlich, D. (2015). A deep proteomics perspective on CRM1-mediated nuclear export and nucleocytoplasmic partitioning. eLife 10, 11466.

Kosugi, S., Hasebe, M., Tomita, M. and Yanagawa, H. (2008) Nuclear export signal consensus sequences defined using a localization-based yeast selection system. Traffic 9, 2053-2062.

Kuiper, R. P., Schepens, M., Thijssen, J., van Asseldonk, M., van den Berg, E., Bridge, J., Schuurin, E., Schoenmakers, E. F. P. M. and van Kessel, A. G. (2003). Upregulation of the transcription factor TFEB in t (6;11) (p21; q13)-positive renal cell carcinomas due to promoter substitution. *Hum. Mol. Genet.* 12, 1661-1669.

Lamming, D. W. and Bar-Peled, L. (2019). Lysosome: The metabolic signalling hub. *Traffic* 20, 27-38.

Lange, A., McLane, L. M., Mills, R. E., Devine, S. E. and Corbett, A. H. (2010). Expanding the definition of the classical bipartite nuclear localization signal. *Traffic* 11, 311-323.

Laplante, M. and Sabatini, D. M. (2012). mTOR signaling in growth control and disease. *Cell* 149, 274-293.

Li, H., Tsang, C. K., Watkins, M., Bertram, P. G. and Zheng, X. F. S. (2006). Nutrient regulates Tor1 nuclear localization and association with rDNA promoter. *Nature* 442, 1058-1061.

Li, L., Friedrichsen, H. J., Andrews, S., Picaud, S., Volpon, L., Ngeow, K., Berridge, G., Fischer, R., Borden, K. L. B., Filippakopoulos, P. and Goding, C. R. (2018). A TFEB nuclear export signal integrates amino acid supply and glucose availability. *Nat. Comm.* 9, 2685.

Li, P., Gu, M. and Xu, H. (2019). Lysosomal ion channels as decoders of cellular signals. *Trends Biochem. Sci.* 44, 110-124.

Li, Y., Xu, M., Ding, X., Yan, C., Song, Z., Chen, L., Huang, X., Wang, X., Jian, Y., Tang, G., Tang, C., Di, Y., Mu, S., Liu, X., Liu, K., Li, T., Wang, Y., Miao, L., Guo, W., Hao, X. and Yang, C. (2016). Protein kinase C controls lysosome biogenesis independently of mTORC1. *Nat. Cell Biol.* 18, 1065-1077.

Lim, C.Y. and Zoncu, R. (2016). The lysosome as a command-and-control center for cellular metabolism. *J. Cell Biol.* 214, 653-664.

Lin, J., Handschin, C. and Spiegelman, B. M. (2005). Metabolic control through the PGC-1 family of transcription coactivators. *Cell Metab.* 1, 361-370.

Liu, Q., Chang, J. W., Wang, J., Kang, S. A., Thoreen, C. C., Markhard, A., Hur, W., Zhang, J., Sim, T., Sabatini, D. M., and Gray, N. S. (2010). Discovery of 1-(4-(4-propionylpiperazin-1-yl)-3-(trifluoromethyl)phenyl)-9-(quinolin-3-yl)benzo[h][1,6]naphthyridin-2(1H)-one as a highly potent, selective Mammalian Target of Rapamycin (mTOR) inhibitor for the treatment of cancer. *Med. Chem.* 53(19), 7146-7155.

Long, X., Lin, Y., Ortiz-Vega, S., Yonezawa, K. and Avruch, J. (2005). Rheb binds and regulates the mTOR kinase. *Curr. Biol.* 15, 702-713.

Lotfi, P., Tse, D. Y., Di Ronza, A., Seymour, M. L., Martano, G., Cooper, J. D., Pereira, F. A., Passafaro, M., Wu, S. M. and Sardiello, M. (2018). Trehalose reduces retinal degeneration, neuroinflammation and storage burden caused by a lysosomal hydrolase deficiency. *Autophagy* 14, 1-16.

Ma, X. M., Yoon, S. O., Richardson, C. J., Jülich, K. and Blenis, J. (2008). SKAR links pre-mRNA splicing to mTOR/S6K1-mediated enhanced translation efficiency of spliced mRNAs. *Cell* 133, 303-313.

Mansueto, G., Armani, A., Viscomi, C., D'Orsi, L., De Cegli, R., Polishchuk, E. V., Lamperti, C., Di Meo, I., Romanello, V., Marchet, S., Saha, P. K., Zong, H., Blaauw, B., Solagna, F., Tezze, C., Grumati, P., Bonaldo, P., Pessin, J. E., Zeviani, M., Sandri, M. and Ballabio, A. (2017). Transcription factor EB controls metabolic flexibility during exercise. *Cell Metabolism* 25, 182-196.

Martina, J. A., Chen, Y., Gucek, M. and Puertollano, R. (2012). MTORC1 functions as a transcriptional regulator of autophagy by preventing nuclear transport of TFEB. *Autophagy* 8, 903-914.

Martina, J. A. and Puertollano, R. (2013). Rag GTPases mediate amino acid-dependent recruitment of TFEB and MITF to lysosomes. *J. Cell Biol.* 200, 475-491.

Martina, J. A., Diab, H. I., Lishu, L., Jeong-A, L., Patange, S., Raben, N. and Puertollano, R. (2014). The nutrient-responsive transcription factor TFE3 promotes autophagy, lysosomal biogenesis, and clearance of cellular debris. *Sci. Signal.* 7, ra9.

Martina, J. A., Diab, H. I., Brady, O. A. and Puertollano, R. (2016) TFEB and TFE3 are novel components of the integrated stress response. *EMBO J.* 35, 479-495.

Medina, D. L., Fraldi, A., Bouche, V., Annunziata, F., Mansueto, G., Spampanato, C., Puri, C., Pignata, A., Martina, J. A., Sardiello, M., Palmieri, M., Polishchuk, R., Puertollano, R. and Ballabio, A. (2011). Transcriptional activation of lysosomal exocytosis promotes cellular clearance. *Dev. Cell* 21, 421-430.

Medina, D. L., Di Paola, S., Peluso, I., Armani, A., De Stefani, D., Venditti, R., Montefusco, S., Scotto-Rosato, A., Prezioso, C., Forrester, A., Settembre, C., Wang, W., Gao, Q., Xu, H., Sandri, M., Rizzuto, R., De Matteis, M. A. and Ballabio, A. (2015). Lysosomal calcium signalling regulates autophagy through calcineurin and TFEB. *Nat. Cell Biol.* 17, 288-299.

Menzies, F. M., Fleming, A. and Rubinsztein, D. C. (2015). Compromised autophagy and neurodegenerative diseases. *Nat. Rev. Neurosci.* 16, 345-357.

Murano, T., Najibi, M., Paulus, G. L. C., Adiliaghdam, F., Valencia-Guerrero, A., Selig, M., Wang, X., Jeffrey, K., Xavier, R. J., Lassen, K. G. and Irazoqui, J. E. (2017). Transcription factor TFEB cell-autonomously modulates susceptibility to intestinal epithelial cell injury in vivo. *Sci. Rep.* 7, 13938.

Nada, S., Hondo, A., Kasai, A., Koike, M., Saito, K., Uchiyama, Y. and Okada, M. (2009). The novel lipid raft adaptor p18 controls endosome dynamics by anchoring the MEK-ERK pathway to late endosomes. *EMBO J.* 28, 477-489.

Najibi, M., Labed, S. A., Visvikis, O. and Irazoqui, J. E. (2016). An evolutionary conserved PLC-PKD-TFEB pathway for host defense. *Cell Rep.* 15, 1728-1742.

Napolitano, G. and Ballabio, A. (2016). TFEB at a glance. *J. Cell Sci.* 129, 2475-2481.

Napolitano, G., Esposito, A., Choi, H., Matarese, M., Benedetti, V., Di Malta, C., Monfregola, J., Medina, D. L., Lippincott-Schwartz, J. and Ballabio A. (2018). mTOR-dependent phosphorylation controls TFEB nuclear export. *Nat. Comm.* 9, 3312.

Nezich, C. L., Wang, C., Fogel, A. I. and Youle, R. J. (2015). MIT/TFE transcription factors are activated during mitophagy downstream of Parkin and Atg5. *J. Cell Biol.* 210, 435-450.

Nnah, I. C., Wang, B., Saqcena, C., Weber, G. F., Bonder, E. M., Bagley, D., De Cegli, R., Napolitano, G., Medina, D. L., Ballabio, A. and Dobrowolski, R. (2019). TFEB-driven endocytosis coordinates MTORC1 signaling and autophagy. *Autophagy* 15, 151-164.

Nojima, H., Tokunaga, C., Eguchi, S., Oshiro, N., Hidayat, S., Yoshino, K., Hara, K., Tanaka, N., Avruch, J. and Yonezawa, K. (2003). The mTOR partner, raptor, binds the mTOR substrates, p70 S6 kinase and 4E-BP1, through their TOS (TOR signaling) motifs. *J. Biol. Chem.* 278, 15461-15464.

Palmieri, M., Impey, S., Kang, H., di Ronza, A., Pelz, C., Sardiello, M. and Ballabio, A. (2011). Characterization of the CLEAR network reveals an integrated control of cellular clearance pathways. *Hum. Mol. Genet.* 20, 3852-3866.

Palmieri, M., Pal, R., Nelvagal, H. R., Lotfi, P., Stinnett, G. R., Seymour, M. L., Chaudhury, A., Bajaj, L., Bondar, V. V., Bremner, L., Saleem, U., Tse, D. Y., Sanagasetti, D., Wu, S. M., Neilson, J. R., Pereira, F. A., Pautler, R. G., Rodney, G. G., Cooper, J. D. and Sardiello, M. (2017). mTORC1-independent TFEB activation via Akt inhibition promotes cellular clearance in neurodegenerative storage diseases. *Nat. Commun.* 8, 14338.

Parenti, G., Andria, G. and Ballabio, A. (2015). Lysosomal storage diseases: from pathophysiology to therapy. *Annu. Rev. Med.* 66, 471-486.

Pastore, N., Blomenkamp, K., Annunziata, F., Piccolo, P., Mithbaekar, P., Sepe, R. M., Vetrini, F., Palmer, D., Ng, P., Polishchuk, E., Iacobacci, S., Polishchuk, R., Teckman, J., Ballabio, A. and Brunetti-Pierri, N. (2013). Gene transfer of master autophagy regulator TFEB results in clearance of toxic protein and correction of hepatic disease in alpha-1-anti-trypsin deficiency. *EMBO Mol. Med.* 5, 397-412.

Pastore, N., Brady, O. A., Diab, H. I., Martina, J. A., Sun, L., Huynh, T., Lim, J. A., Zare, H., Raben, N., Ballabio, A. and Puertollano, R. (2016). TFEB and TFE3 cooperate in the regulation of the innate immune response in activated macrophages. *Autophagy* 12, 1240-1258.

Pastore, N., Vainshtein, A., Klisch, T. J., Armani, A., Huynh, T., Herz, N. J., Polishchuk, E. V., Sandri, M. and Ballabio, A. (2017). TFE3 regulates whole-body energy metabolism in cooperation with TFEB. *EMBO Mol. Med.* 5, 605-621.

Pastore, N., Vainshtein, A., Herz, N. J., Huynh, T., Brunetti, L., Klisch, T. J., Mutarelli, M., Annunziata, P., Kinouchi, K., Brunetti-Pierri, N., Sassone-Corsi, P. and

Ballabio, A. (2019). Nutrient-sensitive transcription factors TFEB and TFE3 couple autophagy and metabolism to the peripheral clock. *EMBO J.* 38, e101347.

Pearce, L. R., Huang, X., Boudeau, J., Pawlowski, R., Wullschleger, S., Deak, M., Ibrahim, A. F. M., Gourlay, R., Magnuson, M. A. and Alessi, D. R. (2007). Identification of Protor as a novel Rictor-binding component of mTOR complex-2. *Biochem. J.* 3, 513-522.

Peña-Llopis, S., Vega-Rubin-de-Celis, S., Schwartz, J. C., Wolff, N. C., Tran, T. A. T., Zou, L., Xie, X. J., Corey, D. R. and Brugarolas, J. (2011). Regulation of TFEB and V-ATPases by mTORC1. *EMBO J.* 30, 3242-3258.

Perera, R. M. and Zoncu, R. (2016). The Lysosome as a regulatory hub. *Annu. Rev. Cell Dev. Biol.* 32, 223-253.

Peterson, T. R., Laplante, M., Thoreen, C. C., Sancak, Y., Kang, S. A., Kuhel, W. M., Gray, N. S. and Sabatini, D. M. (2009). DEPTOR is an mTOR inhibitor frequently overexpressed in multiple myeloma cells and required for their survival. *Cell* 137, 873-886.

Ploper, D., Taelman, V. F., Robert, L., Perez, B. S., Titz, B., Chen, H. W., Graeber, T. G., von Eeuw, E., Ribas, A. and De Robertis, E. M. (2015). MITF drives endolysosomal biogenesis and potentiates Wnt signaling in melanoma cells. *Proc. Natl. Acad. Sci. USA* 112, E420-E429.

Polito, V. A., Li, H., Martini-Stoica, H., Wang, B., Yang, L., Xu, Y., Swartzlander, D. B., Palmieri, M., di Ronza, A., Lee, V. M. Y., Sardiello, M., Ballabio, A. and Zheng,

H. (2014). Selective clearance of aberrant tau proteins and rescue of neurotoxicity by transcription factor EB. *EMBO Mol. Med.* 6, 1142-1160.

Puertollano, R., Ferguson, S. M., Brugarolas, J. and Ballabio, A. (2018). The complex relationship between TFEB transcription factor phosphorylation and subcellular localization. *EMBO J.* 37, e98804.

Rega, L. R., Polishchuk, E., Montefusco, S., Napolitano, G., Tozzi, G., Zhang, J., Bellomo, F., Taranta, A., Pastore, A., Polishchuk, R., Piemonte, F., Medina, D. L., Catz, S. D., Ballabio, A. and Emma, F. (2016). Activation of the transcription factor EB rescues lysosomal abnormalities in cystinotic kidney cells. *Kidney Int.* 89, 862-873.

Rehli, M., Lichanska, A., Cassady, A. I., Ostrowski, M. C., and Hume, D. A. (1999). TFEC is a macrophage-restricted member of the MiT subfamily of bHLH-ZIP transcription factors. *J. Immunol.* 162, 1559-1565.

Robitaille, A. M., Christen, S., Shimobayashi, M., Cornu, M., Fava, L. L., Moes, S., Prescianotto-Baschong, C., Sauer, U., Jenoe, P. and Hall, M. N. (2013). Quantitative phosphoproteomics reveal mTORC1 activates de novo pyrimidine synthesis. *Science* 339, 1320-1323.

Roczniak-Ferguson, A., Petit, C. S., Froehlich, F., Qian, S., Ky, J., Angarola, B., Walther, T. C. and Ferguson, S. M. (2012). The transcription factor TFEB links mTORC1 signaling to transcriptional control of lysosome homeostasis. *Sci. Signal.* 5, ra42.

Rousseau, A. and Bertolotti, A. (2016). An evolutionarily conserved pathway controls proteasome homeostasis. *Nature* 536, 184-189.

Roux, P. P., Ballif, B. A., Anjum, R., Gygi, S. P. and Blenis, J. (2004). Tumor-promoting phorbol esters and activated Ras inactivate the tuberous sclerosis tumor suppressor complex via p90 ribosomal S6 kinase. *Proc. Natl. Acad. Sci. USA* 101, 13489-13494.

Sabatini, D. M., Erdjument-Bromage, H., Lui, M., Tempst, P. and Snyder, S. H. (1994). RAFT1: A mammalian protein that binds to FKBP12 in a rapamycin-dependent fashion and is homologous to yeast TORs. *Cell* 78, 35-43.

Saftig, P. and Klumperman, J. (2009). Lysosome biogenesis and lysosomal membrane proteins: trafficking meets function. *Nat. Rev. Mol. Cell Biol.* 10, 623-635.

Samie, M. and Cresswell, P. (2015). The transcription factor TFEB acts as a molecular switch that regulates exogenous antigen-presentation pathways. *Nat. Immunol.* 16, 729-736.

Sancak, Y., Thoreen, C. C., Peterson, T. R., Lindquist, R. A., Kang, S. A., Spooner, E., Carr, S. A. and Sabatini, D. M. (2007). PRAS40 is an insulin-regulated inhibitor of the mTORC1 protein kinase. *Mol. Cell.* 6, 903-915.

Sancak, Y., Peterson, T. R., Shaul, Y. D., Lindquist, R. A., Thoreen, C. C., Bar-Peled, L. and Sabatini, D. M. (2008). The Rag GTPases bind raptor and mediate amino acid signaling to mTORC1. *Science* 320, 1496-1501.

Sancak, Y., Bar-Peled, L., Zoncu, R., Markhard, A. L., Nada, S. and Sabatini, D. M. (2010). Ragulator-Rag complex targets mTORC1 to the lysosomal surface and is necessary for its activation by amino acids. *Cell* 141, 290-303.

Sarbassov, D. D., Ali, s. M., Kim, D. H., Guertin, D. A., Latek, R. R., Erdjument-Bromage, H., Tempst, P. and Sabatini, D. M. (2004). Rictor, a novel binding partner of mTOR, defines a rapamycin-insensitive and raptor-independent pathway that regulates the cytoskeleton. *Curr. Biol.* 14, 1296-1302.

Sarbassov, D. D., Ali, S. M., Sengupta, S., Sheen, J., Hsu, P. P., Bagley, A. F., Markhard, A. L. and Sabatini, D. M. (2006). Prolonged rapamycin treatment inhibits mTORC2 assembly and Akt/PKB. *Mol. Cell* 22, 159-168.

Sardiello, M., Palmieri, M., di Ronza, A., Medina, D. L., Valenza, M., Gennarino, V. A., Di Malta, C., Donaudy, F., Embrione, V., Polishchuk, R. S., Banfi, S., Parenti, G., Cattaneo, E. and Ballabio, A. (2009). A gene network regulating lysosomal biogenesis and function. *Science* 325, 473-477.

Saxton, R. A. and Sabatini, D. M. (2017). mTOR signaling in growth, metabolism, and disease. *Cell* 168, 960-976.

Schalm, S. S. and Blenis, J. (2002) Identification of a conserved motif required for mTOR signaling. *Curr. Biol.* 12, 632-639.

Settembre, C., Di Malta, C., Polito, V. A., Arencibia, M. G., Vetrini, F., Erdin, S., Erdin, S. U., Huynh, T., Medina, D., Colella, P., Sardiello, M., Rubinsztein, D. C. and

- Ballabio, A. (2011). TFEB links autophagy to lysosomal biogenesis. *Science* 332, 1429-1433.
- Settembre, C., Zoncu, R., Medina, D. L., Vetrini, F., Erdin, S., Erdin, S., Huynh, T., Ferron, M., Karsenty, G., Vellard, M. C., Facchinetti, V., Sabatini, D. M. and Ballabio, A. (2012). A lysosome-to-nucleus signalling mechanism senses and regulates the lysosome via mTOR and TFEB. *EMBO J.* 31, 1095-1108.
- Settembre, C., De Cegli, R., Mansueto, G., Saha, P. K., Vetrini, F., Visvikis, O., Huynh, T., Carissimo, A., Palmer, D., Klisch, T. J., Wollenberg, A. C., Di Bernardo, D., Chan, L., Irazoqui, J. E. and Ballabio, A. J. (2013a). TFEB controls cellular lipid metabolism through a starvation-induced autoregulatory loop. *Nat. Cell Biol.* 15, 647-658.
- Settembre, C., Fraldi, A., Medina, D. L. and Ballabio, A. (2013b). Signals from the lysosome: a control centre for cellular clearance and energy metabolism. *Nat. Rev. Mol. Cell Biol.* 14, 283-296.
- Sha, Y., Rao, L., Settembre, C., Ballabio, A. and Eissa, N. T. (2017). STUB1 regulates TFEB-induced autophagy-lysosome pathway. *EMBO J.* 36, 2544-2552.
- Shen, K. and Sabatini, D. M. (2018). Ragulator and SLC38A9 activate the Rag GTPases through noncanonical GEF mechanisms. *Proc. Natl. Acad. Sci. USA* 115, 9545-9550.
- Silvestrini, M. J., Johnson, J. R., Kumar, A. V., Thakurta, T. G., Blais, K., Neill, Z. A., Marion, S. W., Amand, W. St., Reenan, R. A. and Lapierre, L. R. (2018). Nuclear

export inhibition enhances HLH-30/TFEB activity, autophagy and lifespan. *Cell Rep.* 23, 1915-1921.

Song, W., Wang, F., Savini, M., Ake, A., di Ronza, A., Sardiello, M. and Segatori, L. (2013). TFEB regulates lysosomal proteostasis. *Hum. Mol. Genet.* 22, 1994-2009.

Sorokin, A.V., Kim, E. R. and Ovchinnikov, L. P. (2007). Nucleocytoplasmic transport of proteins. *Biochemistry* 72, 1439-1457.

Spampanato, C., Feeney, E., Li, L., Cardone, M., Lim, J.-A., Annunziata, F., Zare, H., Polishchuk, R., Puertollano, R., Parenti, G., Ballabio, A. and Raben, N. (2013). Transcription factor EB (TFEB) is a new therapeutic target for Pompe disease. *EMBO Mol. Med.* 5, 691-706.

Steingrímsson, E., Tessarollo, L., Reid, S. W., Jenkins, N. A. and Copeland, N. G. (1998). The bHLH-Zip transcription factor Tfeb is essential for placental vascularization. *Development* 125, 4607-4616.

Steingrímsson, E., Tessarollo, L., Pathak, B., Hou, L., Arnheiter, H., Copeland, N. G. and Jenkins, N. A. (2002). Mitf and Tfe3, two members of the Mitf-Tfe family of bHLH-Zip transcription factors, have important but functionally redundant roles in osteoclast development. *Proc. Natl. Acad. Sci. USA* 99, 4477-4482.

Steingrímsson, E., Copeland, N. G. and Jenkins, N. A. (2004). Melanocytes and the microphthalmia transcription factor network. *Annu. Rev. Genet.* 38, 365-411.

Tassabehji, M., Newton, V. E. and Read, A. P. (1994). Waardenburg syndrome type 2 caused by mutations in the human microphthalmia (MITF) gene. *Nat. Genet.* 3, 251-255.

Tsun, Z. Y., Bar-Peled, L., Chantranupong, L., Zoncu, R., Wang, T., Kim, C., Spooner, E. and Sabatini, D. M. (2013). The Folliculin tumor suppressor is a GAP for RagC/D GTPases that signal amino acid levels to mTORC1. *Mol. Cell* 52, 495-505.

Tsunemi, T., Ashe, T. D., Morrison, B. E., Soriano, K. R., Au, J., Roque, R. A., Lazarowski, E. R., Damian, V. A., Masliah, E. and La Spada, A. R. (2012). PGC-1 α rescues Huntington's disease proteotoxicity by preventing oxidative stress and promoting TFEB function. *Sci. Transl. Med.* 4, 142ra97.

Vega-Rubin-de-Celis, S., Peña-Llopis, S., Konda, M. and Brugarolas, J. (2017). Multistep regulation of TFEB by MTORC1. *Autophagy* 13, 464-472.

Visvikis, O., Ihuegbu, N., Labed, S. A., Luhachack, L. G., Alves, A. F., Wollenberg, A. C., Stuart, L. M., Stormo, G. D. and Irazoqui, J. E. (2014) Innate host defense requires TFEB-mediated transcription of cytoprotective and antimicrobial genes. *Immunity* 40, 896-909.

Wang, B. T., Ducker, G. S., Barczak, A. J., Barbeau, R., Erle, D. J. and Shokat, K. M. (2011). The mammalian target of rapamycin regulates cholesterol biosynthetic gene expression and exhibits a rapamycin-resistant transcriptional profile. *Proc. Natl. Acad. Sci. USA* 108, 15201-15206.

Wang, S., Tsun, Z. Y., Wolfson, R. I., Shen, K., Wyant, G. A., Plovanich, M. E., Yuan, E., D., Jones, T. D., Chantranupong, L., Comb, W., Wang, T., Bar-Peled, L., Zoncu, R., Straub, C., Kim, C., Park, J., Sabatini, B. L. and Sabatini, D. M. (2015). Lysosomal amino acid transporter SLC38A9 signals arginine sufficiency to mTORC1. *Science* 347, 188-194.

Willett, R., Martina, J. A., Zewe, J. P., Wills, R., Hammond, G. R. V. and Puertollano, R. (2017). TFEB regulates lysosomal positioning by modulating TMEM55B expression and JIP4 recruitment to lysosomes. *Nat. Comm.* 8, 1580.

Wen, W., Meinkoth, J. L., Tsien, R. Y. and Taylor, S. S. (1995). Identification of a signal for rapid export of proteins from the nucleus. *Cell* 82, 463-473.

Wolfson, R. L., Chantranupong, L., Saxton, R. A., Shen, K., Scaria, S. M., Cantor, J. R. and Sabatini, D. M. (2016). Sestrin2 is a leucine sensor for the mTORC1 pathway. *Science* 351, 43-48.

Wu, L. Zhou, B., Oshiro-Rapley, N., Li, M., Paulo, J. A., Webster, C. M., Mou, F., Kacergis, M. C., Talkowski, M. E., Carr, C. E., Gygi, S. P., Zheng, B. and Soukas, A. A. (2016). An ancient, unified mechanism for metformin growth inhibition in *C. elegans* and cancer. *Cell* 167, 1705-1718.

Xiao, Q., Yan, P., Ma, X., Liu, H., Perez, R., Zhu, A., Gonzales, E., Burchett, J. M., Schuler, D. R., Cirrito, J. R., Diwan, A. and Lee, J. M. (2014). Enhancing astrocytic lysosome biogenesis facilitates A β clearance and attenuates amyloid plaque pathogenesis. *J. Neurosci.* 34, 9607-9620.

Xiao, Q., Yan, P., Ma, X., Liu, H., Perez, R., Zhu, A., Gonzales, E., Tripoli, D. L., Czerniewski, L., Ballabio, A., Cirrito, J. R., Diwan, A. and Lee, J. M. (2015). Neuronal-targeted TFEB accelerates lysosomal degradation of APP, reducing A β generation and amyloid plaque pathogenesis. *J. Neurosci.* 35, 12137-12151.

Xu, D., Farmer, A. and Chook, Y. M. (2010). Recognition of nuclear targeting signals by Karyopherin- β proteins. *Curr. Opin. Struct. Biol.* 20, 782-790.

Xu, H. and Ren, D. (2015). Lysosomal physiology. *Annu. Rev. Physiol.* 77, 57-80.

Xu, L. and Massagué, J. (2004). Nucleocytoplasmic shuttling of signal transducers. *Nat. Rev. Mol. Cell Biol.* 5, 209-219.

Yang, H., Rudge, D. G., Koos, J. D., Vaidialingam, B., Yang, H. J. and Pavletich, N. P. (2013). mTOR kinase structure, mechanism and regulation. *Nature* 497, 217-223.

Yang, T. T. C., Yu, R. Y. L., Agadir, A., Gao, G. J., Campos-Gonzales, R., Tournier, C. and Chow, C. W. (2008). Integration of protein kinase mTOR and extracellular signal-regulated kinase 5 in regulating nucleocytoplasmic localization of NFATc4. *Mol. Cell. Biol.* 28, 4489-3501.

Zachari, M. and Ganley, I. G. (2017). The mammalian ULK1 complex and autophagy initiation. *Essays Biochem.* 61, 585-596.

Zhang, Y., Nicholatos, J., Dreier, J. R., Ricoult, S. J. H., Widenmaier, S. B., Hotamisligil, G. S., Kwiatkowsky, D. J. and Manning, B. D. (2014). Coordinated regulation of protein synthesis and degradation by mTORC1. *Nature* 513, 440-443.

Zhang, X., Shu, L., Hosoi, H., Murti, K. G. and Houghton, P. J. (2002). Predominant nuclear localization of mammalian target of rapamycin in normal and malignant cell in culture. *J. Biol. Chem.* 277, 22127-28134.

Zhao, G. Q., Zhao, Q., Zhou, X., Mattei, M. G. and de Crombrughe, B. (1993). TFEC, a basic helix-loop-helix protein, forms heterodimers with TFE3 and inhibits TFE3-dependent transcription activation. *Mol. Cell. Biol.* 13, 4505-4512.

Zhao, J., Zhai, B., Gygi, S. P. and Goldberg, A. L. (2015). mTOR inhibition activates overall protein degradation by the ubiquitin proteasome system as well as by autophagy. *Proc. Natl. Acad. Sci. USA* 112, 15790-15797.

Zoncu, R., Bar-Peled, L., Efeyan, A., Wang, S., Sancak, Y. and Sabatini, D. M. (2011). mTORC1 senses lysosomal amino acids through an inside-out mechanism that requires the vacuolar H⁺-ATPase. *Science* 334, 678-683.

ACKNOWLEDGEMENTS

Finally, after four long years, this PhD has come to the end and it is time now to thank all the people who have made this important personal achievement possible. Someone told me that I am good in writing down my thoughts, so I hope my words will be worthy to express all my gratitude to these people. First, I have to thank Prof. Andrea Ballabio, who provided me all the equipment and facilities necessary to learn and grow as a young scientist, and all the members of his laboratory, who helped, supported and criticized my work when it was necessary, all their comments made me a more experienced worker and, hopefully, more professional than I used to be before. In particular, I have to thank Gennaro, from whom I learned a lot, and Floriana, who was able to manage my disorganization, and mostly important the colleagues that worked hard with me every single day: Alessandro, who has been a great bench mate; Marianna, who was fundamental when I first arrived in the new laboratory introducing me in the laboratory life and in the new city; Alessandra, who helped me several times with her advices, in particular during the long critical nights spent together in the laboratory. I cannot mention all the member of the laboratory, but I have good memories with all of them, thank you for all the moments and laughs together, in particular a special thanks to Adrien and Raffaele which were positive examples to me for their goodness and authenticity. Then, a huge thanks to the place that has been my “home” during these years, the Telethon Institute of Genetics and Medicine, and all the people that make great this institute with their work and personalities: Graciana; Valeria Rotoli, vital for all the PhD students; all the scientific and administrative offices members; Stefano, Ciro and Sasà, their presence during the weekends at TIGEM is priceless; Lele for his precious help in English presentations; Santoro for his advices in cloning strategies; all the facilities

members, in particular Chiara and Simone from HCS facility, and all the personnel that make our working day easier. Thanks also to Telethon foundation, which gave me a reason to work for when my motivations failed. It has been probably the hardest time in my life, so I would like to spend few more words for those people that have been essential, now and ever, in my life. First of all, my lovely family, I missed them many times but they always gave me a sense of security every time I was giving up. Then, my love, Francesca, she has been the unexpected surprise of destiny, even in the most difficult periods she was able to remember me moments of pure happiness, it was not easy but thank you for being there listening to all my complaints, support from you and all your sweet family was indispensable, I am sure that all the best is coming with you. I am grateful to all my old friends, I missed them but the most were always next to me when I needed, kilometers create distances but never break bonds. Thank you also to all the fantastic people I met in Naples and in TIGEM, I have so many names in my mind that it is impossible to mention all of them here, every single person was gentle and friendly with me, sometimes even when I did not deserve it; I just want to mention the “free dogs” band, we had great moments all together living the city like a huge funfair made just for us and our wild nights. Finally, a huge special thank is for my little family of friends from Cambridge, they supported me from the very beginning during the PhD journey, in addition they have always reminded me the beauty of sharing joys and sorrows together. Lastly, my immense thanks is for Naples, a city that does not ask permissions, takes you and enters you to satisfy its need to reveal the secret of the wonders around you; I loved this city immediately and, for better and for worse, I experienced completely new emotions here, I will never forget it.